MULTI-PROXY APPROACH ON BLACK CARBON CHARACTERIZATION AND COMBUSTION PRODUCTS SOURCE DISCRIMINATION IN ENVIRONMENTAL MEDIA

A Dissertation

by

LI-JUNG KUO

Submitted to the Office of Graduate Studies of
Texas A&M University
in partial fulfillment of the requirements for the degree of

DOCTOR OF PHILOSOPHY

December 2009

Major Subject: Geology

MULTI-PROXY APPROACH ON BLACK CARBON CHARACTERIZATION AND COMBUSTION PRODUCTS SOURCE DISCRIMINATION IN ENVIRONMENTAL MEDIA

A Dissertation

by

LI-JUNG KUO

Submitted to the Office of Graduate Studies of
Texas A&M University
in partial fulfillment of the requirements for the degree of

DOCTOR OF PHILOSOPHY

Approved by:

Co-Chairs of Committee,	Bruce E. Herbert
	Patrick Louchouarn
Committee Members,	Ethan L. Grossman
	Franco Marcantonio
	Terry L. Wade
Head of Department,	Andreas Kronenberg

December 2009

Major Subject: Geology

ABSTRACT

Multi-proxy Approach on Black Carbon Characterization and Combustion Products Source Discrimination in Environmental Media. (December 2009)

Li-Jung Kuo, B.S., National Sun Yat-sen University;

M.S., National Sun Yat-sen University

Co-Chairs of Advisory Committee: Dr. Bruce E. Herbert
Dr. Patrick Louchouarn

Environmental applications of pyrogenic carbon, aka black carbon (BC), have been hampered due to the poor characterization and quantification of environmental BC. This dissertation was dedicated to the better characterization of environmental char/charcoal BC (char-BC), the most heterogeneous and the less identifiable group in the BC continuum. The analytical approach developed for char-BC was further incorporated with other BC methods in environmental samples for a comprehensive assessment of combustion-derived carbon inputs in different environmental systems.

The present study firstly evaluated the feasibility of using levoglucosan, a marker derived from cellulose/hemocellulose combustion, to characterize and quantify char-BC in the environment. Levoglucosan was found exclusively in BC materials derived from biomass combustion albeit in highly variable yields across different char-BC. A further examination of synthetic chars showed that temperature is the most influential factor affecting levoglucosan yield in char. Notably, levoglucosan was only detectable in low temperature char samples (150-350°C), regardless of plant species. These results

demonstrated that levoglucosan could serve as a good qualitative indicator for the presence of char produced under low temperature conditions in soil, sediments, and aerosols.

Results of lignin analysis on the synthetic chars further reveal that combustion can greatly decrease the yield of the eight major lignin phenols with no lignin phenols detected in any synthetic char produced at ≥ 400°C. The values of all lignin parameters show significant shifts with increasing combustion severity (temperature and/or duration), indicating that thermal alteration is an important abiotic lignin degradation process. Hence the input of char-BC in the environments represents a terrestrial organic matter source with highly altered lignin signatures.

Finally, a multi-proxy approach, including elemental (soot-BC) and molecular (levoglucosan, polycyclic aromatic hydrocarbons (PAHs), and lignin oxidation products) proxies, was adopted to investigate the centennial-scale temporal distribution of combustion products in four sediment cores from Puget Sound basins, WA. The observed temporal trends of soot-BC and combustion PAHs fluxes reflect the evolution of energy consumption and the positive effects of environmental regulations. The distinct temporal patterns of soot and PAHs among cores demonstrate that urbanization is a crucial factor controlling the inputs of combustion byproducts to the environment. On the other hand, the trends of levoglucosan may be more relevant to the climate oscillation and thus show a regional distribution pattern. Our results demonstrate that environmental loading of combustion byproducts is a complex function of urbanization and land use, fuel usage, combustion technology, environmental policies, and climate changes.

ACKNOWLEDGMENTS

Thanks God for guiding me all the time.

I would like to thank my family in Taiwan. Your love and continuous support are the main reasons I can go over the sea, pursue the PhD degree in the United States, and complete this dissertation. Thanks to my sister, Liang-Wei. I am very lucky to have you here in Houston. You contribute a lot in my degree pursuing.

I would like to thank Ching-Wen. Thank you for always being there for me, listening to me, and giving me appropriate suggestions. I am very lucky to have you by my side through all those happy moments and terrible periods. Thank you so much!

I would like to express my sincere gratitude to my research advisors, Dr. Bruce Herbert and Dr. Patrick Louchouarn, for guiding me on the research, helping me on the financial aid, and encouraging me on the daily life. Thanks to my thesis committee, Drs. Ethan Grossman, Franco Marcantonio, and Terry Wade, for their valuable advice. Special thanks to Dr. Terry Wade for the full support on the use of facilities in the Geochemical & Environmental Research Group (GERG). Thanks to Drs. Thomas Bianchi and Andreas Kronenberg for allowing me to use their instruments.

I would also like to acknowledge Meng-Der Fang, Brian Jones, Ronald Lehman, Clayton Powell, Erik Smith, and Gilvan Yogui for their great help on the GC-MS, EA, char making, and lignin analysis. I also thank Guy Denoux, Blake Mackan, Lisa McDonald, José Sericano, Cindy Starr, and Steve Sweet, for their technical supports and help in GERG. This dissertation would not have been possible without all their help.

Many thanks to the members in Herbert's group - Omar Harvey, Christopher Markley, Karen McNeal, and Heather Miller - for friendly discussions and experience sharing. It was fun to work with you in the lab and on the field. Also thanks to Daniellè Aguirre for her great help in the lab in Galveston.

To my friends, Chinese Bible Study Group (Mrs. Lee, Ang Li, Chang-Ping (Michael), Hsin-Ya, Li-Yuan (Joan), Li Sun, Jiang-Hui, Tzu-Fen, Ya-Ting (Renee)), Chi-Lin (Terence), Hen-I (Johnny), Ming-Hung (Taco), Ping-Jung (Judy), Szu-Hsuan (Sherry), Xixi. Thank you for listening to me, helping me. You gave me many great times in the past six years.

TABLE OF CONTENTS

Page

LIST OF FIGURES

Page

Page

LIST OF TABLES

1. INTRODUCTION AND RESEARCH OBJECTIVES

1.1. General introduction of black carbon

In recent years, increasing attention has been given to black carbon (BC) due to its potential impacts on many biogeochemical processes. Production of BC has increased during the last centuries owing to dramatically increased deforestation, shifting agriculture, coal and oil combustion for industrial energy supply, vehicle emissions, and the frequent wildfires (Schmidt and Noack, 2000). Kuhlbusch and Crutzen (1995) estimated the annual production of BC from vegetation fire ranges from 50 to 270 Tg BC/year (Tg = 10^{12} gram); while annual BC flux from fossil fuel combustion was estimated to be 13 to 24 Tg BC/year by Penner et al. (1993). However, these published global BC budgets may underestimate total pool of BC due to different analytical methods applied (Masiello, 2004).

As pointed out by Goldberg (1985), the general definition of BC is "an impure form of the element produced by the incomplete combustion of fossil fuels or biomass." Synonyms and analogous terms in the literature include elemental carbon, polymeric carbon, soot carbon, lampblack, coke, acetylene black, charcoal, graphite black carbon, and fusain (Jones et al., 1997; Accardi-Dey, 2003). The combustion sources of the BC materials are considerably diverse including boilers, vehicle engines, fireplaces, natural gas burners, tar pots, wildfire, wear of brakes and tires (Accardi-Dey, 2003). Various BC materials could be easily redistributed in the environments by aeolian transport and/or

---

This dissertation follows the style of *Organic Geochemistry*.

surface runoff and become ubiquitous. BC is often deposited in a wide range of natural environments including soils, marine and lacustrine sediments, freshwater, seawater, ice core and the atmosphere (Goldberg, 1985; Cachier and Pertuisot, 1994; Gustafsson and Gschwend, 1998; Masiello and Druffel, 1998; Middelburg et al., 1999; Schmidt and Noack, 2000; Muri et al., 2002; Skjemstad et al., 2002; Dickens et al., 2004; Masiello, 2004).

BC is refractory and this makes BC an important consideration in a number of geochemical processes. Due to its long lifetime in most environments, BC represents a stable component in the global carbon cycle (Kuhlbusch, 1998; Masiello and Druffel, 1998). It has been suggested that BC deposition may represent a significant sink of atmospheric CO_2 and source of O_2 (Cope and Chaloner, 1980; Kuhlbusch and Crutzen, 1995; Marris, 2006). In addition, because BC is combustion-derived and it can survive over geological time, it also has been widely used as a tracer for the Earth's fire history (Smith et al., 1973; Griffin and Goldberg, 1979; Wolbach et al., 1988; Bird and Cali, 1998).

Researchers have also found that BC is a supersorbent that affects the mobility and toxicity of hydrophobic organic compounds (HOCs) in surface and subsurface environments (Gustafsson et al., 1997; Jonker and Koelmans, 2002; Accardi-Dey and Gschwend, 2003; Burgess et al., 2004; Cornelissen et al., 2006; Cornelissen et al., 2008ab). Studies concerning the bioavailability of HOCs in the environment have started to consider the impact of BC present in the soil or sediment matrix (Burgess and Lohmann, 2004; Kukkonen et al., 2004; Jonker et al., 2004). In general, HOCs with higher planarity show stronger association with BC and such compounds often possess low Biota-Sediment Accumulation Factors (BSAFs) in the presence of BC (Bucheli and Gustafsson, 2003; Cornelissen et al., 2004; Kukkonen et al., 2004; Cornelissen et al., 2005; Cornelissen et al., 2006). Hence, researchers have

indicated that conventional risk assessments of planar HOCs in soils/sediments may need to be re-evaluated by considering the effect of BC (Cornelissen et al., 2006; Koelmans et al., 2006).

In the field of atmospheric science, BC is well known as the principal light-absorbing aerosol component, which can decrease the aerosol single scattering albedo (SSA) and contribute to global warming (Crutzen and Andreae, 1990; Hansen and Sato, 2001; Jacobson, 2001; Novakov et al., 2003; Ramanathan and Carmichael, 2008; Tollefson, 2009). Researchers have suggested that BC aerosols could be linked to the droughts in northern China, flooding in southern China, and the weaker Indian monsoon because it can alter the regional atmospheric stability, affect the atmospheric circulation, and eventually perturb the regional hydrological cycle (Menon et al., 2002; Ramanathan and Carmichael, 2008). In addition, researchers also indicated that BC can alter the snow/ice albedo and induce the thinning of Arctic sea ice, as well as the melting of land ice and permafrost (Hansen and Nazarenko, 2004; Ramanathan and Carmichael, 2008; Shindell and Faluvegi, 2009; Tollefson, 2009). It also indirectly affects cloud processes (Chylek et al., 1999; Ackerman et al., 2000). Finally, due to its small particle size, BC may penetrate deeply into the lungs and adsorbed compounds like polycyclic aromatic hydrocarbons (PAHs) may enter the blood and become distributed systematically. This may cause somatic cell mutations and thus BC is suspected as a major contributor to approximately one million premature deaths per year (Hansen and Nazarenko, 2004; Samet et al., 2004). Study has also shown that BC exposure may enhance the risk of cardiovascular disease (Radomski et al., 2005).

1.2. Black carbon characterization and quantification - a paradox

The above brief review demonstrates the complex role of BC in a number of environmental issues. BC may be detrimental in terms of global warming or human health, but it can also play a positive role in reducing the bioavailability of HOCs in soils/sediments or as an atmospheric CO_2 sink (Koelmans et al., 2006; Lehmann et al., 2008). To better assess the environmental impact of BC, it is crucial to understand the distribution of BC in the environment. However, BC characterization is still an issue due to its inherent chemical and physical complexity.

1.2.1. BC combustion continuum

Hedges et al. (2000) placed BC into the molecularly-uncharacterized components (MUC) of organic matter in natural environments because such combustion products have many forms, ranging from slightly charred biomass to highly refractory soot condensed from the gas phase. Hedges et al. (2000) conceptualized BC as part of the combustion continuum, which is represented as a diagram with different atomic O/C ratio as an index for different BC types. Along this continuum, the BC material increases in carbon content as the combustion process increases in temperature and duration. Masiello (2004) further refined the BC combustion continuum with indications of changes of formation temperature, particle size, reactivity, sources, and primary reservoirs (Figure 1). Though as a class BC exhibits great physiochemical variations, it is generally divided into two major forms: charcoal and soot. Generally, charcoal is considered to be a combustion residue of plants. However, a small portion of charcoal may originate from other sources (e.g. combustion residues of inefficient incineration of municipal solid waste (Louchouarn et al., 2007). Charcoal often retains some physical structure information of the parent fuel and exhibits a wide particle size

range (mm to μm). Soot is derived from the extensive recombination of small free radicals condensing from the gas phase and could come from both plant and fossil fuels combustion. It retains no structural information of parent fuel except for some isotopic signature (Gustafsson et al., 2001; Reddy et al., 2002). The particle size of soot generally is in the submicron scale.

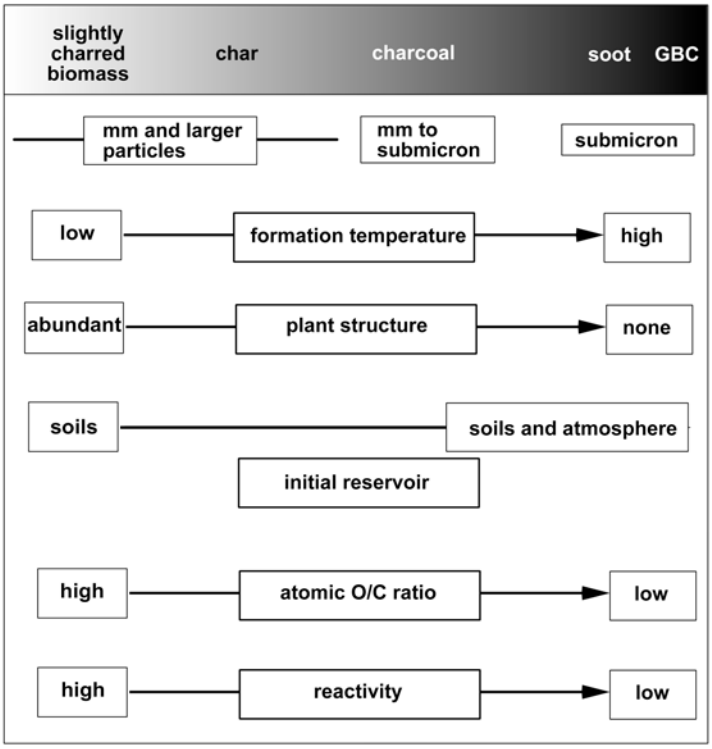

Figure 1. BC combustion continuum modified from the models proposed in Masiello (2004) and Elmquist et al. (2006).

1.2.2. Brief review of BC methods

The lack of clear demarcation between different subclasses of BC combustion products makes it nearly impossible to detect BC with a universal method. Masiello (2004) reviewed most of the available BC analytical methods and their potential detection windows in the BC

continuum (Figure 2). Hammes et al. (2007) provided further knowledge on the comparative nature of these methods through an extensive inter-calibration study of BC quantification on a wide series of reference materials. The BC method continuum resulting from these studies describes the applicability of specific methods to detect different types of black carbon and demonstrates the difficulty in comparing BC values obtained from methods with different detection windows (Schmidt et al., 2001; Masiello, 2004; Hammes et al., 2007).

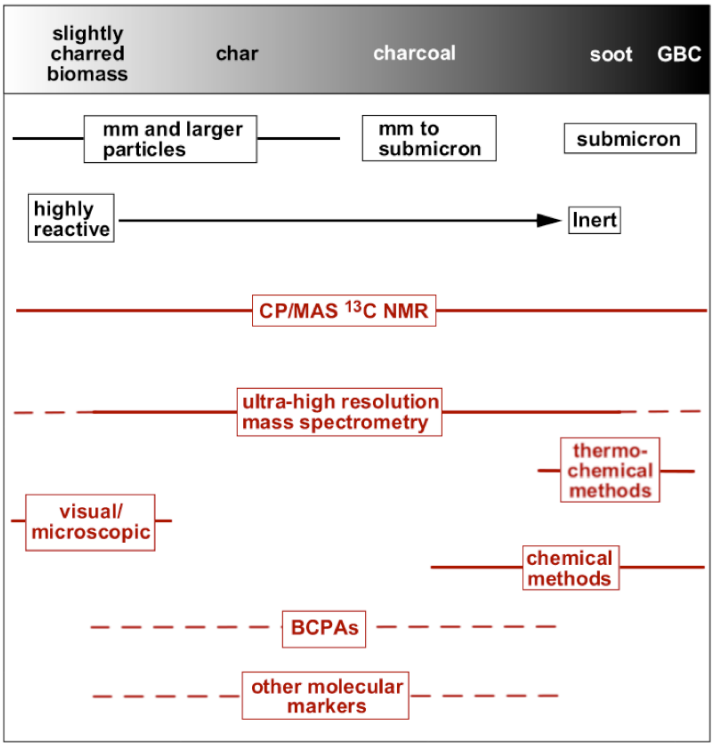

Figure 2. BC method continuum proposed from Masiello (2004).

The available BC methods are grouped into 6 classes: microscopic, optical, thermal, chemical, spectroscopic and molecular markers with some combination of approaches for some of them (Schmidt and Noack, 2000; Masiello, 2004; Nguyen et al., 2004; Hammes et

al., 2007). The microscopic method quantifies the number of charcoal pieces visible under an optical microscope and it is often used to study the fire history in soils/sediments (Clark and Patterson, 1997). In addition to being time-consuming, the major disadvantage of this method is the particle size threshold for identification in the micron range leaving out all ultra-fine combustion materials from detection. The thermal-optical method (Currie et al., 2002; Hitzenberger et al., 2006) is often used to quantify BC in aerosols. It includes thermal treatment and the measurement of transmittance change. The major disadvantage of this method is that it is hard to be applied to soils/sediments samples, which have high inorganic and non-BC organic matter contents. In such samples, the positive bias is large (Hammes et al., 2007). The well-known spectroscopic technique developed by Skjemstad et al. (1999) uses mild UV photo-oxidation treatment to remove the operationally defined non-BC organic fractions followed by ^{13}C NMR for BC quantification. The major disadvantages of this method include the overestimation of BC due to incomplete removal of non-BC organic carbon, and the expense and difficulty of ^{13}C NMR quantification of natural organic matter.

Because of its low cost and relative ease of use, chemo-thermal oxidation (CTO) method is very popular in the environmental science field and widely used to measure the BC in soils/sediments. Gustafsson et al. (1997) developed the most commonly used chemo-thermal oxidation procedure (CTO-375 method). This approach includes the thermal oxidation of samples at 375°C for 18-24 hrs to remove non-BC organic matter, acidification to remove carbonates and silicates and the quantification of residual carbon (the operational defined BC) by elemental analyzer. One major issue with this method is that non-BC organic matter potentially can form char-like material during the thermal oxidation step leading to a positive bias in the estimation of BC in samples. Therefore, Gélinas et al. (2001) modified

this method with the addition of hydrolysis treatments to remove hydrolyzable organic matter before the thermal treatment. This reduces the problem of artificial char production. To distinguish from the CTO-375, the procedure from Gélinas et al. (2001) was named the graphite black carbon (GBC) method. A recent comparison of these two methods (Louchouarn et al., 2007) showed that the positive bias of charring is almost non-existent in soils/sediments containing substantial thermally stable BC (i.e. urban estuaries and lake sediments). Since such samples still are minor proportions of natural soil and sedimentary environment, the CTO-375 method should be used with caution to prevent positive bias during BC quantification. Basically, these two chemo-thermal oxidation procedures work very well in most samples, but a limitation of this type of method is that it nearly exclusively measures the soot/graphite BC that possesses good thermal stability. Nguyen et al. (2004), Elmquist et al. (2006), and Quénéa et al. (2006) have found that charcoal could not be detected by this method.

The use of chemical oxidation methods has also been reported in the literature. The most commonly used chemical oxidation method is the acid dichromate oxidation method. This method was first developed by Wolbach and Anders (1989) to separate kerogen and elemental carbon, including soot and charcoal, in sedimentary rocks based on their different decay rates under the attack of a strong oxidant. This method was also applied to quantify BC in sediments (Masiello et al., 2002) and soils subjected to slash and burn agriculture (Rumpel et al., 2006). The major drawback of this chemical oxidation method is that it is very time-consuming and suffers from some interference (e.g. wax extracts from fresh plants; personal communication with Dr. Masiello). However, two major advantages of this method

are that it has the capability to characterize the isotopic signature of BC and possess a wider detection window than the CTO methods (Masiello, 2004).

Molecular marker approaches quantify the concentrations of specific, identifiable organic compounds that are proxies of BC. A series of such molecular markers are the benzene polycarboxylic acids (BPCA), by-products of the oxidation of BC's condensed polyaromatic units (Glaser et al. 1998). This method has been applied to soil samples (Schmidt et al., 2001; Rodionov et al., 2006) but recent studies showed that results are highly variable, depending on a relatively arbitrary BC "conversion factor", and that there are a number of potential interferences (Brodowski et al., 2005; Hammes et al., 2007; personal communication with Dr. Angela Dickens). Simoneit et al. (1999) proposed another combustion biomarkers, levoglucosan (1,6-anhydro-β-D-glucopyranose), for BC research. Since levoglucosan is a monosaccharide derivative exclusively formed during the thermal breakdown of cellulose during combustion process, it is very source-specific and can be found in solid combustion residues of fuels containing cellulose and hemicellulose (Shafizadeh et al., 1979; Simoneit et al., 1999; Simoneit, 2002; Elias et al., 2001; Otto et al., 2006; Fabbri et al., 2008; Schmidl et al., 2008). In addition, because of levoglucosan's stability under acidic conditions (Fraser and Lakshmanan, 2000; Simoneit et al., 2004), which is typical for atmosphere aerosols, it can be used as a tracer for long-range transport of biomass combustion aerosols (Fraser and Lakshmanan, 2000; Simoneit and Elias, 2000; Nolte et al., 2002; Fraser et al., 2003; bin Abas et al., 2004a; bin Abas et al., 2004b; Fine et al., 2004; Simoneit et al., 2004; Ward et al., 2006; Schmidl et al., 2008; Engling et al., 2009). In a study by Elias and coauthors (2001), the distribution of levoglucosan in a sediment core

was correlated with that of charcoal content suggesting the long-term preservation of this combustion biomarker and its potential to serve as a tracer for historical fire events.

While the methods for identifying and quantifying soot/graphite seem well established (Gélinas et al., 2001; Gustafsson et al., 2001; Louchouarn et al., 2007), the quantitative discrimination of the char/charcoal portion of the BC continuum faces more difficulties. This is because of the wide range of reactivity of char/charcoal caused from the various combustion processes that produce this material (Baldock and Smernik, 2002). Most BC methods are oxidation approaches that remove operationally defined non-BC organics by their presumed high reactivity. These oxidation methods typically remove some or all of the char/charcoal.

The detection of char/charcoal is certainly important in BC research due to the potentially large input to the environment from frequent wildfires in the world. Kuhlbusch and Crutzen (1995) pointed out that more than 80% of BC from vegetation fire remains on the ground after the fire. Hence, the development of sensitive and specific methods for char/charcoal surely is a priority in BC research.

1.2.3. Linking temporal BC distribution with contamination records

Black carbon is an ideal proxy to trace the spatial distribution and history of fossil fuel and other fuels consumption by human society. Karls and Christensen (1998) and Kralovec et al. (2002) isolated BC particles via severe chemical treatments from several sediment cores from Lake Michigan and Lake Erie. With the aid of scanning electron microscope (SEM), they distinguished and counted the BC particles derived from the combustion of coal, oil, and wood. The BC particle distributions were in accord with the historical records of U.S. energy consumption. Temporal BC distribution was also used as an indicator of the impact of

human activities on the environment. Rose et al. (2003) monitored the distributions of spheroidal carbonaceous particles (SCPs), produced from high temperature fossil fuel combustion, in sediment cores of North African coastal lakes to predict the future trend of ecological stress of regional wetlands.

Published research has also explored the relationships between BC loading and HOCs contamination in the environment due to the strong sorption capacity of BC for HOCs and the pyrogenic source of some HOCs (e.g. pyrogenic PAHs) (Gustafsson et al., 1997; Naes et al., 1998; Ghosh et al., 2003; Hong et al., 2003; Bucheli et al., 2004; Cornelissen et al., 2005; Cornelissen and Gustafsson, 2005; Cornelissen et al., 2006; Koelmans et al., 2006). The temporal trends of BC and pyrogenic PAHs, as observed in sediment cores from Lake Washington, were correlated (Wakeham et al., 2004). In a recent work, the temporal distribution of BC, SCPs and pyrogenic PAHs in remote mountain lake sediments were generally correlated though there are slight differences among them (Muri et al., 2006). Different emission sources and limitations of measurement techniques of those three combustion proxies were proposed to explain their observed dissimilarities. Except for some microscopic measurements, the operationally defined BC in the reports cited above was determined by the popular chemo-thermal technique. As mentioned earlier, BC quantified by the chemo-thermal technique (CTO-375 BC or GBC) only represents the soot/graphite region in the BC continuum. Therefore, the temporal BC distribution trends in the above literature didn't represent the "total BC" distribution profile. In a recent study, Louchouarn et al. (2007) addressed such concerns about the total BC profile in sediments. In their study of sediment cores from two urban lakes in the middle of New York City's metropolitan area, comparison of the GBC distribution, elemental analysis (atomic C/N ratio), and molecular

marker (lignin) data showed that another type of black carbon must be present in the sediment. By applying a quantitative mixing model, another potential BC, char-BC, was estimated to contribute up to 35% of the total organic matter in those sediment cores and hence the existence of the char-BC should not be neglected. Their observation again highlighted the limitation of using soot-BC to represent the BC loading and to assess the contamination potential in the environment.

1.3. Research outline

The quality of our understanding of the environmental significance of BC is in large part dependent on our ability to quantify it in a range of soils and sediments. Unfortunately, existing geochemical methods quantify only part of the total BC present in soils and sediments, sometimes resulting in conclusions that are controversial and inconsistent with observations. The major goals of this study are to establish a framework to better quantify BC loading to the environment and use this information to understand (1) the major sources of BC (e.g. biomass burning or fossil fuel combustion), (2) the major forcings affecting the production of BC (i.e. land use, climate or human activities), and (3) the relationship between BC and anthropogenic contaminants, especially PAHs.

To do a comprehensive BC characterization in geologic samples, we need to measure two major BC classes: char-BC and soot-BC. While the well-established GBC method was used to quantify the soot-BC, the molecular marker approach was tested for the char-BC measurement. Most thermal and chemical oxidation techniques have poor char-BC recovery because these approaches utilize intensive oxidation treatments to remove unwanted non-BC organic matter but the char-BC, because of its labile nature to oxidation, is often eliminated simultaneously. To specifically detect char-BC, the feasibility of using levoglucosan, a

cellulose/hemicellulose combustion biomarker, as a proxy of char-BC was evaluated in the first part of my research. A wide range of synthetic chars produced from three different plant species covering woody/non-woody, angiosperm/gymnosperm and C3/C4 plant pairs under controlled combustion conditions were used as model char-BC for this study. The specific objectives of this study are: (1) to evaluate if levoglucosan is a specific marker for char-BC; (2) to understand the effects of combustion temperature and duration, two primary factors in combustion conditions, on the levoglucosan yield; and (3) to compare levoglucosan approach with other BC methods (e.g. acid dichromate oxidation method, GBC method) on analyzing synthetic char.

In the second part of my research, I further analyzed the lignin signatures of the synthetic chars to investigate the effects of biomass combustion on this major biopolymer. Lignin has greater stability than cellulose to biodegradation and thus it represents an important part of soil organic matter. The lignin signatures from CuO oxidation can also tell the type of source plants and the diagenetic status. I used the lignin data of the synthetic chars and environmental samples to understand (1) the effects of combustion severity on the alternation of lignin parameters; (2) the responses of lignin parameters from different plant types to thermal alternation; and (3) the potential effects of char-BC inputs on the characterization of soil organic matter using lignin signatures.

The third part of my research is to conduct a comprehensive BC source and loading assessment on four sediment cores from Hood Canal and central basin of Puget Sound, WA. A multi-proxy approach, including elemental (soot-BC) and molecular (levoglucosan, PAHs), lignin oxidation products) proxies, were used to identify and characterize both char-BC and soot-BC with a thorough combustion source apportionment. The centennial-scale

temporal distribution of BC in these cores provide us a chance to study (1) the effects of urbanization/industrialization on the environmental BC inputs; (2) the potential difference in BC distribution between Pacific Northwest and other regions in US and Europe; (3) the relationship between BC and PAH distribution; and (4) the major forcings affecting the production of BC (i.e. land use, climate or human activities).

2. CAN LEVOGLUCOSAN BE USED TO CHARACTERIZE AND QUANTIFY CHAR/CHARCOAL BLACK CARBON IN ENVIRONMENTAL MEDIA? *

2.1. Introduction

Black carbon (BC) is a generic term that was initially introduced by Novakov (1982) to illustrate the role of soot in atmospheric sulfur chemistry. It was further described by Goldberg (1985) as a spectrum of highly recalcitrant organic residues remaining after combustion of biomass or fossil fuel. Over the past few decades, it has been found widely distributed in many surficial reservoirs (e.g. soil, sediments, freshwater, seawater and the atmosphere; Goldberg, 1985), where it can influence many important biogeochemical and environmental processes (Gustafsson et al., 1997; Kuhlbusch, 1998; Masiello, 2004; Koelmans et al., 2006). In the light of these many applications and interests, Hedges et al. (2000) synthesized the available knowledge on the source and fate of combustion byproducts in the environment. This led to the development of a conceptual continuum representing the diverse nature of BC, from slightly charred material to highly refractory soot. Masiello (2004) and recently Hammes et al. (2007) further refined the BC continuum by providing additional detail of BC characteristics, including temperature of formation, elemental ratios, particle size, reactivity, sources, and reservoirs. One major consensus emerging from these studies is that the BC continuum is comprised of two major categories, char/charcoal and

* Reproduced in part with permission from *Organic Geochemistry* **2008**, *39*, 1466-1478, Kuo, L.-J., Herbert, B. E., and Louchouarn P. "Can levoglucosan be used to characterize and quantify char/charcoal black carbon in environmental media?", Copyright 2008 Elsevier Ltd.

soot/graphite. The first category is a solid residue, which retains some original structural information from the parent material and with particle size in the millimeter to micron range. Although the present "paradigm" defining the spectrum of material within the BC continuum considers that char is mostly derived from biomass burning, municipal and domestic incineration of solid waste can also be a significant source of chars at the local level (Louchouarn et al., 2007). In contrast to char, whose production pathway always remains in the solid phase, soot is formed from the extensive recombination of small free radicals condensing from the gas phase and originates from both biomass and fossil fuel combustion. This formation mechanism leads to submicron soot particles that can remain suspended in the atmosphere on the order of months and be transported over wide geographic scales (Masiello, 2004).

Many techniques have been proposed to characterize and quantify BC in environmental media (Schmidt and Noack, 2000, Schmidt et al., 2001, Gustafsson et al., 2001; Hammes et al., 2007). While the methods for identifying and quantifying the soot/graphite portion of the BC continuum are relatively well established (Gustafsson et al., 2001; Gélinas et al., 2001; Louchouarn et al., 2007), quantifying the char/charcoal portion of the BC continuum suffers from many analytical limitations (Masiello, 2004; Hammes et al., 2007). Many BC methods are based on oxidation approaches that seek to remove non combustion-derived organics by assuming reactivity differences between operationally defined BC and non-BC materials. Because chars/charcoals are usually labile to such treatment, oxidative approaches often fail to detect these complex combustion byproducts in environmental media. In a recent review of the sources and fate of pyrogenic carbon in the environment, Preston and Schmidt (2006) indicated that an appropriate comparative analysis of published charcoal production estimates

is still hampered by variability in the methods used. Hence, the development and validation of a method that is specific for char/charcoal measurement remains a major priority in BC research.

Analytical methods based on molecular markers are potentially attractive for char/charcoal characterization and quantification due to their specificity. Among many biomass combustion markers, levoglucosan (1,6-anhydro-β-D-glucopyranose; CAS 498-07-7) is a good candidate for study. Because it is a monosaccharide derivative formed exclusively from the thermal breakdown of cellulose during combustion, it is source-specific and should hypothetically be found in any combustion residue of fuel containing cellulose and hemicellulose (Shafizadeh et al., 1979; Simoneit et al., 1999; Elias et al., 2001; Otto et al., 2006). The nature of levoglucosan is thus different from benzene polycarboxylic acids (BPCA), a suite of molecular markers proposed for BC quantification (Glaser et al., 1998; Brodowski et al., 2005; Dittmar, 2008). BPCA are the by-products from oxidation of condensed aromatic structures and as such are more indicative of aromatization, whereas levoglucosan is an indicator of thermal alteration of parent structure.

Previous studies have reported the presence of levoglucosan in fire-impacted soils and sediments (Elias et al., 2001; Oros et al., 2002; Otto et al., 2006). Elias and co-workers (2001) also showed that levoglucosan distribution in a lake sediment core was correlated to counted charcoal content. However, to our knowledge, no further study has systematically investigated the relationship between levoglucosan and char-BC.

The present study aims to further evaluate the application of levoglucosan in characterizing and quantifying char-BC in environmental samples. To test the sensitivity of the method for char-BC determination, we conducted an extensive examination of

levoglucosan yield in diverse BC materials (derived from both fossil fuels and biomass combustion), BC-like materials (coals and melanoidin), and soil and sediments with and/or without fire impacts. To evaluate if levoglucosan is a proper molecular marker for the quantification of char-BC, we analyzed the yield from twenty three char samples, produced in the laboratory from three different plant species and different combustion temperature and duration. These were also used to assess the factors that affect levoglucosan yield. Finally, we compared the performance of the levoglucosan approach in char-BC determination with another well-established BC analytical method, namely acid dichromate oxidation.

2.2. Materials and methods

2.2.1. Materials

Three different plant species were used to produce synthetic char. Honey mesquite (*Prosopis glandulosa Torr.*) and cordgrass (*Spartina spartinae*) were sampled from Laguna Atascosa National Wildlife Refuge (Rio Hondo, TX, USA) in June, 2005. Loblolly pine (*Pinus taeda*) was collected from Bastrop State Park (Bastrop, TX, USA) in April, 2006. The three species cover a suite of vascular plant tissue and taxonomy: angiosperm/gymnosperm pair (honey mesquite (HM)-cordgrass (CG)/loblolly pine (PI)), woody/non-woody pair (HM-PI/CG), as well as C3/C4 pair (HM-PI/CG). Twigs of HM and PI were collected using a saw or by hand and the CG stem was collected using shears. In the laboratory, the plants were cut into small pieces (HM and PI: 0.5-1.5 cm long; CG: 2 cm long) and oven dried at 60°C for 3 d before charring. To mimic wildfire conditions in the field, we did not remove the bark from HM and PI and combusted the sample whole. Following drying, small blocks of HM and PI, and stem pieces from CG, were placed in individual quartz crucibles and charred in a muffle furnace (Lindberg Hevi-Duty box furnace

Model 51442 with instrument console Model 59344, Asheville, NC, USA). The quartz crucible was capped with a quartz lid to create an oxygen-limited environment during combustion. The raw materials were heated from room temperature to the desired final temperatures (150-1050°C) at 26°C/min and held there for a scheduled period (0.5-5 h). The combustion duration was counted after the temperature stabilized at its maximum. After combustion, the synthetic char samples were allowed to cool down in the furnace overnight without opening the door to prevent the char from being exposed to excess oxygen at high temperature. All samples were ground to a fine powder (< 60 mesh) and stored in glass vials in a desiccator.

In addition to the lab-produced chars mentioned above, we used a series of "standardized" materials containing combustion-derived constituents or known to generate potential interferences during BC analysis (see Table 1 and short description below). Because some of these were the subjects of a recent multi-author, multi-institutions comparative study, we point to Hammes et al. (2007) for a detailed description of these samples and their BC quantification. Two synthetic chars, chestnut wood char and rice straw char, were obtained from M. W. I. Schmidt (University of Zurich, Switzerland). A detailed description of how these synthetic char samples were produced is provided by Hammes et al. (2006). Urea-glucose melanoidin was also obtained from M.W. I. Schmidt. Four coal standards were purchased from Argonne National Laboratory (ANL; Argonne, IL, USA): Pittsburgh bituminous coal, Pocahontas bituminous coal, Blind canyon bituminous coal and Beulah-Zap lignite. The standard reference materials (SRMs) of diesel particulate matter (SRM 2975), bituminous coal (SRM 1632c), New York/New Jersey waterway sediment (SRM 1944), urban dust (SRM 1649a) and air particulate matter on filter media (RM 8785)

were obtained from the U.S. National Institute of Standards and Technology (Gaithersburg, MD, USA). Additional samples include a natural charcoal recovered from a charred pine (Pinus ponderosa) stump in a forested area of the Catalina Mountains (AZ, USA) that burned during a wildfire in 2003. The charred material was collected into a sealable plastic bag, dried in the laboratory at 45°C overnight and homogenized in an agate mortar. Pre-fire and post-fire soils from a controlled burn site in New Mexico (USA) were provided by P. D'Odorico (University of Virginia, VA, USA). The soil samples were air-dried and passed through a 2 mm sieve. Carbon black (from acetylene; average particle size 0.042 μm) was obtained from Alfa Aesar (Ward Hill, MA, USA). Activated charcoal was obtained from Sigma-Aldrich (St. Louis, MO, USA). Lamp black was obtained from Fisher scientific (Fair Lawn, New Jersey, USA). Finally, charred particulate residues were collected from the wall of a residential wood-fired chimney in College Station, TX.

Table 1. Elemental composition and mass loss for honey mesquite, cordgrass and loblolly pine before and after combustion

Plant species	Sample	Combustion temperature (°C)	Combustion duration (hour)	N%	C%	H%	ash%	O%[a]	Mass loss (%)
Honey mesquite	HM raw			1.39	44.7	6.3	5.51	42.1	
	HM 200	200	1	1.29	47.2	6.0	6.14	39.3	8.75
	HM 250	250	1	1.51	52.3	5.7	6.85	33.7	23.7
	HM 300	300	1	1.60	62.1	4.7	9.44	22.2	46.05
	HM 350	350	1	1.70	63.5	4.2	10.02	20.6	54.64
	HM 400	400	1	1.68	64.6	3.5	11.69	18.6	61.68
	HM 450	450	1	1.55	68.1	3.2	13.43	18.2	65.49
	HM 650	650	1	1.47	72.6	1.8	15.62	8.5	71.58
	HM 850	850	1	1.19	75.1	1.1	17.53	5.1	74.82
	HM 1050	1050	1	0.84	74.9	0.7	18.85	4.7	76.59
	HM 250-0.5	250	0.5	1.34	52.7	5.7	6.07	34.1	21.83
	HM 250-3	250	3	1.39	53.6	5.3	5.72	34.0	28.28
	HM 250-5	250	5	1.42	55.3	5.0	5.55	32.7	31.12
Cordgrass	CG raw			0.46	41.0	6.4	8.79	43.3	
	CG 150	150	1	0.60	43.9	5.9	9.82	39.7	6.97
	CG 200	200	1	0.54	46.2	5.8	10.55	36.9	17.7
	CG 250	250	1	0.57	49.3	5.4	12.40	32.4	29.63
	CG 300	300	1	0.71	56.1	4.2	17.05	22.0	50.12
	CG 350	350	1	0.77	55.2	3.5	20.18	20.3	57.01
	CG 400	400	1	0.75	55.1	3.1	22.98	18.2	63.71
	CG 550	550	1	0.66	54.1	2.2	30.29	12.8	72.21
Loblolly pine	PI raw			0.19	45.9	6.5	1.34	46.1	
	PI 200	200	1	0.27	51.8	6.2	2.06	39.6	6.28
	PI 250	250	1	0.29	55.7	5.8	1.86	36.3	16.88
	PI 300	300	1	0.30	63.8	5.2	2.35	28.3	39.12
	PI 350	350	1	0.40	68.3	4.3	3.42	23.6	55.72

[a] Calculated by difference.

2.2.2. Levoglucosan analysis

All samples were spiked with the internal standard sedoheptulosan (Sigma, MO, USA; Simpson et al., 2004) and extracted via pressurized fluid extraction (PFE) with an accelerated solvent extractor (Dionex ASE 200) using a mixture of CH_2Cl_2 and MeOH (9/1 (v/v)) at 10.3 MPa and 100°C. The extracts were concentrated using a heating mantle with a modified Kuderna-Danish apparatus and dried under a gentle stream of N_2. Samples were redissolved in 500 μL pyridine (absolute, ≥ 99.8%, Fluka, Switzerland). An aliquot (100 μL) was transferred to a glass vial to which 100 μL of *N,O*-bis(trimethylsilyl)trifluoroacetamide (BSTFA) containing 1% trimethylchlorosilane (TMCS; Supelco, PA, USA) was added. The sample was derivatized by heating at 78°C for 1 h in a heating block. After derivatization, 50 μL triisopropylbenzene (Aldrich, MO, USA; Simpson et al., 2004) was added as GC-internal standard.

For gas chromatography-mass spectrometry (GC/MS) we initially used a system (6890N-5973), whose mass selective detector (MSD) was operated at 70 eV in selective ion monitoring (SIM) mode. A DB5-MS capillary column (J&W Inc., 30 m x 0.25 mm i.d., 0.25 μm thickness) was used, with the GC oven temperature programmed from 65°C (2 min) to 300°C (5 min) at 6°C/min. The injector temperature was 270°C and He was used as carrier gas. Data were acquired and processed with the Agilent Chemstation software. During a second phase of testing with low concentration samples (RM 8785), we used a Varian GC/MS-MS system (Varian 3800/4000), with the spectrometer at 70 eV in full scan mode. A VF-5MS ultra-low bleed capillary column (Varian Inc., 60 m length x 0.25 mm i.d., 0.25 μm thickness) was used with the same GC oven and injector temperature programs described above. Data were acquired and processed with the Varian MS Workstation software (version

6.6). Comparative analyses of reference material SRM 1649a on both systems produced similar results ($p > 0.05$).

Positive identification of levoglucosan was performed using retention time and by comparing the relative abundance of quantification/confirmation ions from each sample to those produced by authentic standards (levoglucosan, 99%, Aldrich, St. Louis, MO, USA). The linear response curves ($r^2 = 0.999$) were created from two sets of five point calibration standards with levoglucosan concentration ranging from 0.1-2.0 and 0.1-20 ng/μL. The detection limit was 0.016 ng/μL, equivalent to 20 ng levoglucosan in a sample. The minimum amount reported for any sample was at least 5 times above the limit.

2.2.3. Acid dichromate oxidation

The acid dichromate oxidation approach (Wolbach and Anders, 1989, Bird and Gröcke, 1997, Masiello et al., 2002) was used to determine the different carbon fractions and the BC content of our experimental chars. The methodology was modified from Bird and Gröcke (1997) and Masiello et al. (2002). Briefly, 100 mg char was weighed and transferred to a 42 mL centrifuge tube (Nalgene PPCO Oak Ridge tube with polypropylene screw closure) to which 30 mL 0.25 M $K_2Cr_2O_7$ in 2 M H_2SO_4 were added to oxidize the sample at room temperature. If the solution began to discolor, the tube was centrifuged and the supernatant removed using a glass pipette. Fresh dichromate solution was added for the reaction to continue. During the reaction, the tubes were periodically uncapped to release evolved gas and the contents were re-mixed using a vortex mixer. Oxidation was performed over periods ranging from 0.5 to 1200 h. At the end of the designed oxidation time, samples were centrifuged and rinsed with nano-pure water (x 4) to remove residual oxidation reagent. The oxidized samples were then freeze dried for further analysis.

All glasswares were heated for four h at 450°C to remove organic matter before use. All solutions were prepared by using nano-pure water (Diamond UV ultrapure water system, Branstead International, Iowa, USA). Statistical analysis was performed with SPSS software (SPSS Inc., Chicago, IL, USA).

2.2.4. Elemental analysis and ash content

C and N contents were determined with a Vario EL *III* elemental analyzer (Elementar Americas, Inc., Mt. Laurel, NJ, USA). The temperature of the combustion reactor was set at 1150°C. Quantification was performed using sulfanilic acid (Merck KgaA, Germany) as calibration standard. For soil and sediment samples, the acid vapor acidification method was used to remove inorganic carbon before elemental analysis (Hedges and Stern, 1984; Harris et al., 2001). Char samples were also analyzed for H content at the UC-Davis Stable Isotope Facility (Davis, CA, USA). Atomic C/N and H/C ratios were calculated from the measured C, H and N contents. Oxygen content was calculated by difference. Atomic O/C ratio values were calculated using this oxygen estimate. Ash content was determined using the modified ASTM 1102-84 method (ASTM, 2000).

2.2.5. Hemicellulose/cellulose analysis

Three plants were sent to the Soil, Water and Forage Testing Laboratory in Texas A&M University for neutral detergent fiber (NDF), acid detergent fiber (ADF) and acid detergent lignin (ADL) analyses. Hemicellulose content was calculated from the difference between ADF and NDF contents, while cellulose content was determined by subtracting ADL from ADF (Van Soest and Robertson, 1980). All values were corrected for ash content.

2.3. Results and discussion

2.3.1. Characterization of synthetic chars

The elemental composition and mass loss during pyrolysis of all synthetic chars and their precursor plant materials are presented in Table 1. Similar mass loss percentages were found for synthetic chars of the three plant types at each combustion temperature. These values are all consistent with reported ranges in mass loss during charring of plant materials (Baldock and Smernik, 2002; Braadbaart et al., 2004). The plant chars experienced the most dramatic mass loss between 200 and 300°C. These results are relatively similar to the temperature range (220 to 270°C) reported by Braadbaart et al. (2004) during the combustion of peas in an O_2-free environment. With increasing combustion temperature, the C content increased, while that of H and O decreased. The N content increased initially but then decreased in materials combusted at temperatures > 350°C. N preservation in combustion products formed at relatively low temperature was also documented by Baldock and Smernik (2002), Almendros et al. (2003), Knicker et al. (2005), and Hammes et al. (2006).

Insight into the changes in char composition and possible reactions induced by pyrolysis was inferred from a van Krevelen diagram (Figure 3) with atomic H/C and O/C ratios (Baldock and Smernik, 2002; Braadbaart et al., 2004; Hammes et al., 2006). Char from the three plants have very similar patterns, indicating two major reaction pathways. The first occurs at ≤ 250°C and is dominated by dehydration, resulting in a loss of H approximately twice that of O. The rapid loss of H > 300°C indicates that aromatization occurs. At temperatures > 650°C, aromatization results in highly condensed aromatic structure materials which plot close to typical soot BC such as hexane soot and diesel soot (Baldock and Smernik, 2002; Braadbaart et al., 2004; Nguyen et al., 2004). The combustion temperature

for the transition from dehydration-dominated to aromatization-dominated pathways appears to be between 250 and 300°C, consistent with a transition temperature of 270°C suggested by Braadbaart et al. (2004). However, the results are different from those reported by Baldock and Smernik (2002) for the combustion of red pine (*Pinus resinosa*). The difference is probably due to a longer and variable heating time (24-72 h) in their experiment, which would result in further alteration in atomic H/C and O/C ratios.

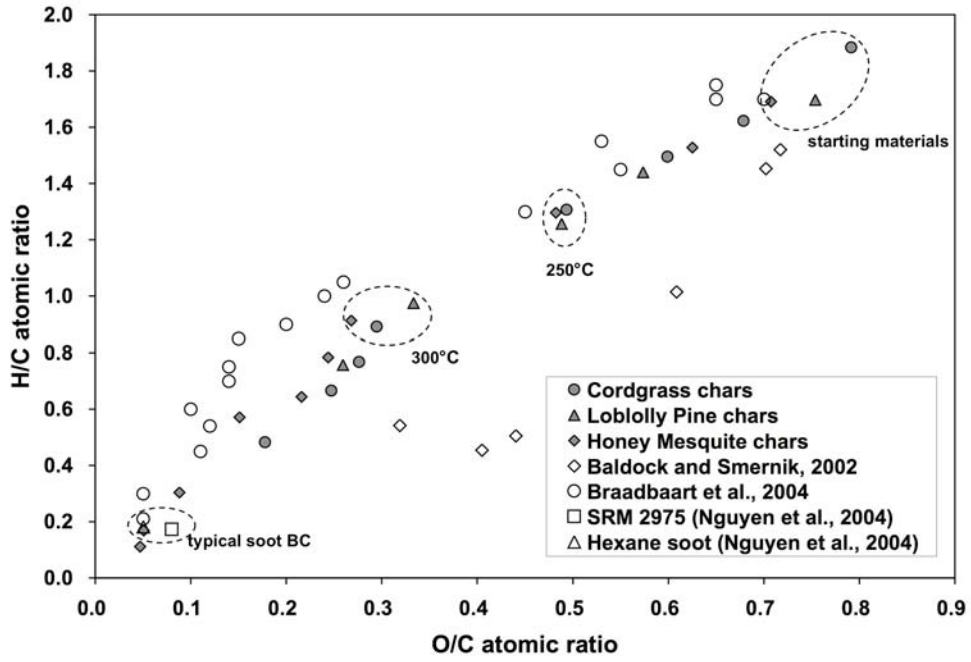

Figure 3. Van Krevelen plot for synthetic chars (including literature data).

2.3.2. Levoglucosan analysis

2.3.2.1. Environmental samples

Levoglucosan levels of a number of environmental materials are shown in Table 2. As expected, the soot residue from diesel combustion (SRM 2975) did not yield any measurable amount of levoglucosan, nor did any of the coal samples (ANL coals and SRM 1632c).

Similarly, no detectable level was observed for melanoidin, a common product of Maillard reaction of amino acids and carbohydrates, which is recognized as a potentially interfering material during BC determination (Schmidt et al., 2001; Hammes et al., 2007). Since carbon black and lampblack are not derived from combustion of biomass precursors, none of these samples yielded any levoglucosan on solvent extraction. It was more surprising, however, that an urban estuarine sediment (SRM 1944), close to sources of combustion, and an activated carbon, derived from the pyrolysis of biomass precursor, did not produce any traces. Similarly, no levoglucosan was produced from a synthetic charcoal sample prepared from chestnut wood under controlled laboratory conditions (450°C, 5 h; Hammes et al., 2006). In comparison, a "companion" charcoal produced from rice straw under the same conditions (Hammes et al., 2006) did produce a significant and reproducible levoglucosan content of 14.7 ± 0.8 μg/g. The analysis of a natural charcoal sample, recovered from a pine stump (*Pinus ponderosa*) after a major wildfire on Mount Lemmon (AZ) in 2003, produced close to 4-5 times more levoglucosan but with greater variability (69.4 ± 12.5 μg/g) than the synthetic rice straw char. Soil samples collected prior to, and subsequent to, a control burn in New Mexico show a distinct change in levoglucosan yield, with a ~ 50 fold increase in the post-fire soil concentration (38.0 ± 11.7 μg/g) with respect to pre-fire conditions (0.85 ± 0.01 μg/g). Three samples showed exceptionally high levoglucosan values. The bulk urban dust NIST standard (SRM 1649a) and its ultra-fine particulate matter isolated on a quartz fiber filter (RM 8785) yielded twice as much levoglucosan (163.9 ± 11.8 and 158.4 ±8.8 μg/g, respectively) than the natural pine charcoal. Finally, particulate black residues recovered from a wood-fired chimney yielded values (26.9 mg/g) of the same order of magnitude as

those measured for fire-derived aerosols (11.6 mg/g) collected in South Texas following massive regional wildfires in Central America (Fraser and Lakshmanan, 2000).

Table 2. Levoglucosan concentration in different environmental materials

Material	Description	Levoglucosan (μg/g)	*n*
SRM 2975	Diesel particulate matter	B.D.L.[b]	2
ANL[a] Coals	Pittsburgh bituminous coal, Pocahontas bituminous coal, Blind canyon bituminous coal, and Beulah-Zap lignite	B.D.L.	2[c]
SRM 1632c	Bituminous coal	B.D.L.	3
Melanoidin	Urea-glucose melanoidin	B.D.L.	1
Carbon black	Acetylene black	B.D.L.	2
Lampblack	Crude oil combustion residue	B.D.L.	2
SRM 1944	NY/NJ water way sediment	B.D.L.	2
Activated Carbon	Commercial product from plant combustion	B.D.L.	2
Char-BC 1	Chestnut wood char	B.D.L.	2
Char-BC 2	Rice straw char	14.7±0.8	2
Natural Charcoal	Pine wood char	69.4±12.5	2
Pre-fire soil	Surface soils from controlled burning site in New Mexico (US)	0.85±0.01	2
Post-fire soil		38.0±11.7	2
SRM 1649a	Urban dust	163.9±11.8	11
RM 8785	Air particulate matter (PM2.5) on filter media	158.4±8.8	2
Chimney soot	Chimney residues from Texas (US) private residence	26888.1	1

[a] Argonne National Laboratory (ANL).
[b] Below detection limit (B.D.L.).
[c] n=2 for each coal standard.

These data confirm that levoglucosan occurs exclusively in biomass combustion residues and is absent from petroleum combustion byproducts or coal materials. The abundant presences of this molecular marker in natural charcoal and solid residues from a wood-fired chimney, as well as its combined occurrence with chars in post-fire soils, demonstrate that this compound can trace inputs of biomass combustion to environmental media.

In addition, the levoglucosan yields for SRM 1649a and RM 8785 are similar to values reported recently by Larsen et al. (2006) for a freezer-stored sample of SRM 1649a (162 ± 8 μg/g) and three filter replicates of RM 8785 (163 ± 37 μg/g). The results suggest that levoglucosan can be reproducibly extracted from particulate phase materials under different laboratory conditions and so point to the potential comparative nature of such results. Moreover, the similar levoglucosan concentration observed for these two reference materials, under different experimental protocols and instrumentation, show that levoglucosan is homogeneously distributed in this urban dust sample and associated with ultrafine particulates (mean diameter from volume distribution in SRM 1649a is 34.6 ± 0.4 μm whereas the RM 8785 consists entirely of the fine fraction ≤ 2.5 μm). The comparative nature of these interlaboratory data points to the potential for SRM 1649a to serve as a working standard for levoglucosan analysis. One discrepancy exists, however, in the study by Larsen et al. (2006), which reported an anomalously low value for a sample of SRM 1649a stored at room temperature for 25 years (81.1 ± 9.4 μg/g). To explain this discrepancy, the authors hypothesized that levoglucosan may be unstable in solid samples over long periods. Since levoglucosan has been shown to resist both photochemical oxidation and acid catalyzed hydrolysis in atmospheric aerosols (Locke, 1988; Fraser and Lakshmanan, 2000), as well as diagenesis during long term preservation in sedimentary deposits spanning over 7000 years (Elias et al., 2001), we believe that the twofold difference between the cluster of SRM replicates and the anomalous value may instead be due to the compromised nature of this specific SRM or to a quantification artifact.

2.3.2.2. Chars made under different combustion conditions

The wide range of levoglucosan concentrations measured in biomass combustion products (Table 2) suggests that the yields from environmental media are not simply proportional to the quantity of combustion residue. We thus tested the impact of combustion conditions and carbon source on yield. Figure 4 presents the organic carbon-normalized levoglucosan levels in synthetic chars made at different temperatures. Interestingly, chars from the three plants all show similar patterns in levoglucosan distribution as a function of temperature, despite significant differences in yield across plant species. For the series, the levoglucosan concentration peaks at 250°C (1800.4 μg/goc, 1542.3 μg/goc, and 521.5 μg/goc for CG, PI, and HM, respectively) and becomes virtually undetectable > 350°C. The CG chars generally gave the highest levoglucosan level, except at 300°C where PI showed the highest value. Our observation of peak levoglucosan production at 250°C matches recent observations by Dickens et al. (2007) who showed similar temperature maxima in the yield of a suite of benzene carboxylic acids extracted from laboratory charcoal samples produced from pine wood at 70, 150, 200, 250, 300 and 350°C. These parallel observations suggest that similar processes are responsible for the production of slightly altered combustion byproducts during the incineration of plant matter.

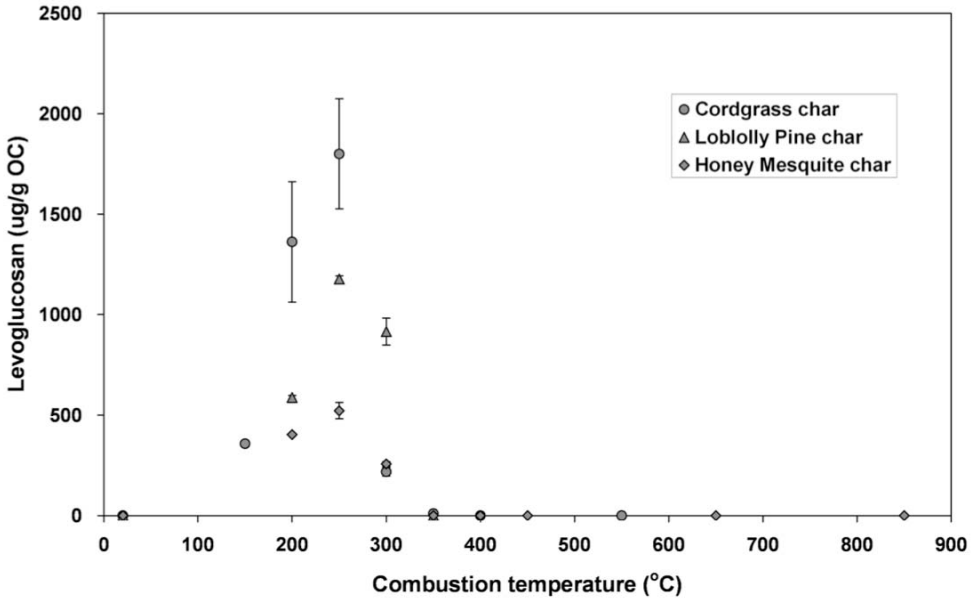

Figure 4. Levoglucosan yield for synthetic chars from three different plant species under different combustion temperatures.

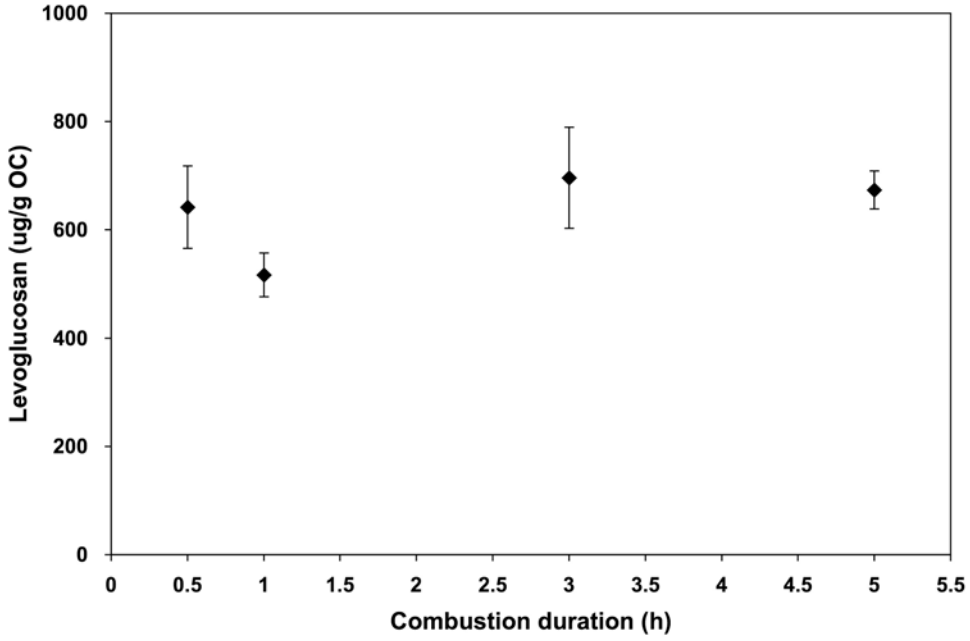

Figure 5. Effect of combustion duration on levoglucosan yield of honey mesquite char combusted at 250°C.

Because temperature duration at a constant temperature was shown to alter the elemental composition of chars (Table 1), we also investigated the potential change in levoglucosan yield under four combustion durations for one char sample (HM at 0.5, 1, 3 and 5 h). As shown in Figure 5, there was no significant impact on concentration.

Pastorova and coworkers (1993) conducted a series of analyses for the characterization of charred microcrystalline cellulose under combustion temperatures ranging from 190 to 390°C. Their study showed that a significant proportion of D-glucose oligosaccharides could be preserved in up to 270°C, followed by a dramatic drop in concentration at higher combustion temperatures. They therefore suggested that, at 270°C, a new thermostable and condensed phase started to dominate the char composition and replace the transglycosylation pathway responsible for levoglucosan formation. The observed yields under different combustion temperatures in the present study are consistent with these proposed mechanisms. Furthermore, Hosoya et al. (2006) reported that thermal degradation of levoglucosan can be substantially suppressed in the presence of some aromatic substances due to interaction among them. Hence the combination of levoglucosan with certain aromatic compounds could maintain its thermal stability at up to 340°C, in contrast to a rapid decomposition at temperatures as low as 240°C when it is heated in isolation. Interestingly, the aromatic nature of lignin structural units found in all vascular plant tissues could potentially stabilize levoglucosan during combustion (Hosoya et al., 2006). Our results add strength to this hypothesis. As shown in Fig. 2, the yield for CG char decreases markedly from 250 to 300°C relative to the change observed for HM and PI chars. Unlike the woody tissue of HM and PI, the CG sample is derived from soft tissue recognized for lower lignin content (Table 3), potentially providing fewer stabilization sites for levoglucosan

preservation. The upper limit (350°C) of levoglucosan occurrence for our synthetic chars is thus consistent with the literature. In the light of these observations, the significant levoglucosan concentration (17.7 ± 0.8 μg/g) measured for rice straw char produced under controlled conditions at 450°C (Hammes et al., 2006), is initially surprising. Hammes et al. (2007) showed that this same charcoal sample yielded more soot BC than the wood charcoal (chestnut) under the same conditions. They suggested that occluded organic matter within phytoliths (silica structures abundant in some grasses) may have been responsible for most of the organic carbon measured as BC in the rice straw char. Since the occluded OC in phytoliths is composed predominantly of carbohydrate (mostly crystalline cellulose; Krull et al., 2003), the apparent resistance of levoglucosan to temperature in the rice straw char may thus be a function of a mineral protection effect and does not contradict the earlier statement that levoglucosan yield for chars is substantial only at combustion temperatures < 400°C.

We also tested the possibility that the highly variable levoglucosan yields across plant species could be "normalized" to the contents of levoglucosan precursor (hemicellulose/cellulose). Roughly estimated hemicellulose, cellulose, and holocellulose contents of HM, CG, and PI via wet chemical method (Table 3) were applied in this correction attempt. However, results showed that cellulose and holocellulose normalizations could not correct for the large differences among chars of different origin, whereas hemicellulose normalization does provide some corrections but only for the two angiosperm plant tissues (CG and HM) (Figure 6).

Table 3. Hemicellulose, cellulose and lignin contents of honey mesquite, cordgrass and loblolly pine

Plant species	Hemicellulose (%)	Cellulose (%)	Holocellulose[a] (%)	Lignin (%)
Honey mesquite (*Prosopis glandulosa* Torr.)	11.5	54.1	65.6	11.5
Cordgrass (*Spartina spartinae*)	31.7	41.7	73.4	4.2
Loblolly pine (*Pinus taeda*)	10.4	56.4	66.8	15.0

[a] Holocellulose = hemicellulose + cellulose.

(a)

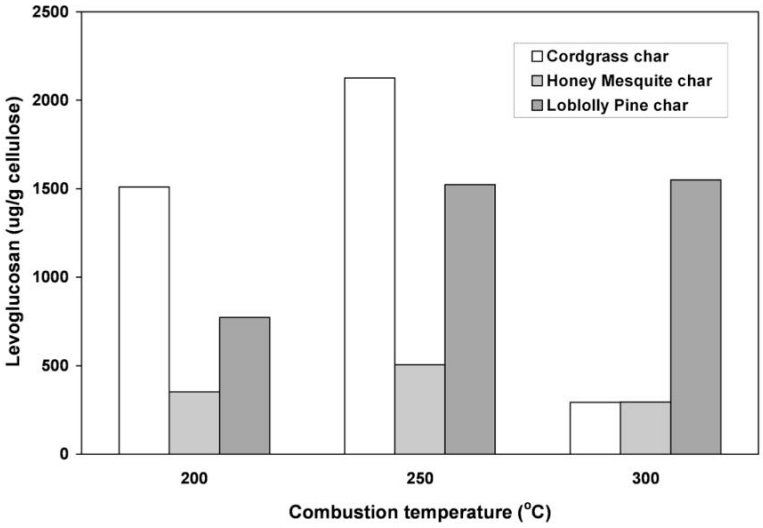

(b)

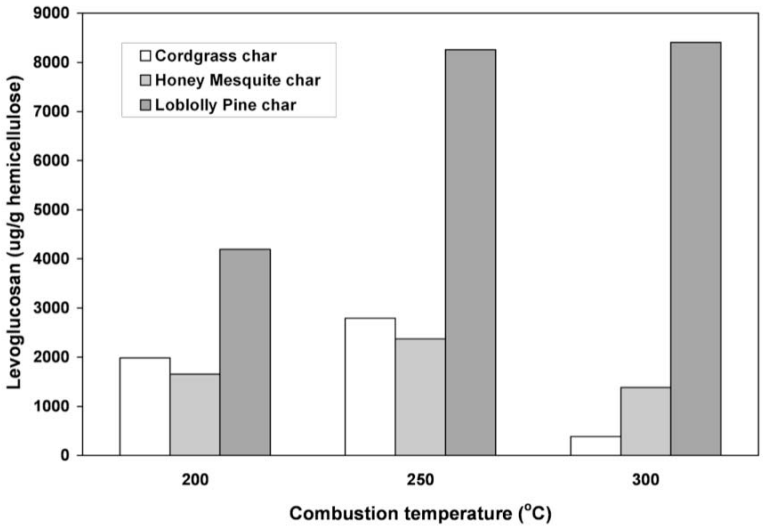

Figure 6. Normalized levoglucosan yields of chars for (a) cellulose and (b) hemicellulose from three different plant species.

The failure to fully normalize the levoglucosan yield for char from different plants highlights the inherent complexity in biomass pyrolysis and the levoglucosan formation mechanism. Several studies have indicated that trace amount of inorganic salts containing alkali or alkaline cations could lead to significant decreases in char yield and levoglucosan formation (Antal and Varhegyi, 1995; Müller-Hagedorn et al., 2003). Piskorz et al. (1989) suggested that highly polar and small alkaline cations could retard the chain reaction leading to the formation of levoglucosan from cellulose through interaction with the terminal chain end of cellulose. This also brings out the competitive nature of several parallel pathways observed during cellulose pyrolysis (Piskorz et al., 1989; Boon et al., 1994; Antal and Varhegyi, 1995). In the study by Boon and co-workers (1994), three major pathways of cellulose dissociation (transglycosylation, cycloreversion and E_i-elimination) were proposed, showing that plant composition, presence of inorganic salts, and combustion conditions influence which pathway might predominate during combustion. This variability in combustion mechanisms may thus explain the level of variability in levoglucosan yield observed across a diverse suite of plant taxonomic groups and tissue types. For example, when the transglycosylation pathway is favoured, levoglucosan would form and accumulate preferentially in the combustion products.

The poor normalization potential also demonstrates that levoglucosan is not a proper quantitative marker for char-BC in environmental matrices such as soils and sediments. Char-BC in these systems is often produced under diverse combustion conditions and plant sources, with potentially large variability in levoglucosan yield. The large-scale fluctuation in levoglucosan yield over a limited temperature range (150-350°C), as well as the large differences across plant species, provides a reasonable explanation for the reported variations

in levoglucosan value among the different biomass combustion products listed in Table 2. For instance, despite its biomass origin, activated charcoal would not be expected to yield any levoglucosan, as a result of the high temperature of formation. In contrast, the inefficient combustion typical of a residential stove results in production of particulate residue enriched in levoglucosan. Similarly, the abundance of levoglucosan in the natural pine char and the post-fire soil imply a relatively low combustion temperature in the field (Scott, 1989). Coupled with the lack of levoglucosan from other materials not derived from biomass burning, our results confirm that levoglucosan could serve as an exclusive marker for a limited set of chars produced under low combustion temperature conditions.

2.3.3. Acid dichromate oxidation of synthetic char

The acid dichromate oxidation method has been widely used for BC quantification in diverse environmental settings (Masiello and Druffel, 1998; Masiello et al., 2002; Rumpel et al., 2006). It was initially developed by Wolbach and Anders (1989) to separate kerogen from elemental carbon, including soot and charcoal, in sedimentary rocks for the purpose of studying historical global fire events over long temporal scales. The method was also applied to quantify the flux of BC to marine sediments (Masiello and Druffel, 1998), as well as assess the impact of slash and burn agriculture on soil erosion and BC carbon export (Rumpel et al., 2006). The major drawback of this chemical oxidation method is that it is very time consuming and rate-dependent, so is influenced by empirical conditions. Its advantages, on the other hand, include the capacity for isotopic monitoring of BC residues and a relatively wide analytical window. There are many modified versions of the method, with varying level of efficiency (Lim and Cachier, 1996; Bird and Gröcke, 1997; Masiello et al., 2002). We adopted the experimental conditions proposed by Masiello et al. (2002) for

comparative purposes of BC half life. This experimental condition has been demonstrated to be as effective as that presented in Wolbach and Anders (1989).

Four synthetic chars, HM 250, HM 350, HM 850 and CG 350, were selected to evaluate the performance of the acid dichromate oxidation method for the quantification of BC in levoglucosan-bearing chars and chars from different sources as well as combustion temperature. The oxidation experiment for each synthetic char was conducted in duplicate. As shown in Figure 7, different chars exhibited very different OC loss curves. HM 250 decayed very quickly and was eliminated at 96 h. In contrast, HM 850 was refractory. Both HM 350 and CG 350 showed intermediate oxidation behaviour. Apparent differences among HM 250, HM 350 and HM 850 show the effect of combustion temperature on the resistance of char-BC. The difference between HM 350 and CG 350 reflects difference in BC resistivity across chars from different plant species. The increased proportion of lignin in woody tissue (HM) may explain this latter difference, as suggested by Bird and Gröcke (1997). Mass-based data showed similar trends to the organic carbon-based data.

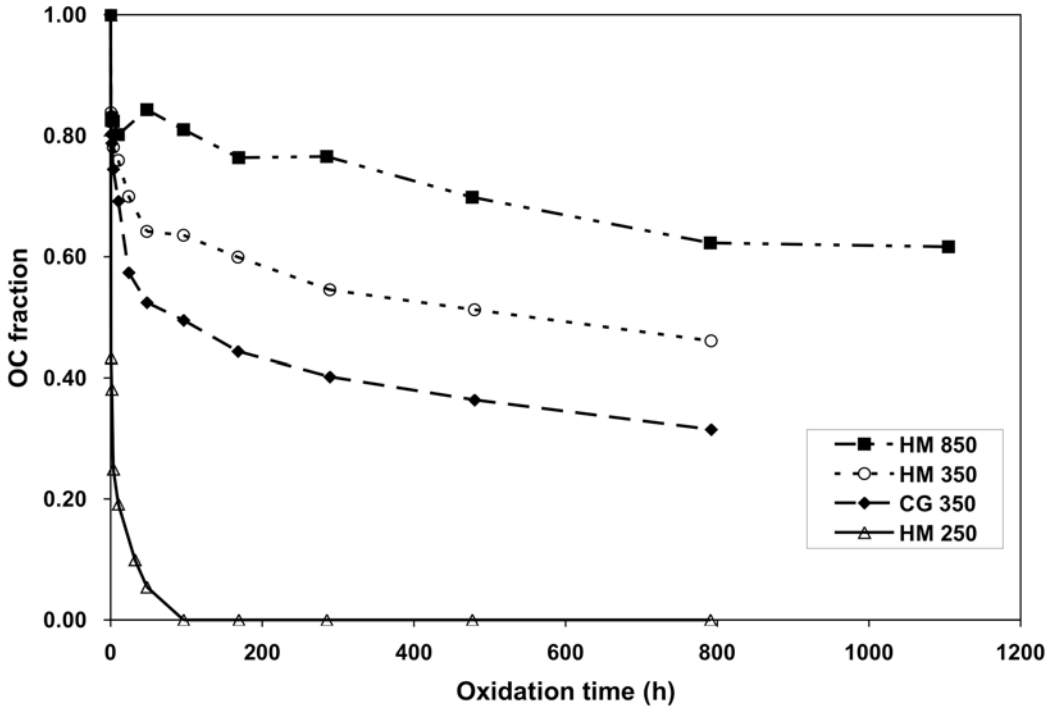

Figure 7. Average organic carbon (OC) remaining for honey mesquite chars HM 850, 350, 250 and cordgrass char CG 350 after acid dichromate oxidation.

We also used multiple component nonlinear regression to model the decay curves of each oxidation treatment according to the method developed by Wolbach and Anders (1989) and Masiello et al. (2002). For HM 250, HM 350 and CG 350, a three term exponential regression equation provided a good fit to the mass-based experimental data (r^2 = 0.992-0.998 for HM 250, 350 and CG 350). The equation is

$$N = N_1 e^{-k_1 t} + N_2 e^{-k_2 t} + N_3 e^{-k_3 t} \qquad \text{(eq. 1)}$$

where N is the mass or OC left at time t; N_1, N_2 and N_3 denote the mass or OC of components 1, 2 and 3 in the original material, respectively; k_1, k_2, k_3 are decay rate constants of components 1, 2, 3, respectively. The three-term equation suggests that these chars are a mixture of three components each characterized by a short, medium, and long half life ($t_{1/2}$; Table 4). In contrast, the decay curve for HM 850 was best fitted by a single term exponential regression, implying that this material is dominated by one component characterized by a long $t_{1/2}$, which is within the range of commercial activated charcoal or soot materials, the common representatives of highly refractory components in the BC continuum in literature (Wolbach and Anders, 1989; Masiello et al., 2002) (Table 4). In addition, the HM 350 and CG 350 chars also showed a substantial proportion of refractory constituents (about 64% and 46%, respectively) with comparable long $t_{1/2}$, no matter in OC- or mass-based data.

Table 4. Half-lives ($t_{1/2}$) and fractions (%) of short, medium and long lived components of synthetic chars in acid dichromate oxidation experiments (values of $t_{1/2}$ and fraction were calculated from a multiple-component nonlinear regression based on mass and organic carbon (OC) data)

Material	Combustion temperature (°C)	Short-life fraction (%)	$t_{1/2}$ short (h)	Medium-life fraction (%)	$t_{1/2}$ med. (h)	Long-life fraction (%)	$t_{1/2}$ long (h)	Reference
HM 250[a.]	250	37 ± 7	0.05 ± 0.03	35 ± 4	1.99 ± 1.28	28.0 ± 2.8	23.1 ±0.0	This study
HM 350[a.]	350	19 ± 1	0.13 ± 0.01	17 ± 0	12.71 ± 1.63	64.5 ± 0.7	1576.2 ± 50.7	This study
HM 850[a.]	850	-	-	-	-	87.5 ± 0.7	3500.7 ± 495.1	This study
CG 350[a.]	350	26 ± 1	0.16 ± 0.02	28 ± 1	13.86 ± 0.00	46.0 ± 1.4	1083.3 ± 23.9	This study
Charcoal briquette[a, c]	unknown	-	-	-	-	62	860	R1[e]
Coconut activated charcoal[a, c]	unknown	-	-	-	-	81	2000	R1[e]
Carbon black[a, d]	unknown	-	-	-	-	101	900	R1[e]
Bone Black (activated)[a, c]	unknown	-	-	-	-	63	910	R1[e]
Norite® activated carbon[a, c]	unknown	-	-	-	-	60	810	R1[e]
HM 250[b]	250	65.0 ± 2.8	0.18 ± 0.04	35.0 ± 2.8	14.04 ± 1.18	-	-	This study
HM 350[b]	350	17.0 ± 1.4	0.13 ± 0.01	19 ± 0	14.37 ± 1.47	64.5 ± 0.7	1541.1 ± 48.4	This study
HM 850[b]	850	-	-	-	-	84.5 ± 0.7	2089.6 ± 675.5	This study
CG 350[b]	350	20.0 ± 1.4	0.09 ± 0.04	30 ± 0	13.96 ± 1.80	50.0 ± 1.4	1083.3 ± 23.9	This study
Coconut charcoal[b]	unknown	-	-	-	-	100 ± 10	637 ± 66	R2[e]
Lampblack soot[b]	unknown	-	-	-	-	101 ± 2	4000	R2[e]

[a] Mass-based data.
[b] OC-based data.
[c] Data of long-life fraction were % mass left after being oxidized in acid-dichromate reagent for 600 hours.
[d] Calculated from the raw data in Wolbach and Anders (1989).
[e] R1=Wolbach and Anders, 1989; R2= Masiello et al., 2002.

The characteristics of the HM250 char sample showed, on the other hand, the largest departure from those of other materials (Table 4). For the mass-based data, even though it was also comprised of three components, the $t_{1/2}$ of its most refractory fraction was only 23 hours, closer to the medium-life fraction for the other chars. For the OC-based data, HM 250 was best fitted with a two-term regression and did not contain the longer half life fraction (Table 4). This indicates that, under the definition of the acid dichromate oxidation method, HM 250 does not contain any highly resistant fraction, i.e. the so-called BC fraction. Because it is the char with the highest levoglucosan yield in the HM series, our results show a lack of overlap between the maxima in the analytical windows for levoglucosan and acid dichromate oxidation. Some overlap exists, however, at the high end of the levoglucosan analytical window (350°C) because parts of HM 350 and CG 350 were defined as BC with the oxidation method. This observation is consistent with the findings of Boon et al. (1994), who showed that an acid resistant and thermally stable fraction will dominate the char at combustion temperatures > 350°C.

2.3.4. The role and applications of the levoglucosan approach in BC studies

As mentioned in the Introduction, BC is a continuum of combustion products originating from different materials and combustion conditions. The lack of clear demarcation lines between combustion products makes it nearly impossible to detect the entire range of BC with a universal method. Masiello (2004) proposed a black carbon method continuum encompassing most of the available BC analytical methods and their possible analytical windows in the BC continuum. This BC method continuum well describes the distinct detectable regions of different methods and demonstrates the difficulty that arises when one seeks to compare BC values produced by two methods with different

analytical windows. In the present study, using systematically produced synthetic chars, we compared the levoglucosan approach to the acid dichromate oxidation approach for the analysis of chars, the broadest and least defined portion of the BC continuum. As shown in Figure 8, we created a simplified BC method continuum diagram for method comparison. With the aid of atomic H/C ratio, the chemothermal oxidation technique (often abbreviated as CTO-375; Gustafsson et al., 2001; Hammes et al., 2007), another popular BC method, is included in this comparison. Based on the low temperature range of chars containing levoglucosan (150-350°C), the analytical window for this molecular marker is located at the low end of the BC continuum, whose upper limit is defined by an atomic H/C ratio of 0.8, the value of both HM 350 and CG 350. The acid dichromate oxidation method could detect BC fractions that include chars and soot. Its lower limit might be located between atomic H/C ratios of 1.3 (adopted from the value of HM 250) and 0.8 (adopted from the value of HM 350). In contrast, CTO-375 is more of a soot-specific method (Hammes et al., 2007). In the literature, two char reference materials (chestnut wood char and rice straw char), both with an atomic H/C ratio of 0.7 (Hammes et al., 2006), have been found to yield no or only very low CTO-375 BC (abbreviated as BC-CTO) (Elmquist et al., 2006; Hammes et al., 2007). This confirmed the work of Nguyen et al. (2004) who only observed measurable BC-CTO in synthetic chars produced at very high temperature (~ 1000°C) and with atomic H/C values ranging 0.08 to 0.14. Quénéa et al. (2006) further demonstrated that char/charcoals are eliminated from soil samples by the CTO-375 treatment. Considering that the atomic H/C values of the recognized BC-CTO are ≤ 0.2 (Nguyen et al., 2004; Hammes et al., 2007), we thus defined the lower limit of the CTO-375 analytical window at an atomic H/C ratio of 0.2, the value for oxidized hexane soot (Nguyen et al., 2004). It should be kept in mind that this

definition is relatively arbitrary since there are many factors controlling the pyrolysis results that may alter the specific analytical window of each BC method. For example, the survivability of BC under CTO-375 is also related to the microporosity of the sample and the presence of mineral oxides (Elmquist et al., 2006). Chars made under different combustion temperature ramp rates may reach slightly different atomic H/C values despite similar final temperatures (Nguyen et al., 2004). All of these may result in the slight differences in the proposed analytical ranges of CTO-375 and acid dichromate oxidation method between Hammes et al. (2007) and our conceptual diagram, which is primary based on our experimental data. Although the atomic H/C ratio may not be a perfect criterion for defining limits of BC ranges, it nevertheless provides a useful basis for method comparison. For example, because the acid dichromate oxidation method produced virtually no resistant BC from low temperature chars (i.e. HM 250), the lower limit of the analytical window of this BC method overlaps only slightly with the levoglucosan analytical window. At its upper limit, the acid dichromate oxidation does produce some overlap with the CTO-375 method.

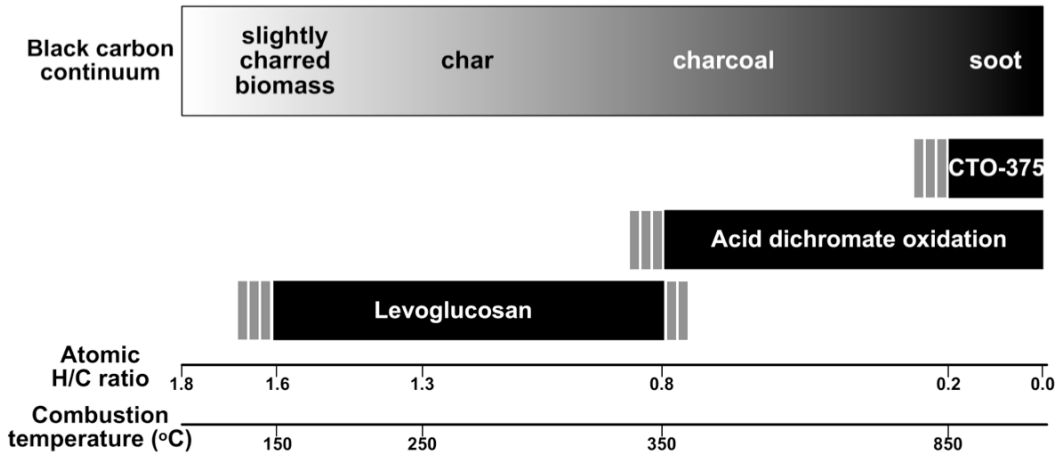

Figure 8. Conceptual diagram of black carbon method continuum showing the analytical windows of levoglucosan, acid dichromate oxidation and chemo-thermal oxidation (CTO-375) based on the observations in this study and literature data. The black bar for each method represents its positive analytical window; while the gray split bars indicate the uncertainty in the method. Values of atomic H/C ratio and corresponding combustion temperature are based on the experimental results in Table 1. The diagram was inspired by Hammes et al. (2007).

The proposed simplified BC method continuum highlights the significance of the molecular marker levoglucsoan in BC research. The levoglucosan-bearing chars were all produced at low temperature (≤ 350°C) and feature a lower aromaticity and thermal resistance, with a higher chemical reactivity. These characteristics make them less amenable to detection with most BC methods. To our knowledge, with the exception of microscopy, there is no other BC method that selectively detects low temperature chars. The relative ease of use and specific analytical window makes the levoglucosan approach a unique addition to the BC method continuum. In addition, the relatively good relationship observed between charcoal particles and levoglucosan in sedimentary archives (Elias et al., 2001) suggests that levoglucosan is a good proxy for paleofire reconstruction and that a substantial portion of the preserved charcoal particles were produced at relatively low temperatures.

Our results also address the concern about the "missing black carbon" conundrum (Druffel, 2004; Masiello, 2004; Schmidt, 2004). Indeed, BC production estimates from biomass burning and fossil fuel combustion exceed the accountable inventories in soils and sediments and loss rates from their standing stocks (Masiello, 2004; Schmidt, 2004). Efforts to reconcile this unbalance are still ongoing but suggest that a combination of processes such as an uncharacterized reactivity in soils, the sequestration in yet poorly quantified reservoirs (i.e. dissolved organic matter in the ocean), and methodological artifacts are standing in our way to a better understanding of the BC cycle in the environment (Druffel, 2004). For example, proposed mechanisms to explain BC losses from soils and sediments include consumption by subsequent fires, slow chemical oxidation and solubilization, biological degradation, as well as the vertical and lateral transports out of these reservoirs (Preston and Schmidt, 2006). The present study highlights two issues faced by BC research: 1. An important portion of the BC continuum is not detected by commonly applied BC methods. 2. This undetected portion of the BC continuum is characterized by a shorter half life as a result of its higher reactivity. Table 2 shows that many natural charcoals and post-fire soils yield substantial amounts of levoglucosan, pointing to potentially low combustion temperatures in the field, an observation that confirms relatively low temperatures measured during controlled burns of savannah in the southeast U.S.A. (Alexis et al., 2007). Therefore, although a significant amount of low temperature char should be found on the ground following wildfires, it is often "missing" in most BC investigations, partly because the applied method could not detect it, or because it is prone to degradation.

2.4. Conclusions

Levoglucsoan is exclusively formed from hemicellulose/cellulose combustion and not found in fossil fuel combustion products. Being a promising vegetation combustion molecular marker, its yield is still affected by several factors. In the present study, combustion temperature was found to be the primary factor governing levoglucosan yield, whereas combustion duration showed no significant effect. The analysis of synthetic chars, made from three different plant species, showed that levoglucosan exists only in low temperature chars (≤ 350°C) unless mineral structures in the plant tissue (i.e. phytoliths) provide physical protection to carbohydrates, allowing this molecular marker to persist at higher temperatures. Large differences among chars from different plant species were also found. Even though efforts were made to correct for this taxonomic effect (i.e. hemicellulose and cellulose normalization), the variable levoglucosan yields observed across plant species suggest heterogeneous processes that may include factors such as the presence of inorganic salts and lignin content in the precursor tissues. Therefore, those unavoidable complexities in biomass combustion make it hard for levoglucosan to act as a quantitative tool for char characterization in environmental media. However, the fact that levoglucosan is specific to low temperature chars imparts a unique role to this molecular marker in the identification of BC materials within the wide range of the BC continuum. In contrast to CTO-375, for example, levoglucosan could be used as a qualitative indicator of low temperature chars, at the low end of the BC continuum. The approach seems particularly useful in characterizing fire-impacted soil samples or aerosols. For examples, it is believed that fire-impacted soils would contain a larger proportion of char/charcoal with respect to soot-BC (Quénéa et al., 2006). As such, to evaluate the presence of such chars in soil samples, we suggest

conducting a quick “low-temperature char assay” using the levoglucosan method before applying other BC methods. In the case of aerosols, the important presence of this biomarker in ultrafine particles suggests that our conventional view of size distribution decreasing and atmospheric residence time increasing along the char to soot continuum may have to be revised to include these small char particles.

3. FATE OF CuO-DERIVED LIGNIN OXIDATION PRODUCTS DURING PLANT COMBUSTION: APPLICATION TO THE EVALUATION OF CHAR INPUT TO SOIL ORGANIC MATTER*

3.1. Introduction

Lignin, the second-most abundant naturally occurring polymer after cellulose, is a complex and important structural component of vascular plants (Sarkanen and Ludwig, 1971). Because of its unique structural features, lignin possesses greater stability to biodegradation than hemicellulose and cellulose and is considered to be among the best preserved components of vascular plants after deposition (Kirk and Farrell, 1987; Hedges, 1991; Dignac et al., 2005). This recalcitrant nature confers a significant role on lignin in the biospheric carbon cycle (Colberg, 1988). In addition, because vascular plants are exclusively terrestrial, lignin is both an important contributor to soil organic matter (SOM) and its presence in aquatic environments helps trace the input of terrigenous OM to such systems (Ertel and Hedges, 1985; Prahl et al., 1994; Louchouarn et al., 1999; Goñi et al., 2000; Benner et al., 2005; Dalzell et al., 2005; Houel et al., 2006).

Alkaline cupric oxide (CuO) oxidation is a technique commonly used to analyze lignin in plant tissue and environmental matrices such as soils, sediments and dissolved OM (Hedges and Mann, 1979a; Ertel and Hedges, 1985; Goñi and Hedges, 1992; Opsahl and Benner, 1998; Louchouarn et al., 2000; Otto and Simpson, 2006). Upon oxidation, the lignin

---

* Reproduced in part with permission from *Organic Geochemistry* **2008**, *39*, 1522-1536, Kuo, L.-J., Louchouarn P., and Herbert, B. E. "Fate of CuO-derived lignin oxidation products during plant combustion: Application to the evaluation of char input to soil organic matter", Copyright 2008 Elsevier Ltd.

macropolymer is hydrolyzed to small structural units belonging to three classes of methoxylated phenols: vanillyl (V), syringyl (S) and cinnamyl (C). Each class of lignin oxidation products (LOPs) is in turn comprised of an acid, an aldehyde and a ketone (for V and S) or only acids (for C). The yields and ratios of these lignin phenols have been extensively used to identify the structure of plant lignin (Hedges and Mann, 1979a; Goñi and Hedges, 1992) and estimate inputs of plant carbon to soils and aquatic systems (Hedges et al., 1982; Prahl et al., 1994; Louchouarn et al., 1999; Goñi et al., 1997, 2000; Farella et al., 2001; Dalzell et al., 2005; Houel et al., 2006), as well as evaluate the diagenetic status of lignin (Goñi et al., 1993; Opsahl and Benner, 1995; Benner and Opsahl, 2001; Otto and Simpson, 2006).

Under aerobic conditions, fungal decomposition is the most important pathway of lignin degradation, whereas bacterial degradation predominates in oxygen-limited environments (e.g. bogs, aquatic environments) (Ruel and Barnoud, 1985; Colberg, 1988). Both biodegradation pathways can alter the yields of lignin phenols due to the preferential degradation of certain phenolic classes or individual lignin phenols, causing a shift in lignin signature and potentially affecting its biogeochemical applications (Hedges et al., 1988a; Nelson et al., 1995; Opsahl and Benner, 1995; Klap et al., 1999). In addition to these biological processes, photochemical oxidation has recently been recognized (Opsahl and Benner, 1998; Hernes and Benner, 2003) to substantially alter the composition of dissolved lignin and change its signature over short time scales (hours to days).

Thermal decomposition is another abiotic process that may lead to lignin alteration and degradation in the environment. For example, following laboratory pyrolysis experiments to assess the usefulness of lignin as a tracer of paleovegetation, Ohta and

Venkatesan (1992) observed substantial modifications to the CuO-derived LOPs in wood combusted at 200°C. Closed system pyrolysis of woods and lignin substructure model-compounds showed that aryl ether bond cleavage, alkylation, and sequential demethoxylation are major reactions during early coalification (Ohta and Venkatesan, 1992; Behar and Hatcher, 1995; Vane and Abbott, 1999; Drage et al., 2002). This led to the use of thermally altered lignin structural models to depict coal structure at different stages of coalification (Hatcher, 1990; Hatcher et al., 1994). However, while most studies of lignin thermal alteration focused on elucidating the coalification process during geothermal alteration, studies of the thermal degradation of lignin in wildfire-induced char/charcoal are scarce (Dickens et al., 2007).

Chars/charcoals are solid combustion residues derived from biomass burning. They are highly heterogeneous resulting from highly variable conditions during combustion (temperature, oxygen availability, presence of mineral oxides) and thus form one of the major groups in the continuum of pyrogenic organic residues, the so-called black carbon (BC), in the environment (Hedges et al., 2000; Masiello, 2004; Hammes et al., 2007). Because of its recalcitrant nature and strong sorption capacity, BC is considered to play an important role in the carbon cycle and many biogeochemical and environmental processes (Gustaffson et al., 1997; Kuhlbusch, 1998; Masiello and Druffel, 1998). The identification and quantification of chars/charcoals is often lacking in many BC studies since most BC methods can not determine them well (Preston and Schmidt, 2006; Kuo et al., 2008). Recently, however, more and more studies have pointed out the significance of chars/charcoals in the environments. Kuhlbusch and Crutzen (1995) estimated that the annual production of pyrogenic carbon from vegetation fires ranges from 50 to 270 Tg/yr, >

80% of which remains on the ground following a fire. Skjemstad et al. (2002) reported that charcoal carbon comprised up to 35% of the total organic carbon (TOC) in five U.S. agricultural soils, whereas DeLuca and Applet (2008) estimated that charcoal comprised 13-43% of the TOC in surface and mineral soils (0-10 cm) from coniferous forest ecosystems. Such a large production of naturally occurring char/charcoal may represent a significant input of thermally altered vascular plants to soils and thus may lead to marked shifts in the overall soil lignin signatures.

In the present study, we selected three plant species covering different taxonomic groups (angiosperm/gymnosperm and woody/non-woody) to produce a series of synthetic chars under controlled combustion conditions. These synthetic chars served as model materials for the diverse natural chars generated from wildfires. We quantified the CuO-derived lignin oxidation products of the chars and used the obtained information to assess: (i) the effect of two primary combustion factors, temperature and duration, on the thermal alteration of lignin parameters. (ii) the response of lignin parameters from different plant types to thermal alteration, and (iii) the potential effect of char input on the characterization of SOM using lignin signatures.

3.2. Materials and methods

3.2.1. Materials

Three different plant species were used. These source materials included two angiosperms, honey mesquite (HM: *Prosopis glandulosa* Torr.) and cordgrass (CG: *Spartina spartinae*) from Laguna Atascosa National Wildlife Refuge (Rio Hondo, TX, USA) in June, 2005. A gymnosperm wood, loblolly pine (PI: *Pinus taeda*), was collected from Bastrop State Park (Bastrop, TX, USA) in April, 2006. Twigs of HM and PI were collected by

sawing or by hand and the CG stem was collected using shears. After transporting them to the laboratory, they were cut into small pieces (HM and PI: 0.5-1.5 cm long; CG: 2 cm long) and dried in an oven at 60°C (3 d) before charring. To mimic wildfire conditions in the field, we did not remove the bark from HM and PI and thus combusted the sample whole. Following drying, small blocks of HM and PI, and stem pieces from CG, were placed in individual quartz crucibles and charred in a muffle furnace (Lindberg Hevi-Duty box furnace Model 51442 with instrument console Model 59344, Asheville, NC, USA). The quartz crucible was capped with a quartz lid to create an oxygen-limited environment during combustion. The raw material was heated from room temperature to the desired final temperature (150-1050°C) at 26°C/min and held there for a scheduled period (0.5-5 h). Duration of combustion was counted after the temperature reached its maximum. After combustion, the synthetic chars were cooled down in the furnace overnight with the furnace door still closed, to prevent the char from being exposed to excess oxygen at high temperature. The chars were then ground to a fine powder (< 60 mesh) and stored in glass vials in a desiccator. With the synthetic chars from above three plant species, we can compare the LOPs of angiosperm chars (HM, CG) vs. those from gymnosperm chars (PI), as well as woody chars (HM, PI) vs. non-woody chars (CG) under identical combustion conditions.

Pre-fire and post-fire surface soils from two control burn sites in New Mexico (USA) were kindly provided by Dr. P. D'Odorico (University of Virginia, VA, USA). They were air-dried and passed through a 2 mm sieve. Standard reference materials (SRMs) of New York/New Jersey waterway sediment (SRM 1944) were obtained from the U.S. National Institute of Standards and Technology (Gaithersburg, MD, USA).

3.2.2. Lignin analysis

Lignin-derived CuO oxidation products were determined using the method developed by Hedges and Ertel (1982) and Goñi and Hedges (1992), with slight modifications by Louchouarn et al. (2006). Briefly, a ground sample, providing 2-5 mg OC (Louchouarn et al., 2000) was mixed with CuO (≈ 300 mg) and $Fe(NH_4)_2(SO_4)_2 \cdot 6H_2O$ (≈ 50 mg) in a stainless steel mini-reaction vessel (3 mL; Prime Focus Inc.), to which 8 wt% nitrogen-sparged NaOH solution was added (3 mL). The headspace of twelve of such reaction mini-bombs was purged with N_2 and the bombs were heated at 155ºC for 3 h in a customized Hewlett-Packard 5890 gas chromatograph. Trans-cinnamic acid (3-phenyl-2-propenoic acid) was used as internal standard and was directly added (≈ 12-20 μg) to each mini-bomb after cooling. The aqueous solution was acidified with 6N HCl and extracted (x 3) with ethyl acetate. Extracts were dried with Na_2SO_4 and evaporated to dryness using a LabConco™ solvent concentrator. The CuO reaction products were re-dissolved in a small volume of pyridine (200-500 μL). After further dilution (1:10 to 1:20), a sub-sample was derivatized with *N,O*-bis(trimethylsilyl)trifluoroacetamide (BSTFA) containing 1% trimethylchlorosilane (TMCS) at 75°C in a heating block (1 h).

Separation and quantification of trimethylsilyl derivatives of CuO oxidation by-products were performed using gas chromatography-mass spectrometry (GC/MS) with a Varian Ion Trap 3800/4000 system fitted with a fused silica column (VF 5MS, 60 m x 0.25 mm i.d.; Varian Inc.). Each sample was injected, under splitless mode, into a straight glass liner inserted into the GC injection port; He was the carrier gas (~ 1.3 mL/min). The GC oven was programmed from 100°C, with no initial delay, to 300°C (held 10 min). The GC injector and GC/MS interface were both maintained at 300°C. The mass spectrometer was operated in

the electron ionization (EI, 70 eV) and in full scan modes. Compound identification was performed using GC retention times and by comparing full mass spectra with those of commercially available standards. Quantification was performed using relative response factors adjusted to the internal standard. The analytical precision of the major CuO-oxidation products and related parameters was derived from replicate analyses of standard estuarine sediments (i.e., NIST SRM 1944), as well as selected charcoal and soil samples, and averaged ~ 5% or less.

3.2.3. Elemental analysis and ash content

Elemental analysis (C and N content) was carried out with an Elementar Vario EL *III* elemental analyzer (Elementar Americas, Inc., Mt. Laurel, NJ, USA). The temperature of the combustion reactor was set at 1150°C. Quantification was based on a calibration equation using sulfanilic acid (Merck KGaA, Germany) as a standard compound. For soil and sediment samples, inorganic carbon was removed prior to analysis using acid vapor acidification (Hedges and Stern, 1984). Char samples were also sent to UC-Davis Stable Isotope Facility (Davis, CA, USA) for H analysis. C/N and H/C atomic ratios were calculated from the obtained C, H, and N contents. Ash content was determined using the modified ASTM 1102-84 method (ASTM, 2000).

3.3. Results and discussion

3.3.1. Thermal alteration of lignin phenols in synthetic chars

3.3.1.1. Characterization of synthetic chars

Table 5 lists the carbon content, % mass and carbon loss, ash content, and concentration of eight primary lignin oxidation products as well as 3,5 dihydroxybenzoic acid (3,5Bd) from synthetic chars. Under identical combustion conditions, the three series experienced similar

mass loss values and changing patterns (Table 5). The steepest rate of change in mass loss occurred between 200 and 300°C. Above 300°C, the mass loss continued but at a much slower rate. The proportion of OC increased steadily in all synthetic chars, reaching maxima and leveling off (HM and CG) for samples made under elevated combustion temperatures. The high temperature chars derived from woody tissue (HM and PI) were more enriched in carbon (> 75%) than the grass char (CG), which only reached 55% OC at 550°C (Table 5). The lower OC proportion in CG chars may be due to their relatively high mineral and ash contents (Table 5), which would dilute the OC content of the bulk samples (grasses can contain up to 50% in silica). We calculated the absolute residual carbon content of chars by correcting the carbon content in Table 5 with the corresponding ash content and mass loss (Figure 9). The proportions of residual OC are very similar in the char series of these three different plants. The large changes in residual carbon content in chars produced between 200 and 400°C point to substantial loss of thermally labile, carbon-rich constituents, such as hemicellulose and cellulose, in this temperature range (Kuo et al., 2008). The relatively consistent residual carbon content in the high temperature chars (≥ 450°C) supports the formation of a graphite-like structure derived from lignin backbone (Mackay and Roberts, 1982). In our previous study on the same synthetic chars, H/C and O/C atomic ratios also showed that the aromatization pathway starts to dominate at combustion temperatures > 300°C (Kuo et al., 2008).

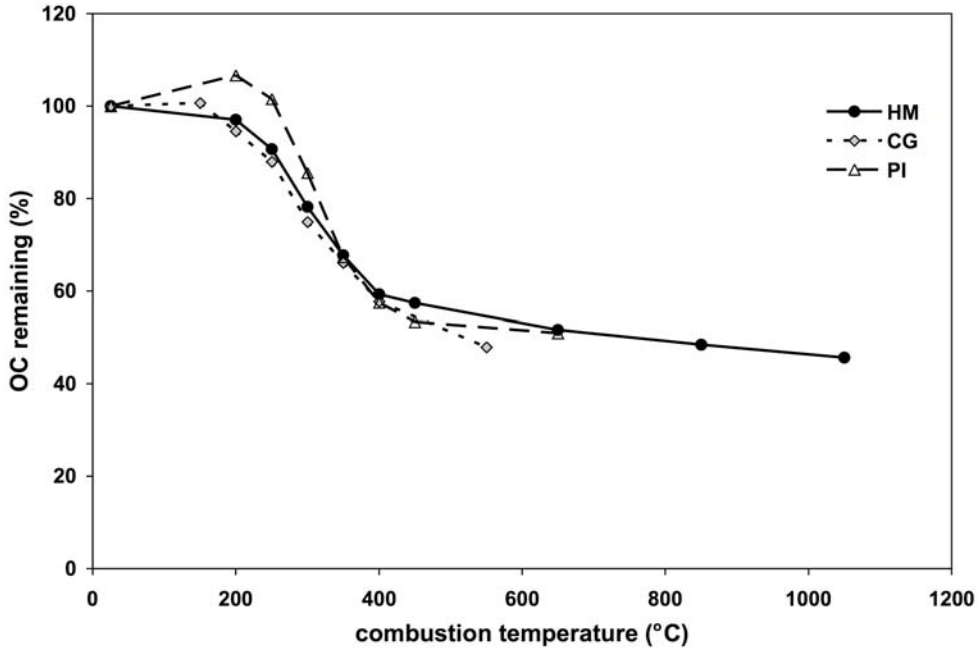

Figure 9. Thermograms of % organic carbon (OC) remaining for honey mesquite (HM), cordgrass (CG), and loblolly pine (PI) chars.

Table 5. Elemental compositions and yields of individual lignin phenols of synthetic chars (values for λ8 are mg/100mg OC; values for other lignin phenols and 3,5Bd are mg/g).

Plant species	Sample ID	Combustion temperature (°C)	Combustion duration (hr)	Mass loss (%)	Ash (%)	%C	Resid.C (%)[a]	Resid.LOP (%)[a]	Σ8[b]	λ8[b]	Vl[b]	Vn[b]	Vd[b]
Honey mesquite	HM raw				5.5	44.7	100.0	100.0	63.7	14.3	20.3	5.0	4.4
	HM 200	200	1	8.8	6.1	47.2	97.1	99.7	69.2	14.7	17.6	5.1	6.4
	HM 250	250	1	23.7	6.9	52.3	90.7	45.1	37.2	7.1	7.4	2.9	5.2
	HM 300	300	1	46.1	9.4	62.1	78.2	7.7	8.7	1.4	1.7	0.56	1.9
	HM 350	350	1	54.6	10.0	63.5	67.7	0.62	0.84	0.13	0.15	0.07	0.41
	HM 400	400	1	61.7	11.7	64.6	59.3	0.00	0.00	-	-	-	-
	HM 450	450	1	65.5	13.4	68.1	57.4	0.00	0.00	-	-	-	-
	HM 650	650	1	71.6	15.6	72.6	51.7	0.00	0.00	-	-	-	-
	HM 850	850	1	74.8	17.5	75.1	48.5	0.00	0.00	-	-	-	-
	HM 1050	1050	1	76.6	18.9	74.9	45.7	0.00	0.00	-	-	-	-
	HM 250_0.5	250	0.5	21.8	6.1	52.7	92.8	59.1	47.7	9.1	9.5	3.9	5.9
	HM 250_3	250	3	28.3	5.7	53.6	86.2	39.2	34.8	6.5	6.5	2.7	5.3
	HM 250_5	250	5	31.1	5.6	55.3	85.2	31.2	28.9	5.2	5.3	2.4	5.2
Cordgrass	CG raw				8.8	41.0	100.0	100.0	62.7	15.3	14.1	2.0	2.0
	CG 150	150	1	7.0	9.8	43.9	100.7	77.6	51.7	11.8	9.6	2.2	2.0
	CG 200	200	1	17.7	10.6	46.2	94.6	41.0	30.7	6.6	5.1	1.4	2.5
	CG 250	250	1	29.6	12.4	49.3	88.0	17.9	15.3	3.1	2.9	0.23	2.5
	CG 300	300	1	50.1	17.1	56.1	75.0	2.7	3.1	0.56	0.83	-	1.1
	CG 350	350	1	57.0	20.2	55.2	66.1	0.59	0.77	0.14	0.13	0.06	0.26
	CG 400	400	1	63.7	23.0	55.1	57.7	0.00	0.00	-	-	-	-
	CG 550	550	1	72.2	30.3	54.1	47.9	0.00	0.00	-	-	-	-
Loblolly pine	PI raw				1.3	45.9	100.0	100.0	71.4	15.6	52.1	8.3	9.0
	PI 200	200	1	6.3	2.1	51.8	106.6	68.6	51.8	10.0	29.9	7.1	9.4
	PI 250	250	1	16.9	1.9	55.7	101.5	34.3	29.3	5.3	15.0	4.0	9.6
	PI 300	300	1	39.1	2.4	63.8	85.5	13.1	15.2	2.4	5.9	2.0	7.1
	PI 350	350	1	55.7	3.4	68.3	67.3	2.1	3.3	0.48	0.94	-	2.4
	PI 400	400	1	64.1	4.1	71.4	57.5	0.00	0.00	-	-	-	-
	PI 450	450	1	68.3	6.4	73.3	53.4	0.00	0.00	-	-	-	-
	PI 650	650	1	73.3	5.5	83.8	51.0		n.d.	n.d.	n.d.	n.d.	n.d.

Table 5. Continued.

Plant species	Sample ID	Sl[b]	Sn[b]	Sd[b]	Cd[b]	Fd[b]	3,5Bd[b]	S/V[c]	C/V[c]	Cd/Fd[c]	$(Ad/Al)_v$[c]	$(Ad/Al)_s$[c]	3,5Bd/V[c]
Honey mesquite	HM raw	17.0	9.3	5.8	0.42	1.5	0.38	1.1	0.06	0.28	0.22	0.34	0.01
	HM 200	19.4	9.8	8.4	0.58	2.0	0.67	1.3	0.09	0.29	0.36	0.43	0.02
	HM 250	9.5	4.8	6.7	0.16	0.60	0.38	1.4	0.05	0.26	0.70	0.70	0.02
	HM 300	1.8	0.60	1.9	0.07	0.21	0.54	1.0	0.07	0.33	1.1	1.1	0.13
	HM 350	0.07	-	0.14	-	-	0.51	0.34	0.00		2.7	1.8	0.82
	HM 400	-	-	-	-	-	0.33						
	HM 450	-	-	-	-	-	0.12						
	HM 650	-	-	-	-	-	-						
	HM 850	-	-	-	-	-	-						
	HM 1050	-	-	-	-	-	-						
	HM 250_0.5	12.5	6.3	8.3	0.27	1.3	0.49	1.4	0.08	0.20	0.62	0.66	0.03
	HM 250_3	8.3	4.3	6.8	0.21	0.66	0.46	1.3	0.06	0.32	0.81	0.82	0.03
	HM 250_5	6.4	2.9	5.9	0.19	0.67	0.70	1.2	0.07	0.28	0.97	0.94	0.05
Cordgrass	CG raw	13.8	6.8	3.5	12.2	8.3	-	1.3	1.1	1.5	0.14	0.25	0.00
	CG 150	12.0	5.5	3.4	10.3	6.7	-	1.5	1.2	1.5	0.21	0.29	0.00
	CG 200	6.3	4.5	4.0	4.2	2.8	0.17	1.6	0.77	1.5	0.50	0.63	0.02
	CG 250	2.4	2.6	3.1	1.1	0.63	0.14	1.5	0.31	1.8	0.85	1.3	0.02
	CG 300	0.32	-	0.75	0.08	0.05	0.47	0.55	0.07	1.6	1.3	2.4	0.24
	CG 350	0.05	0.06	0.10	0.06	0.05	0.57	0.46	0.25	1.3	2.0	1.9	1.3
	CG 400	-	-	-	-	-	0.37						
	CG 550	-	-	-	-	-	-						
Loblolly pine	PI raw	0.82	-	0.15	0.09	0.89	0.12	0.01	0.01	0.09	0.17	0.10	0.00
	PI 200	2.7	0.70	0.73	-	1.4	0.43	0.09	0.03	0.00	0.31	0.27	0.01
	PI 250	-	-	0.13	-	0.71	0.38	0.00	0.02	0.00	0.64		0.01
	PI 300	-	-	-	-	0.26	0.53	0.00	0.02	0.00	1.2		0.04
	PI 350	-	-	-	-	-	0.58	0.00	0.00		2.5		0.18
	PI 400	-	-	-	-	-	0.41						
	PI 450	-	-	-	-	-	0.08						
	PI 650	n.d.	n.d.	n.d.	n.d.	n.d.	n.d.						

[a] Residual carbon content and residual lignin oxidation products (sum of Vl, Vn, Vd, Sl, Sn, Sd, Cd, and Fd) content compared to the unburn plant.

[b] Σ8: sum of eight lignin-derived phenols (Vl, Vn, Vd, Sl, Sn, Sd, Cd, and Fd); λ8: OC–normalized sum of eight lignin-derived phenols; Vl: vanillin; Vn: acetovanillone; Vd: vanillic acid; Sl: syringaldehyde; Sn: acetosyringone; Sd: syringic acid; Cd: *p*-coumaric acid; Fd: ferulic acid; 3,5Bd: 3,5-dihydrobenzoic acid.

[c] S/V: ratio of syringyl to vanillyl phenols; C/V: ratio of cinnamyl to vanillyl phenols; Cd/Fd: ratio of *p*-coumaric acid to ferulic acid; $(Ad/Al)_v$: ratio of vanillic acid to vanillin; $(Ad/Al)_s$: ratio of syringic acid to syringaldehyde; 3,5Bd/V: ratio of 3,5-dihydrobenzoic acid to vanillyl phenols.

-: Undetectable

n.d.: Not determined

3.3.1.2. Thermal alteration of lignin oxidation products and lignin parameters

3.3.1.2.1. Total lignin oxidation products

All three charred plants experienced a dramatic decrease in LOPs in the early stages of combustion (Figure 10). Less than 20% of the original LOPs remained in 300°C chars and no detectable levels were observed in chars produced at temperatures ≥ 400°C. Dickens et al. (2007) reported a similar finding for a suite of synthetic chars made from red pine (*Pinus resinosa*) in a temperature range of 70-350°C. However, they found that lignin phenols reached undetectable levels at slightly lower temperatures (250-350°C) than those reported here. This may be due to the prolonged combustion duration (24-72 h) these authors used. In the present study, we observed that extended combustion does have a negative impact on LOP yield (Table 5). The substantial decrease in LOP yield during combustion demonstrates the thermal lability of lignin even at relatively low combustion temperature (≤ 350°C). This observation is also in accord with the results of earlier thermogravimetric analysis which showed that lignin decomposes over a broad range of temperature, overlapping with the temperature of hemicellulose and cellulose degradation (about 250°C and 350°C, respectively; Antal and Varhegyi, 1995; Lopez-Capel et al., 2005; Kuo et al., 2008).

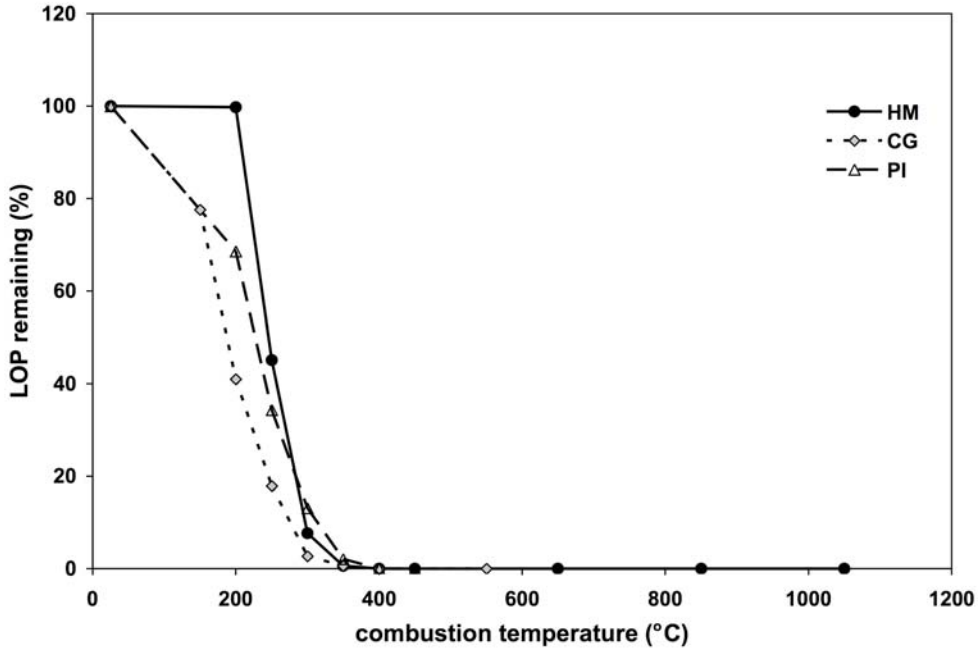

Figure 10. Thermograms of % total lignin oxidation products (LOP) remaining for honey mesquite (HM), cordgrass (CG) and loblolly pine (PI) chars.

3.3.1.2.2. Ratio of syringyl to vanillyl phenols

In addition to the information from mass- or carbon-normalized lignin content, internal parameters based on specific phenolic lignin oxidation products highlight compositional differences in lignin source and thus provide a means for discriminating between taxonomic vascular plant groups (gymnosperms vs. angiosperms), tissue types (soft tissue vs. woody tissue), and diagenetic state or alteration of the original lignin material (Hedges and Mann, 1979a; Hedges et al., 1985, 1988b; Goñi and Hedges, 1992; Goñi et al., 1993; Opsahl and Benner, 1995). For example, a ratio of syringyl (S) to vanillyl (V) phenols appreciably greater than zero for complex environmental mixtures is indicative of the presence of at least some angiosperm tissue because syringyl structural units are only incorporated in significant amounts in angiosperm lignin but virtually absent from gymnosperm tissue (Sarkanen and

Ludwig, 1971; Hedges and Mann, 1979b; Goñi and Hedges, 1992; Opsahl and Benner, 1995). Similarly, a ratio of cinnamyl (C) to vanillyl phenols greater than zero is indicative of the presence of non-woody material because cinnamyls are abundant in most herbaceous and soft tissues (i.e., leaves and needles) but virtually absent from wood (Sarkanen and Ludwig, 1971; Hedges and Mann, 1979b; Goñi and Hedges, 1992; Opsahl and Benner, 1995).

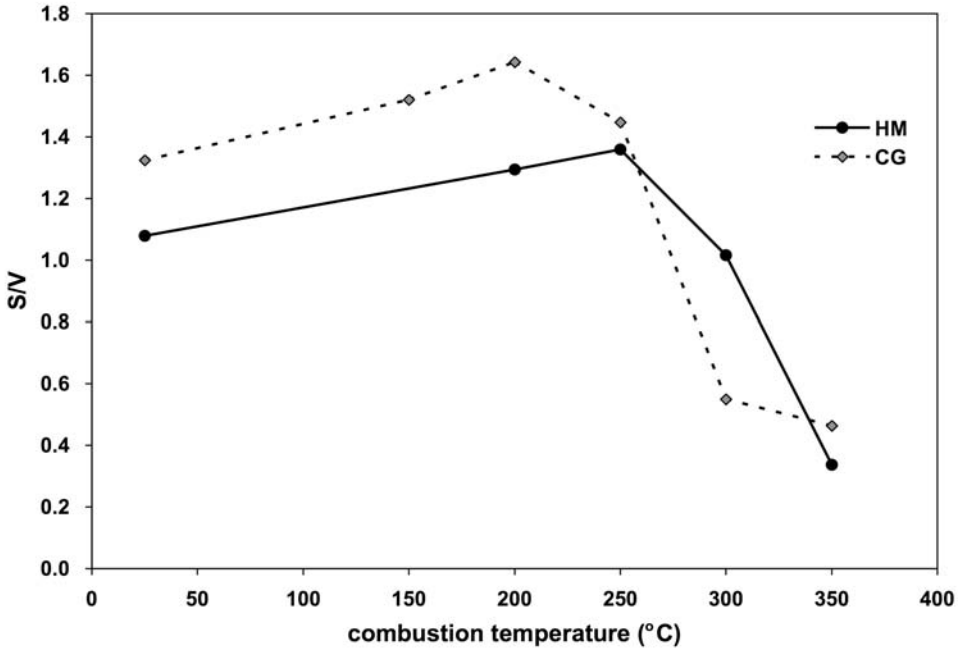

Figure 11. Thermograms of ratio of syringyl to vanillyl phenols (S/V) for honey mesquite (HM) and cordgrass (CG) chars. The S/V values are plotted only for samples ≤ 350ºC since S and V are not detected in chars produced at temperatures above that limit.

In the present study, the two unburned angiosperm plant tissue samples possess high S/V values (HM: 1.06; CG: 1.32), while the value for unburned gymnosperm (PI) is only 0.01. The effect of combustion on the S/V signature is thus only shown for HM and CG (Figure 11). Interestingly, these two plant tissues show similar two-stage trends with increasing

combustion temperature. During combustion, their S/V values show an initial increase up to 200-250°C, followed by a steep decrease, with values approaching zero at 400°C. The main difference between the two species is the turning point temperature between the two stages (HM 250°C; CG 200°C).

This two-stage S/V ratio trend in thermal degradation suggests that different lignin subunits have different thermal stabilities and/or that ultrastructural components of plant tissues themselves have different thermal stabilities. Differences in stability of different ultrastructural components have been shown to occur during fungal attack and partly contribute to the diverging results for lignin degradation by white-rot and brown-rot fungi (Ruel and Barnoud, 1985; Hedges et al., 1985; Hedges et al., 1988a). In hardwoods, the middle secondary cell wall layer (S2 layer) is enriched in syringyl structural units, while the outer and inner secondary cell wall layers (S1 and S3 layer, respectively) and the compound middle lamella (CML) are predominantly composed of vanillyl and condensed *p*-hydroxy structural units (Terashima and Fukushima, 1989). Because the S2 layer is more labile to attack by white-rot fungi than other cell wall substructures, the preferential degradation of syringyl phenols vs. vanillyl phenols was often found in white-rot fungal degradation (Ruel and Barnoud, 1985; Hedges et al., 1985; Hedges et al., 1988a). The features of these cell wall ultrastructures have also been shown to be susceptible to thermal treatment (McGinnes et al., 1971; Scott, 1989; Jones and Chaloner, 1991). Jones and Chaloner (1991) indicated that the stratification of cell wall layers (e.g. S1 and S2 layers) is still visible in wood pyrolyzed at 180-220°C, but that the cell wall layers become homogenized (no layering) at 230-340°C, with further cracking of the homogenized cell wall along the CML at 340-600°C. These features of ultrastructural change are often used for fossil charcoal identification and

may relate to the observed two-stage S/V ratio change in the present study because the turning point temperatures of S/V values of HM and CG are close to that of cell wall homogenization.

The generation of extra vanillyl phenols from syringyl phenols through demethoxylation may be an alternate process leading to a decrease in S/V values upon thermal degradation. However, our data show that the yields of vanillyl and syringyl phenols decrease with increasing combustion temperature (Table 5). Studies of lignin thermal degradation have indicated that direct demethoxylation of lignin phenols is not a predominent reaction during combustion (Ohta and Venkatesan, 1992; Behar and Hatcher, 1995; Vane and Abbott, 1999). For example, Ohta and Venkatesan (1992) found no accumulation of vanillyl phenols with thermal degradation of syringyl phenols for heating at 200°C for up to 200 hours. In their confined system pyrolysis of a fossil angiosperm wood, Behar and Hatcher (1995) found that, with increased severity of pyrolysis (increase temperature and/or duration), a loss of lignin-related compounds was accompanied by an increase in alkylated benzenediols (such as alkylcatechols and methoxycatechol). The authors associated the abundance of these catechols in pyrolyzed wood with an increased presence of lignin residues that had undergone demethylation during combustion. As catechols themselves began to diminish under more severe pyrolysis conditions, other aromatic compounds (phenols, cresols, alkyl phenols, alkyl benzenes, and alkyl naphthalenes) became predominant in the residues. The authors thus indicated that the multi-step mechanism, demethylation in the early stage followed by dehydroxylation and/or ring opening, was most likely responsible for the observed thermal degradation of lignin. This proposed multi-step mechanism was further supported by Vane and Abbott (1999), who monitored the thermal degradation products of

two lignin model compounds, 2-methoxyphenol and 2,6-dimethoxyphenol, under closed system pyrolysis and pointed out that demethylation is the dominant reaction during early coalification of lignin. The prevailing demethylation of lignin during combustion would alter the structure of the lignin polymer (Hatcher, 1990) and hence remove the common lignin oxidation phenols from the analytical window of the CuO oxidation method. This may explain the substantial decrease in LOP yield observed in the present study (Table 5, Figure 10).

(a)

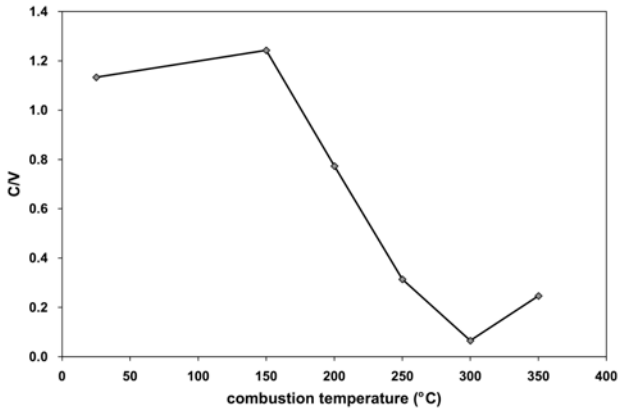

(b)

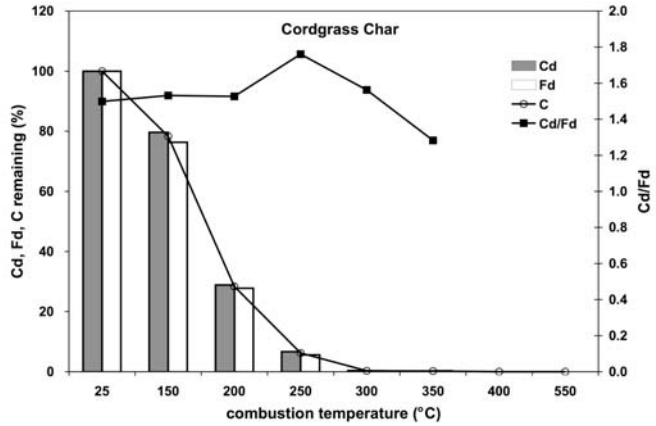

Figure 12. Thermograms of (a) ratio of cinnamyl to vanillyl phenols (C/V); and (b) *p*-coumaric acid (Cd), ferulic acid (Fd), sum of two cinnamyl phenols (C), and ratio of Cd to Fd (Cd/Fd) from cordgrass (CG) char. The C/V and Cd/Fd values are plotted only for samples ≤ 350ºC since V, Cd, and Fd are not detected in chars produced at temperatures above that limit. The x-axis of Fig. 12b is nonlinear.

3.3.1.2.3. Ratio of cinnamyl to vanillyl phenols and p-coumaric acid to ferulic acid

As expected, the unburned cordgrass, a non-woody plant, is characterized by a much higher C/V value (1.13) than the two other woody tissues (HM and PI, 0.06 and 0.01, respectively). As we observed for the S/V values of HM and CG chars, the C/V ratio of the CG char shows a two-stage trend with increasing temperature (Figure 12a). Although the C/V value did not change significantly at low temperature (< 150°C), it dropped dramatically > 200°C and approached zero at 400°C. The increased C/V value at 350°C may be an artifact due to the very low concentrations of cinnamyl and vanillyl phenols in the sample. This thermogram implies that cinnamyl phenols are more susceptible to thermal degradation than vanillyl phenols. However, the significant depletion in these two lignin phenol families with increasing combustion temperature (Table 5) demonstrates that they are all labile with respect to combustion.

Looking specifically at the changes in the two cinnamyl phenols, *p*-coumaric acid (Cd) and ferulic acid (Fd), we found no preferential thermal degradation for either of these (Figure 12b), suggesting that they have similar thermal stability.

3.3.1.2.4. Ratios of acid to aldehyde phenols

In addition to the taxonomic parameters discussed above, both V and S classes afford acid and aldehyde phenols in proportions characteristic of the state of degradation of the parent lignin polymer. For example, low ratio values of acid over aldehyde moieties [(Ad/Al): 0.1-0.5] are typical of fresh lignin (Hedges and Mann, 1979a; Goñi and Hedges, 1992), whereas increased proportions of acidic groups in oxidatively altered lignin yield elevated acid/aldehyde values (> 0.5) upon alkaline CuO oxidation (Hedges et al., 1988b; Goñi et al., 1993; Nelson et al., 1995; Opsahl and Benner, 1995, 1998). Other processes,

such as selective dissolution of acid moieties and their sorption onto minerals, can also lead to increased (Ad/Al) ratios in environmental samples (Houel et al., 2006; Hernes et al., 2007). Thus, elevated Ad/Al ratios in environmental samples, particularly within the vanillyl family ($(Ad/Al)_v$), suggest that lignin has either been altered by microbial and/or photochemical degradation ((Hedges et al., 1988b; Kögel-Knabner et al., 1991; Goñi et al., 1993; Opsahl and Benner, 1995, 1998; Hernes and Benner, 2003), or that dissolution/sorption processes have selectively enriched the matrix in acid groups (Kaiser and Guggenberger, 2000; Rumpel et al., 2002; Houel et al, 2006; Hernes et al., 2007). In this thermal alteration study of plant residues, the latter process is not at play and potential changes in (Ad/Al) ratios will track changes in composition rather than losses/enrichment due to dissolution/sorption.

The values of $(Ad/Al)_v$ of unburned HM, CG and PI (0.22, 0.14 and 0.17, respectively) are all within the reported values of fresh vascular plants discussed above. However, these values increased dramatically across the temperature range over which LOPs were detectable (up to 350°C; Figure 13). The maximum $(Ad/Al)_v$ values reached for HM, CG and PI chars (2.7, 2.0,and 2.1, respectively) are at the higher limit reported for humic and fulvic acid fractions (0.7-2.5) extracted from soil/sedimentary OM (Ertel and Hedges, 1984; Sánchez-García, 2007) or DOM sorbed onto soil minerals (Hernes et al., 2007). The five- to tenfold increase in $(Ad/Al)_v$ from unburned plants (in which vanillin is up to 5 times more concentrated than vanillic acid) to 350°C char (in which the concentration of vanillic acid is twice that of vanillin; Table 5) may reveal the role of side chain oxidation of aldehyde precursors in lignin macromolecules during combustion (Hedges et al., 1988a). However, vanillin might also be lost via cleavage of C_α-$C_{aromatic}$ bond (Ohta and Venkatesan, 1992).

This mechanism, coupled with a potentially greater thermal stability of vanillic acid, could reasonably explain the significant decrease in vanillin content *vs*. the relatively minor change of vanillic acid in low temperature chars (Figure 13). Changes in $(Ad/Al)_v$ are also incurred by lengthening the combustion duration. As shown in Figure 4d, the $(Ad/Al)_v$ value for the 250°C HM char increases from 0.6 to 1.0 over the 0.5-5.0 h combustion periods. These results confirm those of Ohta and Venkatesan (1992) who observed a similar effect on $(Ad/Al)_v$ in their experiment on chars (200°C) made from red alder (*Cunonia capensis*) and pine (*Pinus pinea*) over combustion periods of 20-200 hours.

We also found that the the syringyl phenols, abundant in the two angiosperm plants, are susceptible to thermal alteration with $(Ad/Al)_s$ ratios increasing concomitantly with increasing combustion temperature (Table 5). The highest value for HM (1.8) occurs at 350°C, whereas the highest value for CG (2.4) is produced at 300°C. These two very high values are above the reported range for soil/sediment humic and fulvic acids (0.42-1.6, Ertel and Hedges, 1984; Sánchez-García, 2007), showing the highly oxidized nature of these two chars. Notably, the similarity between $(Ad/Al)_s$ and $(Ad/Al)_v$ ratios during combustion is in contrast to the results obtained from soft-rot fungal degradation and photochemical oxidation, which showed no or only little change in $(Ad/Al)_s$ (Hedges et al., 1988a; Opsahl and Benner, 1998). This observation reflects the nonselective nature of thermal alteration.

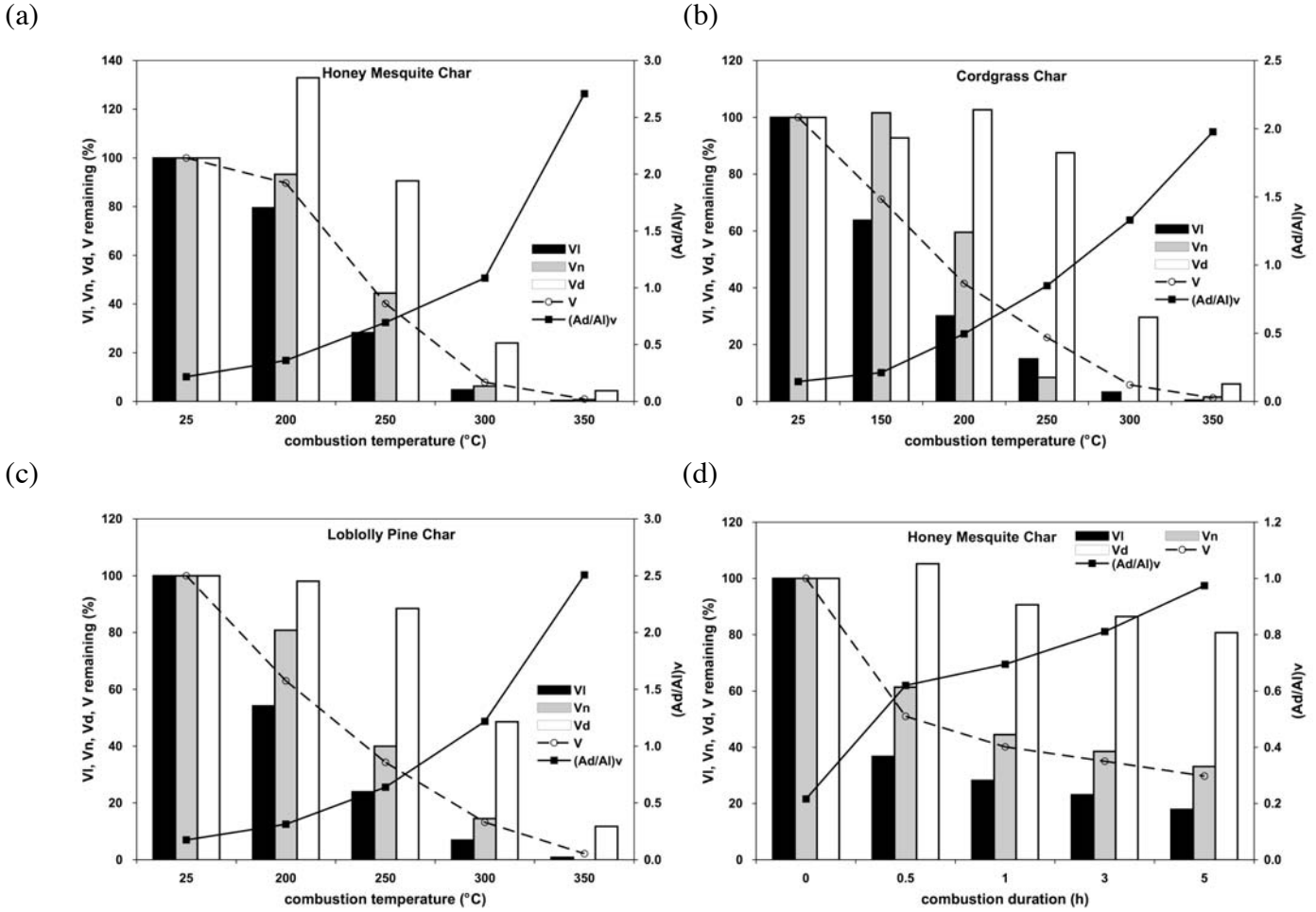

Figure 13. Thermograms of vanillin (Vl), acetovanillone (Vn), vanillic acid (Vd), sum of three vanillyl phenols (V), and $(Ad/Al)_v$ ratio from (a) honey mesquite char, (b) cordgrass char, and (c) loblolly pine char. (d) Changes of Vl, Vn, Vd, V, and $(Ad/Al)_v$ ratio from honey mesquite char (250 °C) as a function of combustion duration. The $(Ad/Al)_v$ values in (a), (b), and (c) are plotted only for samples ≤ 350ºC since vanillin is not detected in chars produced at temperatures above that limit. Note the x-axis is nonlinear.

3.3.1.2.5. Ratio of 3,5-dihydroxybenzoic acid to vanillyl phenols

Among additional CuO oxidation products, the phenolic compound 3,5-dihydroxybenzoic acid (3,5Bd) is a common product of soil degradation (Christman and Oglesby, 1971; Ugolini et al., 1981; Prahl et al., 1994) and has been regularly found within freshwater and marine sediments (Hedges and Parker, 1976; Gough et al., 1993; Prahl et al., 1994; Louchouarn et al., 1999; Houel et al., 2006; Dickens et al., 2007). It has been shown to derive mostly from the oxidation of SOM (Ugolini et al., 1981), except for some marine sediments receiving large inputs from brown macroalgae (Goñi and Hedges, 1995). In turn, the ratio of 3,5Bd to total vanillyl phenols (3,5Bd/V) has been shown to be much higher for humic matter than for bulk sediment OM (Sánchez-García, 2007), confirming the use of the ratio for determining the degree of oxidation of different soil OM (Otto et al., 2005; Otto and Simpson, 2006). Recently, Dickens et al. (2007) and Sánchez-García et al. (2009) further validated the use of this ratio as a robust tracer for SOM input to aquatic systems, including coastal and shelf environments. The likely precursors of this phenolic product are not altered lignin macropolymers but tannins and other flavonoids (Christman and Oglesby, 1971; Goñi and Hedges, 1995). Because tannin-like materials tend to accumulate within decaying cells (de Leeuw and Largeau, 1993), the relative increase in this compound in soils may be related to the extent of degradation and humification of fresh vascular plant tissue (Prahl et al., 1994; Houel et al., 2006). However, although Dickens et al. (2007) have shown that charring can increase the yield of 3,5Bd in vascular plants, the effect of thermal degradation on the 3,5Bd/V ratio has not been addressed. In all plant charcoals, the value of 3,5Bd/V remains negligible under combustion temperatures ≤ 250°C and peaks at 350°C; while values of chars from ≥ 400°C combustion could not be calculated for lack of detectable vanillyl phenols in

those chars (Table 5). The large difference in maximum value across char types probably reflects a plant species effect. For example, the relatively low values for the PI chars are probably a direct result of relatively high yields of vanillyl phenols from gymnosperm wood (Table 5). Nevertheless, the extremely high 3,5Bd/V and $(Ad/Al)_v$ values for 350°C chars are striking, demonstrating that combustion can alter these two diagnostic indicators and suggesting that 350°C may be a critical temperature in terms of thermal degradation of lignocellulose. Furthermore, the lack of sensitivity of the 3,5Bd/V ratio to low temperature combustion (≤ 250°C), contrasting with the behavior of the $(Ad/Al)_v$ ratio could be used to roughly estimate the combustion temperature for environmental chars. However, such an application may suffer from serious interferences when chars are mixed with soils containing highly degraded non-char OC since the latter also yields elevated $(Ad/Al)_v$ and 3,5Bd/V ratios. Although $(Ad/Al)_s$ responds differently between thermal alteration and some other degradation pathways, this ratio still increases during diagenesis (Opsahl and Benner, 1995). It is unlikely we can differentiate the presence of char and other lignin degradation pathways in complex environmental matrices by using shifts in LOP patterns alone. But this task may be possible at least qualitatively only when other char identification approaches are available (see example in next section).

3.3.2. Effect of char input on OM characterization

The influence of thermal alteration on CuO-derived lignin parameters in synthetic chars implies that combustion in natural environments can alter the lignin signals in burned residues of vascular plants. A more significant question is: Does the input of these thermally altered vascular plants (char/charcoal) in soils/sediments have the potential to induce a shift in the lignin signal of environmental matrices? Here we apply a simple two-end-member

mixing model to characterize the changes in bulk lignin parameters of selected SOM on input of specific chars. Biomarker signatures from a soil litter layer and a mineral soil collected from B horizon were adapted from Houel et al. (2006) as "model" end members for SOM with characteristics from the two ends of the soil spectrum (carbon-rich litter *vs*. carbon-poor mineral soil). Pine chars (PI 300, 350 and 400°C) were used in this mixing model because the soil endmembers come from podzols from a northern Canadian forest, which consist predominantly of pine/spruce stands (Houel, 2003). Using the elemental and biomarker concentration data for each end-member (Table 6), we can calculate OC-normalized total lignin phenols (λ6, which only contain vanillyl and syringyl phenols) and 3,5Bd/V ratio by using the equation:

$$\left(\frac{A}{B}\right)_{obs} = \frac{(A_{char} \times f_{char}) + [A_{SOM} \times (1 - f_{char})]}{(B_{char} \times f_{char}) + [B_{SOM} \times (1 - f_{char})]} \qquad \text{(eq. 2)}$$

where *A* represents the mass-normalized value of the parameter in the numerator of the ratio (3,5Bd and Σ6); *B* represents the mass-normalized value of the parameters in the denominator (V and OC); subscripts char and SOM denote added char and SOM, respectively; f_{char} is the fraction of char in the mixture; $(A/B)_{obs}$ is the observed ratio of the mixture. Note that, for the undetectable values of HM 400, we use zero in the calculations. Because we have no prior knowledge of pre-existing charcoal in these soils, we assume here that the soil endmember signatures are entirely due to uncharred plant residues. The presence of chars in the soils, however, would not change the overall result of the mixing models since we use the measured soil compositions rather than theoretical values calculated from a composite of plant tissue inputs, and only model the potential impact on soil signatures due to char inputs. Using such a model to assess quantitatively the amount of char

inputs to the soil requires additional information such as additional indicators of char or BC and lignin content/signature prior and after burning (see discussion below).

Table 6. Elemental and biomarker mass-normalized concentrations of diverse end-members for modeling. All units are in mg (g dry wt)$^{-1}$

End-members	C_{org}[a]	Σ6[b]	V[b]	S[b]	Vd[b]	Vl[b]	3,5Bd[b]
Soil litter[c]	526.0	16.8	13.2	3.6	3.2	7.4	0.69
Mineral soil[c]	30.0	0.11	0.09	0.02	0.04	0.03	0.07
PI[d]: 300ºC char	638.1	14.9	14.9	-	7.1	5.9	0.53
PI[d]: 350ºC char	682.7	3.3	3.3	-	2.4	0.94	0.58
PI[d]: 400ºC char	714.2	-	-	-	-	-	0.41

[a] C_{org}: organic carbon.
[b] Σ6: mass-normalized summation of three vanillyl phenols (V) and three syringyl phenols (S); Vd: vanillic acid; Vl: vanillin; 3,5Bd: 3,5-dihydroxybenzoic acid.
[c] Data cited from Houel et al. (2006).
[d] PI: loblolly pine.
-: Undetectable

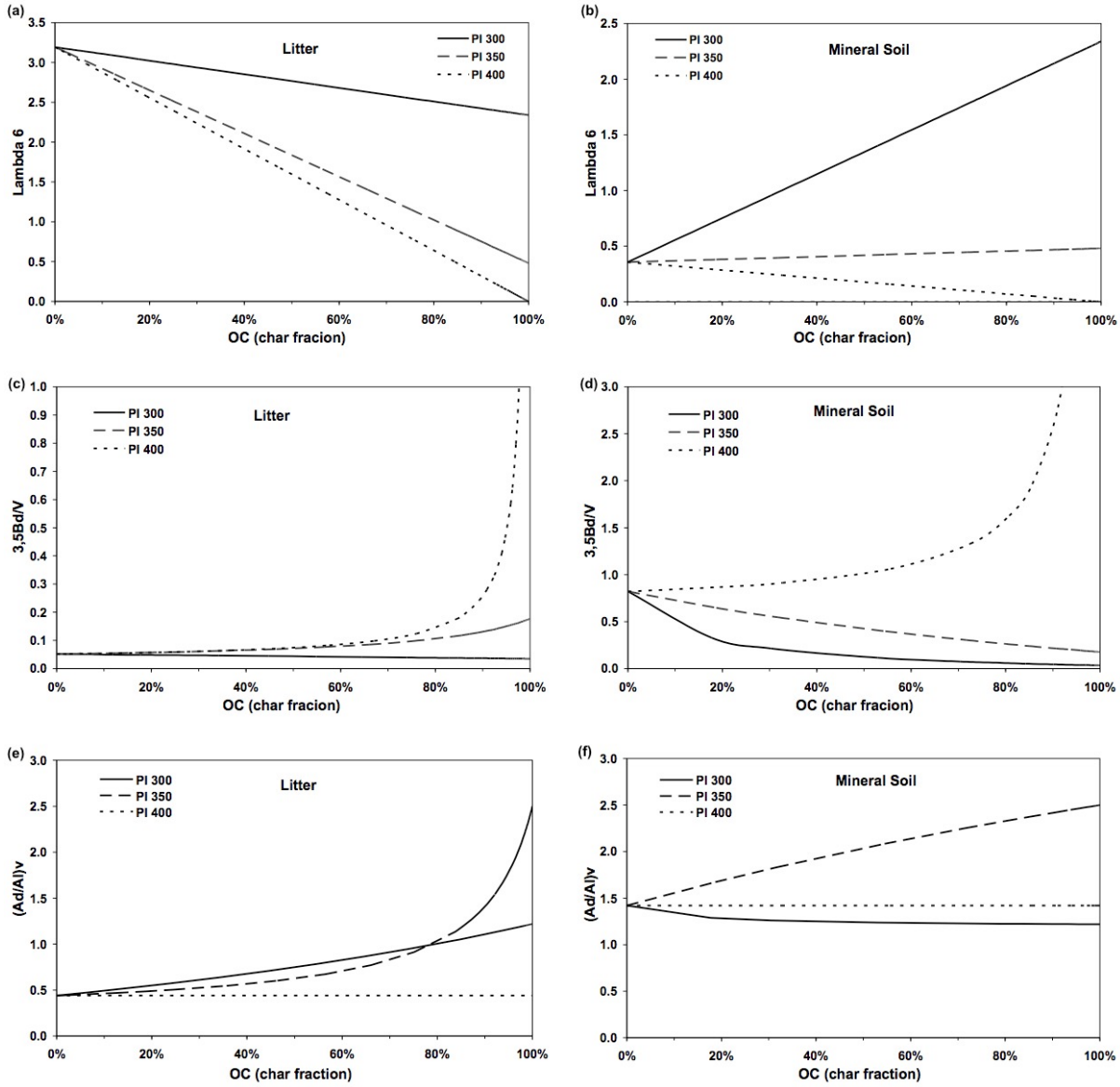

Figure 14. Predictions of (a) λ6 of soil litter; (b) λ6 of mineral soil; (c) 3,5Bd/V of soil litter; (d) 3,5Bd/V of mineral soil; (e) $(Ad/Al)_v$ of soil litter; and (f) $(Ad/Al)_v$ of mineral soil while mixed with increasing amount of 300, 350, and 400°C pine chars (PI 300, 400, and 450, respectively) based on simple two-end-member mixing model.

Figure 14 shows the estimated trends for selected CuO parameters (λ6, 3,5Bd/V, and $(Ad/Al)_v$) in soil litter and mineral soil under increasing char inputs. The lignin yield (λ6) of soil litter and mineral soil are affected differently by the addition of char (Figure 14a,b).

Lignin yields for the soil litter, which is OC-rich and comprised of relatively abundant plant debris (λ6 = 3.2 mg/100 mg OC), decreases continuously (Figure 14a) with the addition of relatively lignin-depleted char (λ6 = 2.3, 0.5, and 0.0 mg/100 mg OC for PI 300, 350 and 400, respectively). In contrast to litter, the mineral soil possesses low OC content and is lignin-poor (λ6 = 0.4 mg/100 mg OC). In this type of soil sample, inputs from PI 300 increases the overall lignin yield, whereas those from PI 350 and 400 result in almost constant and decreasing λ6 signal, respectively, for the mineral soil-char mixture (Figure 14b). This model suggests that the impact of char input on soil lignin yield will greatly depend on both the type of soil and the combustion temperature generating the char particles that reach the soil.

Figures 14c and 14d show the change in 3,5Bd/V in soil-char mixtures. The addition of these char end members does not lead to significant shifts in litter signatures (initial 3,5Bd/V = 0.05) unless they are derived from high temperature and become the predominant OC fraction (> 75%; Figure 14c). This is resulted from the abundance of vanillyl phenols in soil litter, effectively diluting the potential impact of char inputs with high 3,5Bd (Table 6). In the mineral soil (3,5Bd/V = 0.82), char input results in distinct 3,5Bd/V trends depending on the relative difference in biomarker yields among the three chars and mineral soil (Figure 14d). The input of low to mid-temperature chars (PI 300 and 350; 3,5Bd/V = 0.04 and 0,17, respectively) results in decreasing trends, while inputs of high temperature chars (PI 400; 3,5Bd = 0.41 mg/g; V undetectable) lead to an exponential increase in the mixture's 3,5B/V ratio and a significant shift above a char fraction of 60%. Finally, it is notable that our modeling does not include the high temperature charcoals produced > 500°C, which do not possess detectable 3,5Bd and V. Based on our simple mixing model, the input of such high

temperature charcoal to soils/sediments should not affect the 3,5Bd/V ratio but may greatly reduce the OC-normalized lignin value due to its enriched OC content and lack of LOP.

The vanillic acid to vanillin ratio ($(Ad/Al)_v$) of both the litter and mineral soil also shows substantial shifts in signature upon char addition (Figure 14e-f). The substantial increase in the proportion of vanillic acid in the PI 300 and 350 chars (Table 5; $(Ad/Al)_v$ = 1.2 and 2.5, respectively) contribute to a significant increase in the $(Ad/Al)_v$ of the litter-char mixture even at a 20-30% proportion of char inputs. The lack of vanillyls (acid and aldehyde) in the PI 400 char results in no impact, upon char addition, to the $(Ad/Al)_v$ ratio in this modeled mixture. Similarly, no change is observed when this charcoal is mixed with the mineral soil endmember. In contrast, the PI 300 and 350 chars have opposite effects on mineral soil overall $(Ad/Al)_v$ signature with a slight decrease in value under the PI 300 addition and a rapid and large increase under the PI 350 addition. The increase proportion of acid moieties in mineral soil horizons has been well documented in the literature (Kaiser and Guggenberber, 2000; Rumpel et al., 2002; Houel et al., 2006) and suggest that the acid enrichment in deep soils is the result of a combination of processes such as oxidative degradation of lignin, selective dissolution of acid constituents, and their sorption on active mineral sites (aluminosilicates, oxydo-hydroxides) following their vertical transport in soil columns (Kaiser and Guggenberger; Rumpel et al., 2002; Houel et al., 2006). Hence, because of the already high proportion of vanillic acid in mineral soils, only the addition of the most acid-rich chars can lead to substantial increases in $(Ad/Al)_v$ ratios.

Table 7. Elemental compositions, lignin oxidation products values and ratios and levoglucosan yields of two New Mexico soils before and after the control burning. Abbreviations of lignin parameters are the same as Table 5

Soil	Soil 1			Soil 2		
Type	Pre-burn	Post-burn	% change[a]	Pre-burn	Post-burn	% change[a]
N (%)	0.06	0.12	100	0.06	0.17	183
C (%)	0.60	1.48	147	0.55	1.66	202
(C/N)a[b]	11.7	14.4	23	10.7	11.4	7
Σ6 (mg/g)	0.16	0.54	229	0.14	0.43	211
λ6	2.72	3.28	20	2.49	2.57	3
S/V	1.03	0.87	-15	0.97	0.98	1
C/V	0.54	0.41	-24	0.29	0.25	-11
(Ad/Al)v	0.41	0.48	18	0.41	0.44	8
(Ad/Al)s	0.39	0.48	23	0.33	0.38	16
3,5Bd/V	0.08	0.07	-9	0.07	0.07	-3
Cd/Fd	1.39	1.00	-28	0.99	0.92	-7
Levoglucosan (ug/g OC)	141.7	2565.5	1711	60.0	1324.1	2107

[a] % change = (post-burn – pre-burn) (pre-burn)$^{-1}$ (100%)
[b] Atomic C/N ratio

To test the predictions from this simple mixing model, we analyzed two pairs of pre-burn/post-burn soil samples from control burning sites at an experimental station in the desert grassland/scrubland ecosystem of the Sevilleta National Wildlife Refuge (New Mexico, USA). The sites were described previously by Ravi et al. (2007) in a study focused on the link between fire and wind erosion in such arid environments. The vegetation consists of grassland/scrubland with a mosaic of soil patches dominated by grasses and shrubs. Soil samples were collected from the surface (top 2 cm) under the grasses and around the shrubs at several replicated plots before and after the prescribed burning. Table 7 shows the elemental and biomarker information for these soils before and after burning. The pre-burn soils contain low OC contents while their high λ6 and low $(Ad/Al)_v$, $(Ad/Al)_s$, and 3,5Bd/V values point to inputs of fresh plant debris. After the control burn, the OC content in the soils

increases, showing the input of chars or fire induced litter fall from plants (Alexis et al., 2007).

Since the HM and CG samples are the closest to the plant species found in the shrub/grass land cover at these sampling sites, we selected their synthetic chars to test our model on the New Mexico soils (Figure 15). The observed shifts in biomarker signatures (slightly increasing λ6 and $(Ad/Al)_v$ values with stable 3,5Bd/V) can actually only be explained by a mixture of the pre-burn New Mexico soil with a small proportion of char produced at ≤ 250°C (maximum 10-20% depending on the plant source of the char). The order of magnitude increase in levoglucosan concentration (Table 7), an exclusive molecular marker of cellulose/hemicellulose combustion (Simoneit et al., 1999; Elias et al., 2001; Otto et al., 2006), provides strong evidence for inputs of chars to the soils. Because levoglucosan is only present in char produced under low combustion temperature (≤ 350°C), elevated levoglucosan yields in environmental samples thus help confirm inputs from relatively low temperature chars. Moreover, the significant increase in Σ6 in the post-burn soils suggests that these soils predominantly received unaltered or slightly charred plant debris. This observation is in line with the findings of Alexis et al. (2007) who showed that, during prescribed fires in an scrub-oak ecosystem in Florida, USA, the vast majority (~ 75%) of OC released from vegetation to the soil was due to leaf litter fall in the form of unburned tissue.

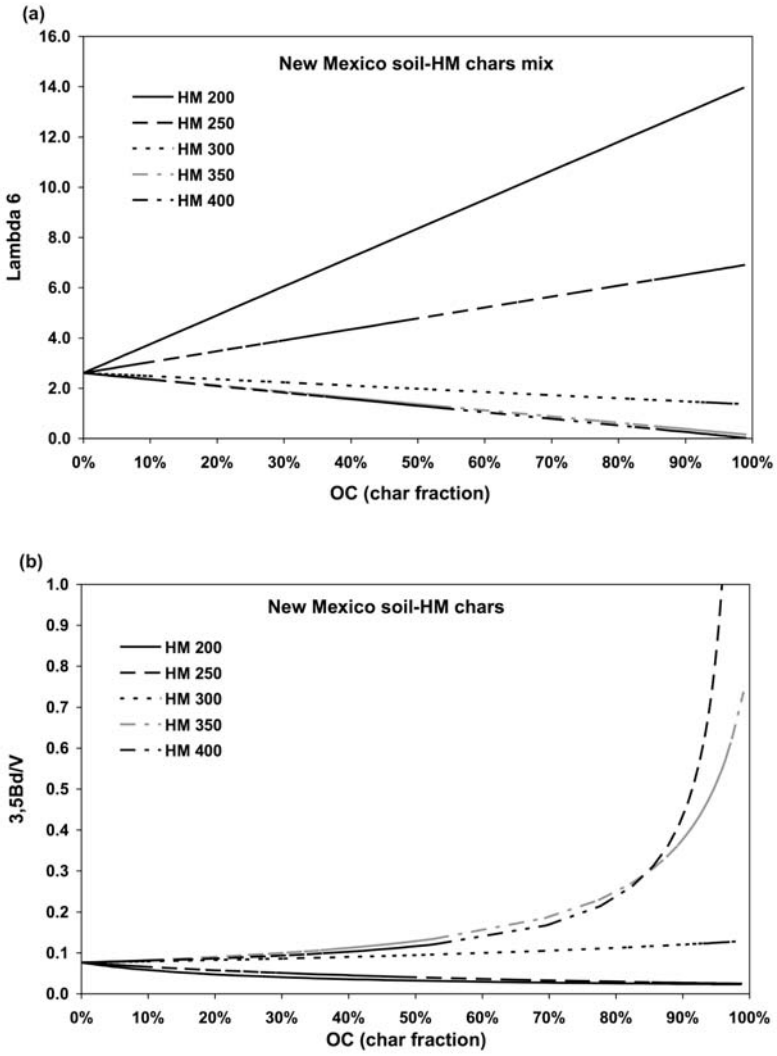

Figure 15. Predictions of (a) λ6; (b) 3,5Bd/V; (c) $(Ad/Al)_v$ of New Mexico soil while mixed with increasing amount of 200, 250, 300, 350, and 400 honey mesquite chars (HM 200, 250, 300, 350, and 400, respectively); (d) λ6; (e) 3,5Bd/V; (f) $(Ad/Al)_v$ of New Mexico soil while mixed with increasing amount of 200, 250, 300, 350, and 400 cordgrass chars (CG 200, 250, 300, 350, and 400, respectively) based on simple two-end-member mixing model.

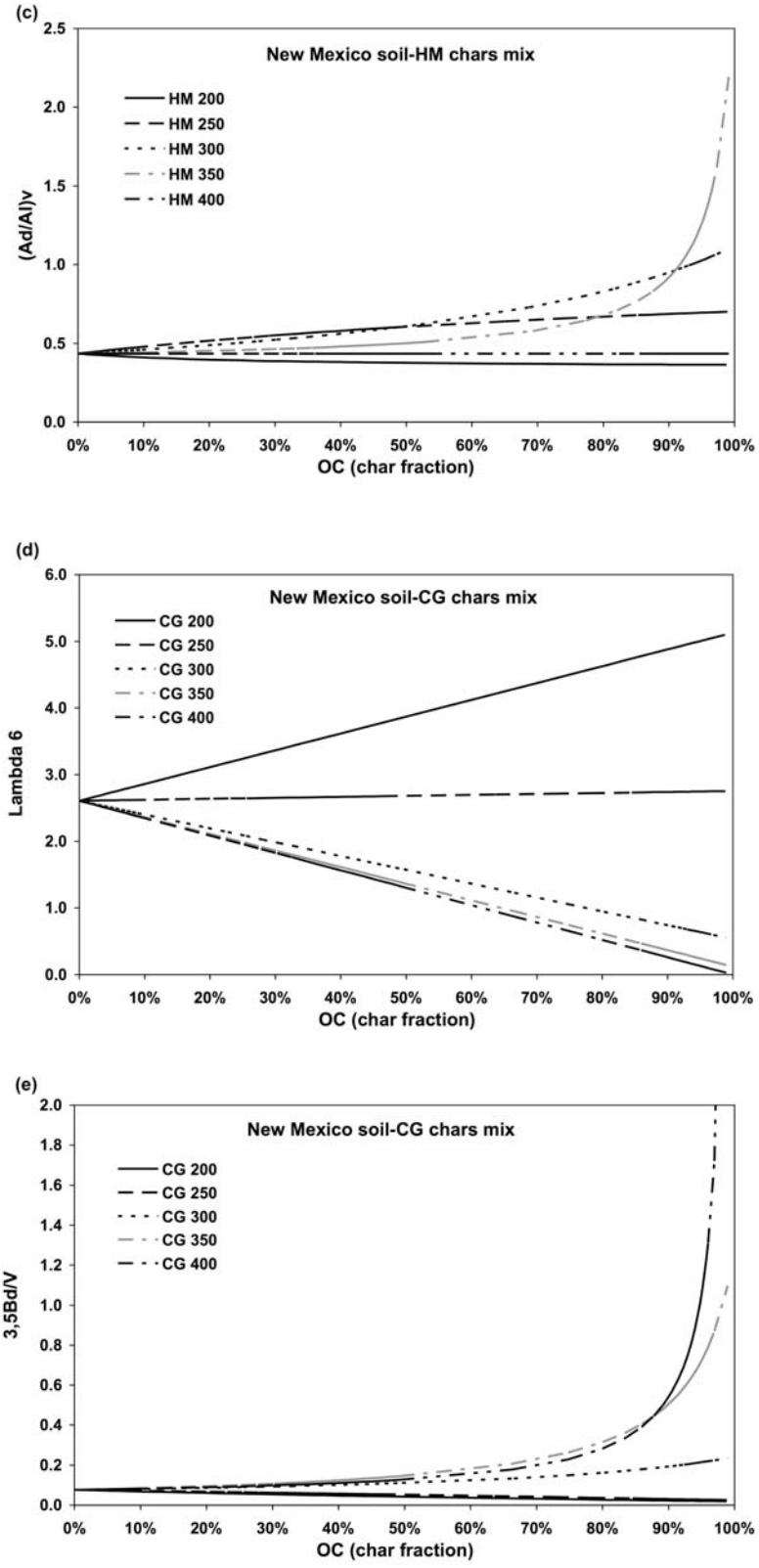

Figure 15 continued.

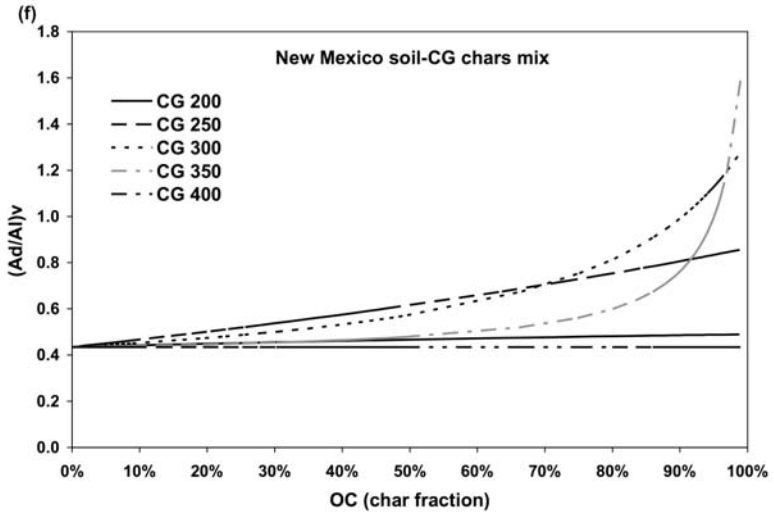

Figure 15 continued.

The above example of New Mexico soils shows that such a mixing model has the potential to roughly assess the fraction of char inputs following a major fire when the LOP data of soil before and right after burning are known. This "environmental reconstruction", however, is presently over simplified and bound to suffer from complex factors such as diverse char inputs (different combustion conditions and/or different parent materials), secondary combustion at the site, alteration of LOP signatures of pre-burn soils due to combustion, and the further decomposition of post-burn soils. An obvious caveat to this application is the difficulty in teasing apart the source inputs from highly degraded, but unburned, soil organic matter with those from high temperature chars. Both would have high $(Ad/Al)_v$ and 3,5Bd/V ratios and relatively low lambda values. One of the main differences expected from major inputs of the latter organic materials, however, would be a higher OC content and significant presence of thermally stable BC. Low temperature chars, on the other hand, should be simultaneously traced by the presence of low-temperature charcoal markers such as levoglucosan. Hence, we acknowledge that a simple modeling application to

distinguish between types of charcoal inputs to natural environmental matrices is fraught with problems and can only be useful when performed in combination with supporting analyses (biomarkers of chars, thermal or chemical oxidation to measure soot-BC). Nevertheless, our results demonstrate that thermal alteration of lignin should be considered in LOP data interpretation when there is positive evidence of char inputs.

3.4. Conclusions

Because of its relative recalcitrant nature and good preservation potential over long timescales, lignin is often used as a proxy for estimating the input of terrestrial OM to diverse environments. However, when lignin undergoes degradation, its signature is modified, complicating its source interpretation. The present study systematically investigated the thermal alteration of lignin by analyzing the CuO-derived LOPs in synthetic chars made from selected angiosperms and gymnosperms under controlled combustion conditions. The results showed that thermal alteration greatly affects the lignin signature even at low temperature, ultimately eliminating the common CuO-derived LOPs (syringyl, vanillyl and cinnamyl phenols) under severe combustion conditions (≥ 400ºC). Furthermore, the observed removal of all these LOPs in chars demonstrates that thermal alteration of lignin is different from biological degradation and photochemical oxidation in that it is predominantly an nonselective degradation process. Our results also showed that three CuO-derived diagenetic indicators, $(Ad/Al)_v$, $(Ad/Al)_s$, and 3,5Bd/V, can provide some qualitative indication of the extent of thermal degradation, with the 3,5Bd/V ratio providing the narrowest temperature range (250-350°C). Because of their altered lignin signatures, substantial inputs of chars to environment mixtures can generate artifacts during the characterization of organic matter native of such mixtures. The results of a simple two-end-member mixing model showed that

the effects of char input will be most influenced by the combustion temperature during char production and the relative difference in biomarker yields between char and soil organic matter. The real situation in environments would be further complicated since natural char from biomass burning is actually a mixture of chars with variable characteristics. Hence, in environments with potential char input, the characterization of terrestrial organic matter source via lignin analysis should probably be confirmed/contrasted with additional biomass combustion markers such as levoglucosan.

4. COMBUSTION-DERIVED HYDROCARBONS IN DEEP BASINS OF PUGET SOUND: HISTORICAL INPUTS FROM FOSSIL FUEL AND BIOMASS COMBUSTION

4.1. Introduction

Black carbon (BC) is the carbonaceous residue from incomplete combustion of organic matter and has been found widely distributed in many surficial reservoirs, such as soils, sediments, waterbodies, and the atmosphere (Goldberg, 1985). It is now recognized that BC can be described as a continuum of physically and chemically heterogeneous materials ranging from slightly charred biomass to highly refractory soot (Hedges et al., 2000; Masiello, 2004; Hammes et al., 2007). Major sources of BC include biomass burning (which produces both char-BC and soot-BC) and fossil fuel combustion (which produces soot-BC). Due to its highly recalcitrant nature, BC can be preserved in environmental matrices for tens of thousands of years and thus represents a stable component in the global carbon cycle (Kuhlbusch, 1998; Masiello and Druffel, 1998; Pessenda et al., 2001; Masiello, 2004; Preston and Schmidt, 2006; Czimczik and Masiello, 2007). Because of its long environmental lifetime and combustion origin, BC is an ideal fire proxy for assessing paleofire history and climate change (Wolbach et al., 1988; Verardo and Ruddiman, 1996; Bird and Cali, 1998; Marlon et al., 2006; Whitlock et al., 2008).

Environmental BC loading has been tied to anthropogenic activities since the industrial revolution due to the associations between combustion practices and the rapid increases in human populations and energy usage (Griffin and Goldberg, 1979; Kralovec et al., 2002; Rose et al., 2003). Recent researches have shown that BC can exert adverse environmental

impacts ranging from local health effects on humans (Lighty et al., 2000; Samet et al., 2004; Radomski et al., 2005) to potentially influence on the Earth's radiation budget (Ramanathan et al., 2001; Hadley et al., 2007). In addition, toxic combustion-derived pollutants such as polycyclic aromatic hydrocarbons (PAHs) can be co-generated with BC and/or adsorb on its surfaces due to BC's high affinities for these aromatic compounds (Gustafsson et al., 1997; Cornelissen et al., 2004; Cornelissen et al., 2005). To understand the linkages between the development of human society and inputs of BC and PAHs to the environment, evaluate the effectiveness of environmental regulations in the past century, and assess current environmental status, researchers have tried to utilize sediment cores to reconstruct the temporal trends of combustion byproducts (Gustafsson et al., 1997; Muri et al., 2002; Buckley et al., 2004; Wakeham et al., 2004; Muri et al., 2006; Louchouarn et al., 2007; Elmquist et al., 2007). These studies have successfully confirmed the significant increase of soot-BC emissions in the early-to-mid 20th century and its later decrease due to changes in fuel usages and improvement of combustion efficiency as well as emission reduction technologies. However, discrepancies in the sedimentary BC records among studies have also been revealed. Cores from different regions show that BC maxima occurred at different times and were generated from different sources. For example, a soot-BC maximum in a rural Swedish lake was observed in 1920, at the same time as PAH molecular signatures suggest predominant wood combustion (Elmquist et al., 2007). In comparison, a sediment core from Central Park Lake in New York City showed that soot-BC peaked around 1950s while molecular and elemental evidences pointed to oil combustion and incineration of municipal solid waste as predominant sources (Louchouarn et al., 2007). Furthermore, the observed BC trends are often not in agreement with the modeling results for historical BC

emissions, which are generally estimated from consumption profiles of different fuels and corresponding average emission factors of BC (Novakov et al., 2003; Ito and Penner, 2005; Bond et al., 2007; Louchouarn et al., 2007). The discrepancies may result from uncertainties in the emission factors of different fuels, various combustion efficiencies from different sectors and also the technology improvement over time (Cooke et al., 1999; Bond et al., 2004; Bond et al., 2007). In addition, BC emission modeling is often performed at a national or continental-scale whereas sedimentary BC profile is often connected to regional or local sources.

While most temporal BC reconstructions were conducted in the eastern US and Europe, studies in the western US are scarce. Recently, Wakeham and collaborators (2004) investigated the vertical distributions of hydrocarbons in a core from Lake Washington, WA. They included a soot-BC analysis in the same core and found that BC and combustion-derived PAHs, both peaked in the 1950s, were contributed by fossil fuel combustion. In the present study, we conducted a more comprehensive investigation on historical BC deposition records from four dated sediment cores in central Puget Sound basin and Hood Canal basin, WA. The metropolitan area of Seattle/Tacoma is located on the eastern shore of the Puget Sound, a major urban coastal system in Pacific Northwest. The population of the three coastal counties (King, Pierce, and Kitsap) around central Puget Sound has grown rapidly over the last 50 years compared to the sparsely populated counties surrounding Hood Canal (State of Washington Office of Financial Management, 2007). We conducted the soot-BC and PAH analyses to construct centennial-scale input trends of combustion-derived products of these cores. In addition, levoglucosan analysis was applied in this study to assess the historical inputs of low temperature char-BC, which is mostly derived from wildfires (Kuo et

al., 2008). PAH diagnostic ratios were also utilized to deduce the potential sources of BC and PAHs. This multi-core, multi-proxy study enables us to identify the spatial and temporal distributions of combustion-derived materials across this region and gain further insight into (i) the effects of urbanization/industrialization on the environmental BC inputs (Puget Sound cores *vs*. Hood Canal cores), (ii) the potential differences in regional BC distribution patterns (Pacific Northwest *vs*. eastern US & Europe), and (iii) the major forcings affecting the production of BC (i.e. climate, human activities).

4.2. Materials and methods

4.2.1. Site description and sediment collection

The central basin of Puget Sound is an urban fjord-like estuary bounded on the north by a sill at Admiralty Inlet (66 m) and on the south by a sill at the Tacoma Narrows (44 m). The main basin stretches 70 km from Whidbey Island in the north to Commencement Bay in the south. Hood Canal is also a glacially carved fjord. It opens from Admiralty Inlet southward about 110 km to the southern terminus. Hood Canal is separated from the Puget Sound main basin by the Kitsap Peninsula. The southern end of Hood Canal is called The Great Bend, which extends eastward into Lynch Cove. The water column in the central basin of Puget Sound reaches a depth of approximately 250 m compared to that in Hood Canal, which ranges from 150 m to < 50 m at The Great Bend.

Figure 16. Satellite image of study area and core locations in Puget Sound, WA.

Sediment cores were collected from four sites in the central basin of Puget Sound (PS-1 and PS-4) and Hood Canal (HC-3 and HC-5; see Figure 16) using a stainless steel, open barrel gravity corer (Kasten corer) as described elsewhere (Brandenberger et al., 2008a,

2008b). Coring was conducted aboard the University of Washington research vessel, RV Barnes. After collection, the cores were subsectioned immediately using an acid-rinsed ceramic knife. Sediment cores from PS-1, PS-4, and HC-5 were sectioned at 2 cm intervals from 0-50 cm, 0-60 cm, and 0-100 cm, respectively, then at 5 cm intervals down to the core catcher. HC-3 core was sampled every 2 cm throughout the entire core. Sectioned sediments were collected in 8 oz. precleaned glass jars and stored in coolers until transport back to the Pacific Northwest National Marine Science Laboratory in Sequim, WA. Each core segment was homogenized and freeze-dried for further analyses.

4.2.2. Methods

4.2.2.1. Graphite black carbon (GBC) analysis

The soot-BC in the sediment was quantified with the GBC method developed by Gélinas et al. (2001) and modified by Louchouarn et al. (2007). Briefly, samples were first treated with 1N HCl for 30 min to remove the carbonates, salts, and sesquioxide coatings. The residue was separated from the supernatant by centrifugation (3000 rpm, 20 min). Silicate minerals were then removed by two successive 12 h treatments with a mixture of 1N HCl and 10% HF in PTFE tubes at room temperature. To remove hydrolyzable organic matter (HOM), the demineralized samples were hydrolyzed by sequential treatments with 2N, 4N and 6N trifluoroacetic acid (TFA) at 100°C for 3 h, 18 h and 18 h, respectively, in glass tubes. Finally, the residual hydrolyzable organic matter was removed with 6 N HCl at 100°C for 24 h. Prior to heating, the solutions and headspaces were purged with N_2 for at least one minute before sealing the tube with a Teflon-lined cap. Following each hydrolysis, the supernatants were separated from the solid residues by centrifugation. The samples were rinsed with nano-pure water after the last TFA treatment and HCl hydrolysis. The residues

were then dried at 60°C in an oven until reaching constant weight. GBC content was then determined with a Vario EL *III* elemental analyzer (Elementar Americas, Inc., Mt. Laurel, NJ, USA) on dried samples that had been combusted at 375°C for 24h to remove all non-soot-BC organic carbon (Gélinas et al., 2001; Louchouarn et al., 2007).

4.2.2.2. PAHs analysis

The analytical procedure for PAHs extraction and quantification follows that stated in Park et al. (2002). Briefly, dry sediment samples were spiked with PAH surrogates (d10-phenanthrene and d10-chrysene) and extracted via pressurized fluid extraction (PFE) with an accelerated solvent extractor (Dionex ASE 200) using dichloromethane at 1500 psi and 100°C. The extracts were then reduced in volume using a water bath and exchanged into hexane. Elemental sulfur in the extracts was removed by treating with pre-cleaned copper powder overnight. The concentrated extracts were then purified using silica gel/alumina column chromatography consisting of 20 g silica gel (deactivated 5% with nano-pure water) and 10 g alumina (deactivated 1% with nano-pure water) with dichloromethane/pentane (1/1 (v/v)) mixture. The resulting extracts were further concentrated and solvent exchanged to 1 mL hexane using a water bath. GC-internal standards (d10-fluorene and d12-benzo(a)pyrene) were added to each sample prior to GC-MS analysis.

The GC-MS system was an Agilent 6890N GC interfaced to an Agilent 5973 Network mass selective detector (MSD). The MSD was operated at 70 eV in selective-ion-monitoring (SIM) mode. A DB5-MS capillary column (J&W, Inc., 30m length, 0.25mm diameter, 0.25 μm thickness) was used to separate the analytes with helium as the carrier gas at a constant flow of 0.8 mL/min. Samples were injected under splitless mode. The injector temperature was maintained at 300°C and the temperature program of the GC oven was 60°C to 150°C at

a temperature ramp rate of 15°C/min, 150°C to 220°C at a temperature ramp rate of 5°C/min, and 220°C to 300°C (10 min isothermal) at a temperature ramp rate of 10°C/min. Data were acquired and processed with the Agilent Chemstation software. Identification of PAHs was based on their retention times and confirmed by the abundance of a secondary ion relative to the molecular ion. Average recoveries of d10-phenanthrene and d10-chrysene were 65±9% and 79±16%, respectively.

4.2.2.3. Levoglucosan analysis

Sediment samples were spiked with the internal standard sedoheptulosan (Simpson et al., 2004) and extracted via pressurized fluid extraction (PFE) with an accelerated solvent extractor (Dionex ASE 200) using a mixture of dichloromethane and methanol (9/1 (v/v)) at 1500 psi and 100°C. The extracts were concentrated in a water bath and treated with pre-cleaned copper to remove elemental sulfur. Samples were then further evaporated to dryness using a LabConco™ solvent concentrator and were redissolved in 500 μL pyridine. An aliquot (75 μL) was transferred into a combusted glass vial to which 75 μL of silylation reagent *N,O*-bis(trimethylsil)trifluoroacetamide (BSTFA) containing 1% trimethylchlorosilane (TMCS) was added. Samples were then derivatized by heating at 75°C for 1 hour in a dry bath.

Separation and quantification of levoglucosan were performed using GC-MS with a Varian Ion Trap 3800/4000 system fitted with a fused silica column (VF 5MS, 30 m x 0.25 mm i.d.; Varian Inc.). Each sample was injected under splitless mode with helium as the carrier gas (1 mL/min). The GC oven was programmed from 65°C (2 min) to 300°C (5 min) at 6°C/min ramp rate. The GC injector and GC/MS interface were maintained at 280°C and 270°C, respectively. The mass spectrometer was operated in the electron ionization (EI, 70 eV) and in selective ion scan (SIS) modes. Data were acquired and processed with the Varian MS Workstation software (version 6.6). Identification of levoglucosan was performed using retention times and by comparing the relative abundance of quantification/confirmation ions in each sample to those produced by authentic standards (levoglucosan, 99%, Aldrich, St. Louis, MO, USA). Quantification was performed using relative response factors adjusted to the internal standard and multiple one-point calibrations (n=6). The analytical precision was derived from replicate analyses of NIST SRM 1649 and 1649a (urban dust) and averaged ~ 5% (Kuo et al., 2008).

Table 8. Data of GBC, OC, levoglucosan concentrations, and porosity of selected sediment sections, and the calculated GBC/OC ratios, GBC and levoglucosan fluxes of four cores

Core	Depth interval (cm)	Estimated Year[a]	OC[a] (%)	GBC (%)	GBC/OC (%)	Levoglucosan (ng g^{-1})	Porosity[a]	GBC flux[b] (mg cm^{-2} yr^{-1})	Levoglucosan flux[b] (ng cm^{-2} yr^{-1})
PS-1	0-2	2004	2.31	0.024	1.0	n.d.	0.87	0.017	
	4-6	2002	2.35	0.028	1.2	81.5	0.86	0.021	6.3
	8-10	1999	2.34	0.028	1.2	104.2	0.85	0.024	8.9
	14-16	1995	2.33	0.030	1.3	n.d.	0.83	0.028	
	18-20	1991	2.27	0.028	1.2	98.6	0.83	0.026	9.4
	24-26	1987	2.25	0.029	1.3	135.1	0.83	0.027	12.7
	32-34	1981	2.21	0.024	1.1	111.9	0.83	0.023	10.6
	36-38	1977	2.34	n.d.		117.4	0.82		11.5
	40-42	1974	2.24	0.025	1.1	132.2	0.82	0.025	13.2
	50-52	1965	2.31	0.030	1.3	104.2	0.82	0.030	10.7
	56-58	1960	2.32	0.027	1.1	135.5	0.83	0.026	13.2
	60-65	1956	2.24	0.035	1.6	108.5	0.83	0.034	10.4
	70-75	1948	2.23	0.034	1.5	159.3	0.81	0.035	16.6
	80-85	1939	2.28	0.029	1.3	110.7	0.80	0.032	12.1
	85-90	1934	2.21	0.024	1.1	82.8	0.80	0.026	9.0
	95-100	1925	2.25	0.026	1.2	103.9	0.80	0.029	11.5
	100-105	1920	2.14	0.026	1.2	127.2	0.80	0.029	14.5
	110-115	1910	2.20	0.027	1.2	n.d.	0.80	0.030	
	120-125	1901	2.22	0.024	1.1	60.1	0.79	0.028	7.1
	130-135	1891	2.05	0.023	1.1	63.9	0.78	0.028	7.7
	135-140	1886	1.85	0.023	1.2	n.d.	0.79	0.027	
	165-170	1858	1.71	0.024	1.4	68.0	0.81	0.026	7.3
	205-210	1822	1.64	0.024	1.5	142.0	0.80	0.026	15.6
	235-240	1793	1.59	n.d.		117.7	0.79		13.8
PS-4	0-2	2005	2.13	0.021	1.0	-	0.87	0.028	
	8-10	2002	2.18	0.028	1.3	n.d.	0.84	0.048	
	12-14	2000	2.21	0.024	1.1	-	0.82	0.045	
	16-18	1998	2.18	0.033	1.5	n.d.	0.81	0.065	
	24-26	1995	2.12	0.031	1.5	n.d.	0.81	0.061	
	36-38	1989	2.13	0.029	1.4	-	0.82	0.054	
	55-60	1979	2.05	0.017	0.8	n.d.	0.79	0.037	
	95-100	1959	2.15	0.022	1.0	-	0.80	0.048	
	105-110	1954	2.04	0.021	1.0	n.d.	0.80	0.044	
	115-120	1949	2.02	0.028	1.4	n.d.	0.79	0.061	
	125-130	1944	1.90	0.020	1.1	-	0.79	0.044	
	130-135	1942	1.89	0.036	1.9	n.d.	0.79	0.080	
	140-145	1937	1.89	0.088	4.7	n.d.	0.78	0.204	
	150-155	1931	2.16	0.029	1.3	n.d.	0.79	0.065	
	160-165	1926	2.20	0.021	1.0	-	0.79	0.047	
	175-180	1918	2.05	0.025	1.2	n.d.	0.79	0.057	
	190-195	1910	1.87	0.024	1.3	-	0.78	0.054	
	215-220	1896	1.67	0.031	1.9	-	0.78	0.073	

Table 8 continued

Core	Depth interval (cm)	Estimated Year[a]	OC[a] (%)	GBC (%)	GBC/OC (%)	Levoglucosan (ng g^{-1})	Porosity[a]	GBC flux[b] (mg cm^{-2} yr^{-1})	Levoglucosan flux[b] (ng cm^{-2} yr^{-1})
HC-3	0-2	2004	2.62	0.024	0.9	433.9	0.91	0.005	8.9
	2-4	2001	2.54	n.d.		283.2	0.88		7.2
	4-6	1998	2.57	0.021	0.8	305.9	0.88	0.005	7.9
	8-10	1992	2.44	0.023	0.9	421.0	0.88	0.006	11.2
	10-12	1989	2.44	n.d.		440.6	0.88		11.5
	12-14	1986	2.46	0.021	0.9	727.9	0.88	0.005	18.7
	18-20	1977	2.44	0.020	0.8	782.4	0.87	0.006	22.0
	22-24	1971	2.56	n.d.		541.9	0.87		15.7
	24-26	1968	2.51	0.023	0.9	393.1	0.86	0.007	12.4
	26-28	1964	2.41	0.022	0.9	334.0	0.86	0.007	10.6
	30-32	1957	2.28	0.021	0.9	299.4	0.85	0.007	9.5
	36-38	1944	2.14	0.019	0.9	263.3	0.84	0.006	9.1
	46-48	1937	2.13	0.016	0.8	379.4	0.84	0.006	13.6
	48-50	1933	2.19	n.d.		541.5	0.84		19.1
	50-52	1929	2.16	0.017	0.8	442.2	0.84	0.006	15.2
	54-56	1921	2.12	0.017	0.8	226.9	0.83	0.006	8.4
	58-60	1913	2.32	0.014	0.6	273.1	0.84	0.005	9.5
	60-62	1909	2.29	n.d.		563.8	0.84		20.2
	62-64	1905	2.32	0.017	0.8	594.8	0.83	0.006	21.7
	64-66	1901	2.31	n.d.		520.5	0.83		19.1
	68-70	1893	2.30	0.018	0.8	69.0	0.83	0.007	2.6
	74-76	1881	2.24	n.d.		93.6	0.83		3.5
	82-84	1865	2.18	0.015	0.7	160.7	0.83	0.006	6.1
	84-86	1861	2.19	n.d.		163.7	0.82		6.3
	88-90	1853	2.19	n.d.		277.7	0.83		10.6
	90-92	1849	2.17	0.016	0.8	372.3	0.83	0.006	14.0
	92-94	1844	2.17	n.d.		183.5	0.83		6.9
	96-98	1836	2.13	n.d.		122.0	0.82		4.8
	102-104	1824	1.95	0.014	0.7	389.1	0.83	0.005	14.5
	104-106	1819	1.97	n.d.		122.8	0.82		4.9
	110-112	1806	2.02	n.d.		125.0	0.81		5.3
	112-114	1801	2.01	n.d.		144.6	0.81		6.1
	116-118	1792	2.03	n.d.		97.8	0.80		4.2
	122-124	1778	1.77	n.d.		100.9	0.80		4.3
	124-126	1773	1.75	0.015	0.8	127.3	0.82	0.006	5.1
	128-130	1765	1.75	n.d.		138.6	0.82		5.6
	132-134	1756	1.77	n.d.		157.0	0.82		6.3
	140-142	1738	1.72	n.d.		175.4	0.80		7.5
	150-152	1714	1.82	0.017	0.9	n.d.	0.80	0.007	
HC-5	0-2	2004	2.48	0.031	1.2		0.88	0.012	
	2-4	2002	2.44	n.d.		104.7	0.87		4.4
	4-6	2000	2.55	0.040	1.6	322.6	0.86	0.019	15.1
	8-10	1996	2.54	0.038	1.5	289.0	0.86	0.018	14.0
	12-14	1991	2.48	0.039	1.6	308.4	0.84	0.021	16.4
	16-18	1986	2.47	0.029	1.2	266.7	0.84	0.015	14.1

Table 8 continued

Core	Depth interval (cm)	Estimated Year[a]	OC[a] (%)	GBC (%)	GBC/OC (%)	Levoglucosan (ng g^{-1})	Porosity[a]	GBC flux[b] (mg cm^{-2} yr^{-1})	Levoglucosan flux[b] (ng cm^{-2} yr^{-1})
HC-5	20-22	1981	2.41	0.035	1.5	195.4	0.83	0.020	11.1
	26-28	1973	2.41	0.041	1.7	255.2	0.84	0.023	14.2
	32-34	1966	2.48	0.035	1.4	258.4	0.83	0.019	14.5
	36-38	1961	2.48	0.033	1.3	283.7	0.84	0.018	15.7
	40-42	1955	2.38	0.032	1.4	n.d.	0.83	0.019	
	42-44	1953	2.26	n.d.		162.7	0.83		9.5
	46-48	1947	2.30	0.032	1.4	254.9	0.82	0.019	15.2
	50-52	1942	2.20	0.031	1.4	79.4	0.82	0.019	4.9
	54-56	1936	2.19	0.029	1.3	n.d.	0.82	0.018	
	56-58	1933	2.19	n.d.		112.1	0.82		6.9
	62-64	1925	2.06	0.030	1.4	305.3	0.81	0.019	19.1
	66-68	1920	2.05	0.029	1.4	165.5	0.82	0.018	10.1
	72-74	1911	2.13	0.025	1.2	163.4	0.82	0.016	10.0
	76-78	1906	2.07	n.d.		103.0	0.82		6.2
	78-80	1903	2.15	0.029	1.4	210.0	0.83	0.017	12.3
	84-86	1895	2.14	n.d.		199.3	0.82		12.3
	88-90	1889	2.18	0.026	1.2	n.d.	0.82	0.016	
	90-92	1886	2.20	n.d.		163.5	0.81		10.5
	94-96	1880	2.13	0.026	1.2	n.d.	0.81	0.017	
	100-105	1869	2.14	n.d.		196.1	0.81		12.8
	110-115	1854	2.09	0.025	1.2	167.4	0.81	0.016	10.9
	115-120	1847	n.d.	n.d.		157.7	0.79		11.1
	120-125	1839	2.11	n.d.		201.0	0.81		13.1
	135-140	1818	2.05	0.026	1.2	n.d.	0.83	0.015	
	205-210	1715	2.03	0.026	1.3	n.d.	0.79	0.018	

a. Data from Brandenberger et al. (2008a, b).

b. Sediment accumulation rates (±1σ) (g cm^{-2} yr^{-1})for flux calculation: PS-1: 0.556±0.052; PS-4: 1.05±0.048; HC-3: 0.218±0.030; HC-5: 0.337±0.018 (Brandenberger et al., 2008a, b).

-: not detected.

n.d.: not determined.

4.3. Results and discussion

4.3.1. Temporal profiles of combustion-derived products in Puget Sound/Hood Canal cores

4.3.1.1. Puget Sound cores

The level of GBC contents in two Puget Sound cores ranged between ~0.02 to 0.09% (Table 8). The observed GBC levels are comparable to the reported GBC content in a sediment core from the nearby Lake Washington, WA (~0.02-0.06%, Wakeham et al., 2004), as well as the Washington coast sediments (~0.01-0.08%, Dickens et al., 2004). However, the GBC levels in Puget Sound cores are 1-2 orders of magnitude lower than the reported BC contents in sediment cores from urban lakes in New York City and Boston (Gustafsson et al., 1997; Louchouarn et al., 2007).

In the present study, GBC fluxes were calculated for a better comparison of the temporal variation in GBC inputs among different cores. The calculation of flux can eliminate the potential interferences from the concurrent input of any larger detrital material that would dilute the concentration of the interested minor components in each sediment interval. Equation (3) was used in the flux calculation:

$$F = C \times \rho_D \times (1 - \phi_h) \times R \qquad \text{(eq. 3)}$$

where F is the flux of GBC (mg cm^{-2} yr^{-1}); C is the GBC concentration (mg g^{-1}); ρ_D is the dry density (g cm^{-3}) ; ϕ_h denotes the porosity at depth h; R is the sedimentation rate (cm yr^{-1}). Large differences in GBC fluxes were observed between PS-1 and PS-4 (Figure 17a,b, Table 8). Throughout the entire core, the GBC fluxes in PS-4 are higher than those corresponding sections of PS-1. Because there is not much difference in GBC concentrations in these two cores except for the GBC maximum in PS-4 (0.024-0.035 and 0.017-0.036 % for PS-1 and PS-4, respectively), the distinct GBC fluxes result from their distinct sedimentation rates (1.2

and 2.1 cm yr^{-1} for PS-1 and PS-4, respectively, Brandenberger et al., 2008a,b). The pre-industrial GBC fluxes in PS-1 (0.026 mg cm^{-2} yr^{-1}) are comparable to those in Stora Frillingen Lake in Sweden (0.029 mg cm^{-2} yr^{-1}) and Solvenian mountain lakes (0.025-0.075 mg cm^{-2} yr^{-1}) (Muri et al., 2006; Elmquist et al., 2007). The GBC fluxes in the two Puget Sound cores showed a major peak in 1940s-1950s. After this peak, GBC fluxes dropped dramatically toward the surface, with the exception of a second peak in the 1980s-1990s observed at both sites (Figure 17a,b). The magnitude of the GBC flux maximum in PS-1 (0.035 mg cm^{-2} yr^{-1}) is similar to the historical peak of BC flux in Stora Frillingen Lake observed around 1920s (~0.04 mg cm^{-2} yr^{-1}, Elmquist et al., 2007). The GBC flux maximum in PS-4 (0.20 mg cm^{-2} yr^{-1}) is about 6-fold higher than the maximum value in PS-1 and is the highest GBC flux observed in this study. A sediment core with a similar flux of BC was found in an urban lake near central Stockholm, Sweden (~0.2 mg cm^{-2} yr^{-1}, Routh et al., 2004).

(a)

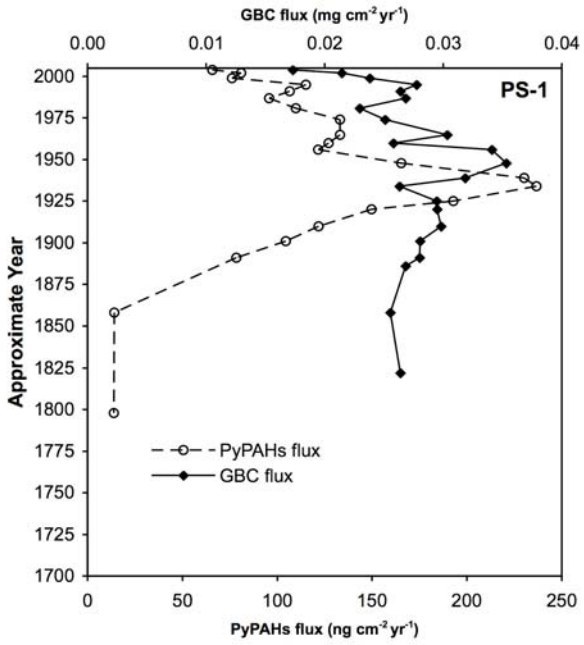

(b)

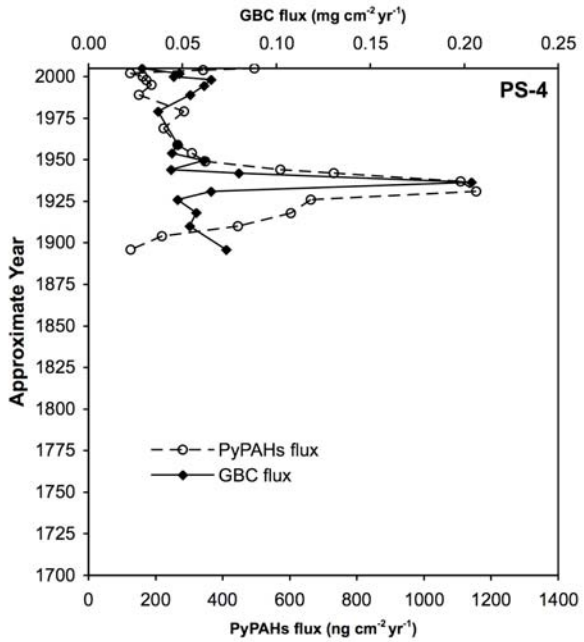

Figure 17. Temporal profiles of fluxes of graphite black carbon (GBC) and total combustion PAHs (PyPAHs) for (a) PS-1, (b) PS-4, (c) HC-3, and (d) HC-5.

(c)

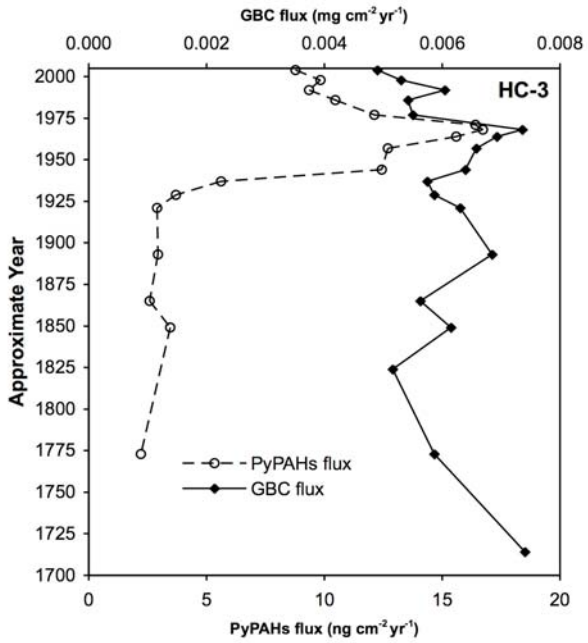

(d)

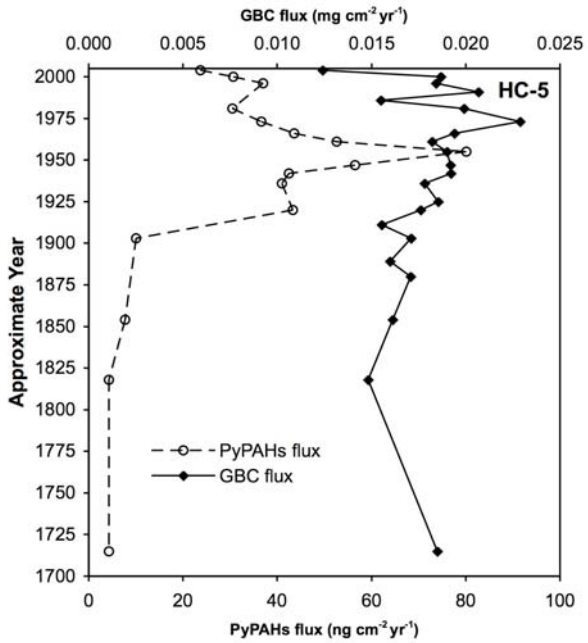

Figure 17 continued.

The temporal flux profiles of total combustion PAHs (PyPAHs) of PS-1 and PS-4 are also shown in Figure 17a,b. Total combustion PAHs are the summation of fluoranthene (Fl), pyrene (Py), benzo[*a*]anthracene (BaA), chrysene (Chy), benzo[*b*]fluoranthene(BbF), benzo[*k*]fluoranthene (BkF), benzo[*a*]pyrene (BaP), indeno[1,2,3-*c,d*]pyrene (InP), dibenz[*a,h*]anthracene (DBA), and benzo[*g,h,i*]perylene (BghiP). The concentrations of individual PAHs are listed in Table 9. In both cores, PyPAHs fluxes increased steeply and synchronously after 1850s (based on PS-1) and reached maxima during the 1930s-1940s. The fluxes then experienced a ~50% decrease during 1940s-1960s, followed by a slight increase in 1970s, and decreased again in 1970s-1980s. In recent decades, PS-1 shows a slight increase in PyPAHs around 1990s followed by a decrease in the surficial sediments. In contrast, PS-4 showed relatively constant fluxes of PyPAH during the 1990s before an abrupt increase in recent years. The observed timing of PAH flux maxima in our study match well with prior findings for the same region. An earlier study by Lefkovitz et al. (1995) investigated the historical trends of metals and organic contaminants at the same sites as those from PS-1 and PS-4. The combustion PAH maxima in these earlier cores also occurred in the 1930s-1940s. In addition, the peak values reported in this earlier study (1516 and 6788 ng/g for cores in PS-1 and PS-4 locations, respectively) are comparable to the PyPAH concentration maxima from the present study (2170 and 5144 ng/g for PS-1 and PS-4, respectively). The accordance between these two sets of cores confirms the synchronous changes in anthropogenic inputs to this system during the 20th century and the valid geochronological dating of these cores. Similar results have been reported for heavy metals and terrestrial OM inputs to the cores from central Puget Sound basin by Brandenberger et al. (2008a). Our results are also consistent with earlier studies that reported PAH maxima in the

1940s in sites from the central Puget Sound basin close to Seattle and Tacoma (Bates et al., 1984; Barrick and Prahl, 1987). In the present study, the concurrent GBC and combustion PAHs maxima point to the strong inputs from combustion sources in Puget Sound. This may be attributed to the high coal usage for domestic heating in the Seattle/Tacoma area at that time (Bates et al., 1984; Barrick and Prahl, 1987; Lefkovitz et al, 1995). Indeed, the US historical energy consumption trend shows that coal was the dominant energy source from late 19th to mid-20th century and that prior to 1970, coal consumption peaked in the 1910s-1920s and 1940s (Figure 18a). We didn't find a significant peak in PyPAHs during the 1910s-1920s in Puget Sound cores though PS-4 shows a small hump during that period (Figure 17b). Therefore, this potential PAH peak was probably overshadowed by the steep increase in PAHs in the early 20th century due to the urbanization of Seattle/Tacoma area. Interestingly, our GBC profiles do show a small peak in 1910s-1920s (Figure 17a,b), presumably resulting from coal combustion.

The sharp decline in PyPAHs fluxes during the 1940s-1960s, together with the concurrent drop in GBC fluxes, might be due to a lower dependence on coal for domestic heating and the dominant energy switchover to petroleum (Figure 18a) as well as changes in technologies leading to more efficient combustion (Novakov et al., 2003). In Washington State, starting in the 1930s, coal production and consumption declined markedly due to the development of hydroelectricity as an alternative energy source. Washington is known for its abundant hydroelectric resources and it is the leading hydroelectric power producer in the US. During 1930s-1970s, the coal production in Washington dropped from over 2 million short tons to only 37000 short tons (State coal profile, EIA, 1994). The slight PyPAHs increases in 1970s in Puget Sound cores, in agreement with the observations in a sediment

core from Pettaquamscut River in Rhode Island (Lima et al., 2003), probably correspond to a petroleum usage peak during that time (Figure 18a). The further decrease in PAH fluxes during the 1970s-1980s, which brought the PAH flux back to the levels of the early 1900s, might be due to the OPEC oil embargo and the use of catalytic converters in vehicles (Lima et al., 2003). The Washington State smoke management plan, which was enacted in 1970, also contributed to the reduced PAHs emissions (Fahnesstock and Agee, 1983).

The relatively constant PyPAHs flux in 1990s in PS-4 is similar to the observations in Lake Michigan and Pettaquamscut River (Schneider et al., 2001; Lima et al., 2003), showing the stabilized inputs of combustion PAH. However, GBC fluxes of PS-4 show a significant peak during this period (Figure 17b). PS-1, in contrast, showed peaks in both PAH and GBC fluxes in the same timeframe. Further discrepancy between PS-1 and PS-4 was shown in the most recent sediments. The continuous decline in both PAHs and GBC fluxes in PS-1 are similar to the findings in Lake Washington (Wakeham et al., 2004). In contrast, PyPAHs fluxes in PS-4 return to the levels observed during the early-to-mid 20th century. Since the corresponding GBC trend went in the opposite direction, the observed high PAHs in the recent years is not likely the results of remobilization of old sediments from other sites. It also should be noted that during 2003-2004 dredging activities in the Lower Duwamish Waterway, a highly contaminated (PAHs, PCBs, phthalates) Superfund site located south of Elliot Bay near downtown Seattle, were undertaken. The remobilization of contaminated sediments during dredging could have contributed to the observed high PAHs in PS-4. However, this possibility is unlikely since PCB analysis of 1998-2004 sediments in PS-4 did not show elevated PCB levels concomitant with high PAH levels. Notably, Van Metre and collaborators (2000, 2005) also reported an increasing trend of PAH concentrations in

recently deposited sediments from many urban lakes (mostly in intensive urbanized watersheds) around the US, including Lake Ballinger in north Seattle. The authors attributed the recent rises in PAH concentrations to the increase in vehicle traffic and large changes in urban land use. PS-4 may resemble the features of Lake Ballinger due to its location (close to Seattle). Further evidence for this hypothesis is provided in the following discussions on PAH signatures.

(a) (b)

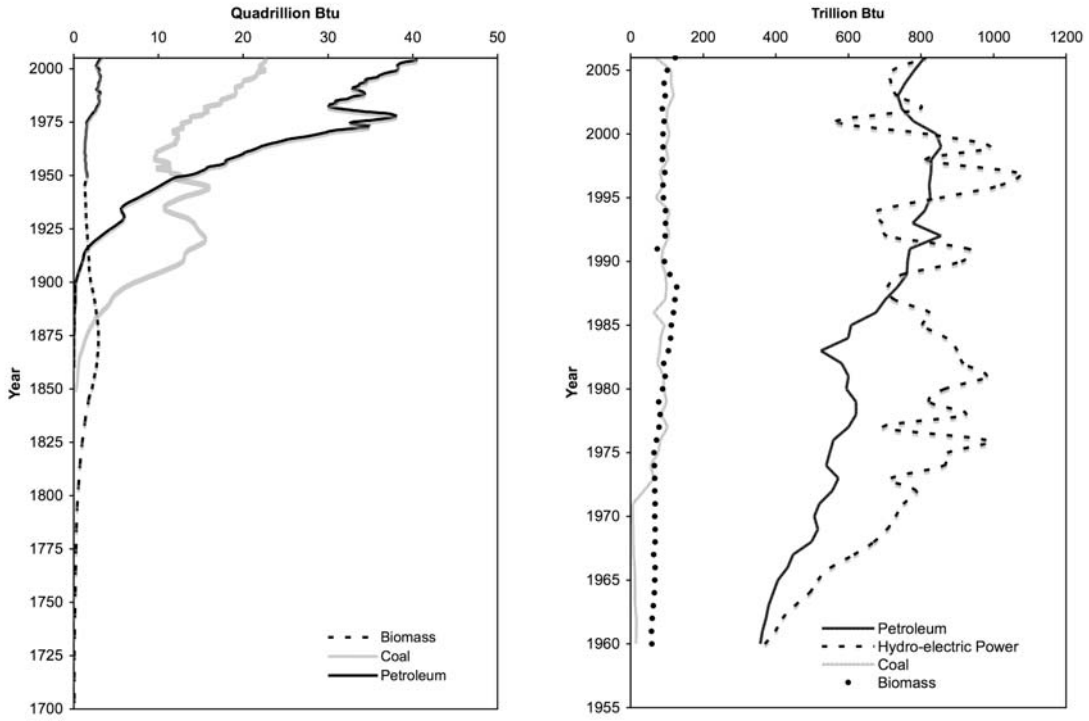

Figure 18. Historical energy consumption profile of (a) United States (Energy Information Administration, 2007), and (b) Washington State (1960-2006) (State energy consumption extimates, EIA, 2006).

Table 9. Measured PAH concentration (ng/g dw) in four dated Puget Sound/Hood Canal cores. The explanation of abbreviation[a] of each PAH is listed in the bottom

Core	Depth (cm)	Estimated year	Phe	An	MP	DMP	1-MP	2,6-DMP	1,7-DMP	Fl	Py	Ret	BaA	Chy	BbF	BkF	BeP	BaP	InP	DBA	BghiP
PS-1	0-2	2004	163.0	40.8	245.7	296.2	92.6	33.9	164.2	172.9	193.0	710.0	52.5	77.1	120.6	37.3	74.4	67.6	75.8	13.4	84.8
	4-6	2002	426.4	63.7	362.5	277.8	128.0	34.8	147.4	207.4	194.9	685.2	73.2	122.0	149.0	45.2	89.0	82.8	76.6	12.9	82.2
	8-10	1999	165.9	40.6	225.1	273.4	82.2	30.4	147.4	175.9	185.7	686.6	57.3	86.3	122.9	37.7	75.5	68.0	70.5	11.6	77.8
	14-16	1995	804.7	74.8	515.7	361.5	176.2	47.7	176.8	269.1	274.6	756.1	79.3	106.7	150.5	45.9	93.9	93.2	93.8	16.0	102.8
	18-20	1991	193.4	42.3	262.2	331.3	96.7	35.7	176.3	202.0	232.5	810.5	76.3	106.6	152.3	46.8	95.9	88.2	96.4	13.4	106.9
	24-26	1987	442.9	51.0	340.3	283.6	120.3	34.6	145.7	199.4	206.5	685.7	63.1	93.6	140.2	44.4	87.8	83.1	84.3	12.1	91.8
	32-34	1981	168.4	44.3	289.6	376.4	102.5	43.2	182.1	205.1	252.7	779.7	73.3	105.8	160.4	48.8	96.6	87.7	98.9	14.6	115.3
	40-42	1974	1400.8	99.2	861.1	466.0	272.7	65.1	201.9	306.3	320.4	839.8	76.3	114.0	158.3	52.6	97.8	90.4	93.2	13.8	111.1
	50-52	1965	178.2	50.1	275.3	347.8	99.2	39.0	182.0	218.4	273.3	847.1	88.5	120.3	175.9	53.6	113.4	98.8	115.9	16.1	133.6
	56-58	1960	177.0	53.0	295.9	361.1	109.6	39.8	205.3	222.8	293.5	922.0	87.9	117.9	175.1	53.9	114.2	102.1	110.6	14.5	126.6
	60-65	1956	169.8	48.2	282.4	368.6	107.2	37.1	199.4	198.7	266.2	884.1	86.6	119.2	170.8	52.7	111.2	102.2	114.9	18.6	133.6
	70-75	1948	217.6	62.3	366.6	480.5	140.9	49.3	278.7	264.5	359.8	1326.7	112.5	142.8	187.0	57.5	125.3	135.9	145.5	19.9	166.1
	80-85	1939	266.2	77.1	434.1	560.3	163.0	57.0	309.3	350.1	496.3	1473.8	144.1	180.0	236.6	77.9	161.7	179.8	191.6	24.0	221.4
	85-90	1934	341.5	77.3	478.2	585.1	188.4	60.2	360.4	381.1	531.9	1780.9	145.8	177.5	239.7	81.6	160.3	181.4	185.8	24.4	221.8
	95-100	1925	302.6	71.8	522.5	696.6	220.1	69.2	462.2	306.2	394.5	2167.4	124.9	151.9	195.2	62.7	127.7	142.6	155.2	20.9	179.4
	100-105	1920	235.9	58.3	559.6	814.8	231.6	79.1	519.2	236.5	299.2	2426.3	98.5	113.6	148.2	48.2	91.8	103.6	112.4	14.9	137.3
	110-115	1910	371.6	60.0	805.0	1138.6	355.9	106.8	790.4	233.8	258.4	3782.0	83.0	107.1	116.3	37.5	75.2	77.5	78.1	0.0	98.6
	120-125	1901	390.4	57.1	852.0	1157.0	352.5	106.2	797.7	213.7	234.1	5202.3	59.0	82.0	81.1	31.8	53.5	57.3	52.9	0.0	66.3
	130-135	1891	936.5	79.0	798.7	673.0	284.1	69.7	416.6	169.8	160.3	2985.8	44.5	63.3	63.4	20.7	35.2	38.1	36.9	5.6	45.1
	165-170	1858	890.8	35.6	440.9	160.0	121.0	27.7	35.0	54.6	43.0	68.3	3.9	13.3	7.9	1.6	5.3	0.0	2.0	0.0	5.2
	230-235	1798	774.9	27.5	389.2	143.1	105.9	25.1	30.2	48.4	41.9	54.7	2.7	10.5	5.8	1.1	4.5	0.0	1.3	0.0	4.1
PS-4	0-2	2005	476.1	127.4	357.7	264.9	104.6	37.5	74.6	714.4	861.3	189.6	247.9	326.5	379.3	116.6	250.9	335.9	288.7	42.7	306.5
	2-4	2004	343.4	68.0	318.9	199.9	87.8	29.8	51.3	484.8	628.9	195.1	157.1	214.8	232.9	89.8	156.5	209.0	170.1	22.1	184.6
	8-10	2002	167.9	33.0	181.4	183.8	55.3	23.1	60.6	153.0	160.7	218.4	41.6	73.4	92.8	32.7	55.7	53.8	51.3	10.0	61.8
	12-14	2000	210.2	30.6	181.1	140.5	56.1	21.1	43.1	167.0	184.4	190.4	56.5	89.7	110.6	36.2	68.7	72.4	61.0	10.0	74.3
	16-18	1998	286.7	41.2	230.7	161.0	67.9	23.9	53.1	188.5	200.7	219.6	50.7	76.9	108.4	38.8	65.3	67.6	62.6	10.2	74.1
	24-26	1995	2338.1	162.2	1047.5	333.1	294.6	54.2	81.0	242.7	239.6	223.2	52.0	83.6	103.4	35.1	62.4	56.9	56.3	9.9	59.1
	36-38	1989	785.5	54.5	474.0	258.4	148.1	35.8	80.7	204.5	192.7	239.2	43.0	66.9	94.9	30.9	55.4	51.5	50.0	7.5	57.5
	55-60	1979	176.2	41.7	168.1	143.8	53.3	20.3	55.3	249.6	299.8	233.0	86.4	125.7	161.0	53.4	96.8	105.3	99.1	14.9	114.4
	75-80	1969	152.1	40.1	175.0	169.1	54.7	22.6	61.1	188.6	239.1	222.9	72.9	102.2	144.9	52.4	88.3	86.2	87.8	14.3	103.9
	95-100	1959	155.2	40.8	196.7	197.9	61.5	25.2	65.4	209.6	280.7	227.6	83.1	120.1	167.6	58.6	107.4	100.1	105.0	13.1	115.0

Table 9 continued

Core	Depth (cm)	Estimated year	Phe	An	MP	DMP	1-MP	2,6-DMP	1,7-DMP	Fl	Py	Ret	BaA	Chy	BbF	BkF	BeP	BaP	InP	DBA	BghiP
PS-4	105-110	1954	192.0	49.2	177.4	163.7	50.8	21.9	58.9	211.2	305.5	253.5	97.4	134.8	189.0	68.2	121.8	125.2	130.9	19.0	150.8
	115-120	1949	347.7	65.2	292.7	225.9	90.3	32.3	81.3	316.3	416.6	323.9	90.3	128.7	171.5	60.2	114.7	110.2	124.3	13.4	132.0
	125-130	1944	286.4	76.7	262.4	227.0	78.8	30.1	82.8	444.5	657.7	317.1	170.8	228.4	286.0	87.8	201.3	220.4	226.7	28.0	252.9
	130-135	1942	375.9	106.9	329.7	307.6	99.4	41.9	102.7	593.6	868.0	400.3	217.0	275.5	329.2	121.0	228.2	270.7	261.2	34.8	285.2
	140-145	1937	544.7	144.8	412.8	316.0	127.1	43.7	113.2	887.6	1332.3	421.8	289.8	384.7	471.5	165.4	329.4	400.7	393.5	47.7	429.1
	150-155	1931	566.8	147.8	458.0	360.7	135.1	45.2	126.1	917.4	1459.9	506.1	293.8	401.7	498.2	152.1	344.5	437.0	433.8	56.5	493.5
	160-165	1926	363.7	98.7	338.8	286.5	110.3	37.8	121.1	458.3	720.1	494.0	198.4	263.0	326.4	100.1	219.4	267.8	267.5	33.9	299.7
	175-180	1918	615.1	118.6	584.5	470.2	189.9	58.1	205.3	477.6	682.6	799.9	194.9	246.4	278.8	90.7	181.4	220.5	215.8	25.9	235.3
	190-195	1910	2180.3	193.5	967.3	444.5	286.5	55.4	178.6	344.0	458.5	850.9	170.0	201.0	209.7	78.8	129.6	161.6	142.4	19.8	159.9
	200-205	1904	501.3	67.5	467.5	371.2	150.4	47.1	169.2	252.5	204.5	860.0	58.6	76.3	95.4	34.1	51.9	53.5	61.6	6.1	56.8
	215-220	1896	227.8	31.3	249.7	228.3	83.5	26.3	108.1	140.0	121.4	664.2	31.3	42.1	58.5	23.3	31.9	31.2	38.4	4.3	41.0
HC-3	0-2	2004	145.4	21.8	236.6	345.1	70.3	39.3	97.8	98.1	141.6	183.0	15.1	26.5	37.1	12.9	25.0	22.1	31.7	6.6	37.0
	4-6	1998	124.5	18.6	108.5	87.7	32.0	11.6	25.7	88.9	101.0	117.4	13.5	23.6	42.1	12.8	25.7	23.6	31.1	6.3	39.5
	8-10	1992	111.5	16.5	149.9	161.2	46.5	22.0	51.2	78.4	93.8	119.7	13.1	23.7	38.9	12.4	24.1	20.0	29.6	4.7	36.9
	12-14	1986	122.7	19.0	110.0	100.0	33.7	13.8	32.1	95.8	117.3	123.0	14.5	25.1	42.3	12.7	25.4	21.1	33.5	5.1	39.5
	18-20	1977	141.7	20.2	155.5	158.2	46.2	19.4	46.1	95.3	119.8	120.2	15.4	26.9	48.3	15.1	29.1	22.7	38.5	4.7	44.7
	22-24	1971	124.8	22.2	136.2	157.6	43.3	19.1	47.8	129.3	180.2	215.2	19.6	33.3	55.3	16.9	36.0	28.7	44.1	5.7	53.2
	24-26	1968	124.1	23.4	118.0	108.9	35.9	14.6	38.7	118.6	158.7	164.3	18.5	30.5	55.1	17.5	33.4	27.7	43.1	6.0	53.3
	26-28	1964	113.8	19.1	119.4	113.8	36.4	14.5	36.6	107.7	147.8	154.2	17.8	30.1	49.2	17.0	30.6	25.8	41.9	5.2	50.8
	30-32	1957	105.9	15.8	104.0	97.1	33.3	13.5	32.8	86.8	111.8	130.9	13.9	23.7	40.9	12.4	24.4	22.7	37.0	3.8	45.9
	38-40	1944	158.9	12.9	161.6	197.6	54.7	24.5	59.5	88.0	142.8	296.1	12.0	19.5	24.5	10.5	14.3	15.0	21.8	3.7	27.9
	46-48	1937	69.8	6.9	98.4	114.2	29.2	15.5	30.0	32.5	75.0	107.5	4.1	12.1	10.2	3.5	6.2	0.0	7.1	1.9	10.7
	50-52	1929	107.9	7.4	178.6	200.2	55.2	25.8	55.6	28.0	38.7	95.1	3.4	10.0	8.6	2.7	6.0	0.0	5.2	1.5	9.4
	54-56	1921	98.8	5.8	98.4	82.9	28.0	12.7	23.7	17.6	40.7	99.7	1.8	7.3	4.9	0.6	3.0	0.0	1.3	0.0	4.0
	68-70	1893	84.2	4.8	90.0	96.2	29.0	11.9	28.1	19.9	32.5	103.7	2.9	9.1	4.9	1.6	3.4	0.0	2.4	0.0	4.7
	82-84	1865	60.2	4.3	81.3	85.8	25.6	11.0	23.5	15.5	31.9	88.4	1.8	8.1	4.4	1.1	3.1	0.0	1.4	0.0	4.2
	90-92	1849	83.5	6.2	230.3	339.8	72.8	38.1	91.6	21.0	50.3	109.6	2.2	8.8	3.9	1.2	2.7	0.0	1.3	0.0	3.3
	124-126	1773	135.9	8.1	91.9	57.8	27.0	8.5	14.0	13.9	11.4	64.3	2.0	6.6	5.0	2.4	4.9	0.0	4.3	2.7	6.9
HC-5	0-2	2004	1827.9	130.5	917.8	302.9	254.5	48.1	62.4	184.6	171.1	127.1	19.3	36.7	49.6	17.9	30.1	28.2	31.3	6.8	41.3
	4-6	2000	2233.6	112.7	1099.1	379.9	317.1	63.4	81.8	244.1	182.5	141.5	18.9	37.8	50.1	16.5	29.5	26.3	32.6	5.0	40.1
	8-10	1996	2958.1	145.6	1486.1	459.9	438.3	86.1	94.3	321.6	221.6	135.7	20.0	38.7	48.4	15.1	29.6	24.5	30.2	4.7	37.3
	20-22	1981	139.1	21.9	154.9	123.5	46.2	18.1	34.7	121.2	121.5	114.0	26.4	44.4	66.6	21.4	40.8	35.4	42.0	6.0	51.2

Table 9 continued

Core	Depth (cm)	Estimated year	Phe	An	MP	DMP	1-MP	2,6-DMP	1,7-DMP	Fl	Py	Ret	BaA	Chy	BbF	BkF	BeP	BaP	InP	DBA	BghiP
HC-5	26-28	1973	1260.7	82.1	518.1	201.8	142.9	32.5	51.5	163.6	160.8	128.1	30.6	50.5	74.0	27.8	46.5	38.0	46.5	7.1	60.2
	32-34	1966	991.6	74.3	587.4	241.9	179.1	40.0	57.2	214.2	193.1	131.6	30.4	55.3	83.6	27.9	52.4	44.3	54.6	7.4	68.5
	36-38	1961	1815.7	128.9	903.6	313.2	262.4	51.6	70.3	267.3	243.7	140.3	38.3	58.6	91.4	30.5	59.5	54.6	69.7	9.3	88.6
	40-42	1955	5065.8	232.7	2359.4	630.1	678.7	110.5	118.8	480.3	377.2	163.8	42.9	67.6	96.9	36.6	64.5	62.8	82.8	10.4	101.1
	46-48	1947	1333.4	76.4	663.6	255.3	199.0	40.6	62.6	242.3	221.5	155.8	37.3	59.6	93.9	33.1	62.1	62.3	83.3	9.1	105.7
	50-52	1942	130.8	22.5	134.2	115.8	40.8	15.2	37.8	136.7	146.9	151.3	32.2	49.0	79.8	31.4	49.6	47.1	69.9	7.1	87.8
	54-56	1936	1800.6	101.8	747.1	269.8	213.7	40.0	68.9	164.3	150.3	175.8	27.6	40.3	68.0	26.1	41.8	39.7	60.1	7.3	77.3
	66-68	1920	3166.9	136.2	1641.6	563.6	491.5	92.0	118.1	297.4	211.7	193.3	17.1	28.8	40.5	15.1	23.8	21.8	32.3	4.4	40.6
	78-80	1903	121.6	6.2	130.7	148.2	42.6	18.2	44.5	34.8	66.1	194.6	6.2	18.5	13.7	4.5	9.2	7.8	8.0	0.0	12.2
	110-115	1854	106.2	4.5	126.7	136.4	38.4	17.0	34.8	26.9	53.2	135.7	3.9	15.1	7.6	1.6	5.1	0.0	2.4	0.0	6.7
	135-140	1818	76.3	3.6	101.2	104.5	30.5	14.3	27.7	15.1	30.6	119.6	3.1	12.1	5.9	1.2	4.2	0.0	1.4	0.0	4.5
	205-210	1715	87.6	3.6	91.8	86.7	28.6	11.6	24.2	14.2	22.5	97.5	2.4	10.3	6.1	0.6	4.2	0.0	1.4	0.0	4.0

a. phenanthrene (Phe), anthracene (An), mono-methylphenanthrenes (MP), 1-methylphenanthrene (1-MP), 1,7-dimethylphenanthrene (1,7-DMP), 2,6-dimethylphenanthrene (2,6-DMP),fluoranthene (Fl), pyrene (Py), retene (Ret), benzo[a]anthracene (BaA), chrysene (Chy), benzo[b]fluoranthene (BbF), benzo[k]fluoranthene(BkF), benzo[e]pyrene (BeP), benzo[a]pyrene (BaP), indeno[1,2,3-c,d]pyrene (InP), dibenz[a,h]anthracene (DBA), and benzo[g,h,i]perylene (BghiP).

(a)

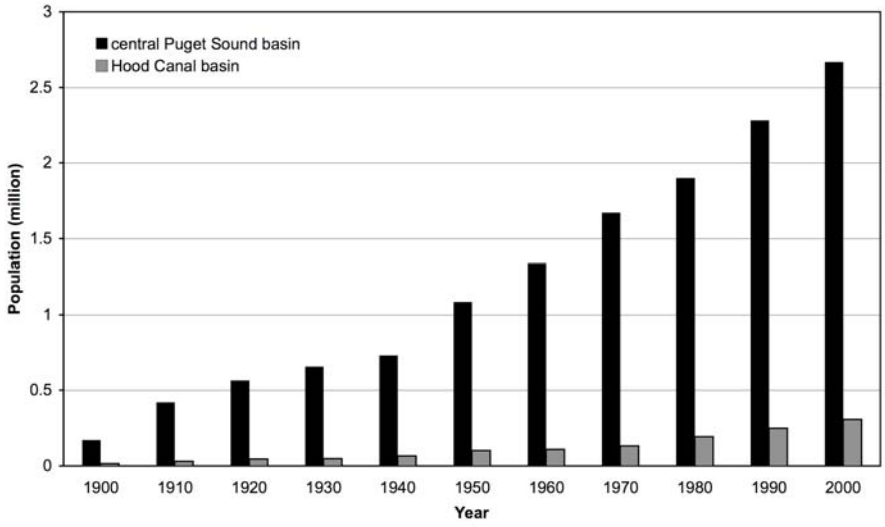

(b)

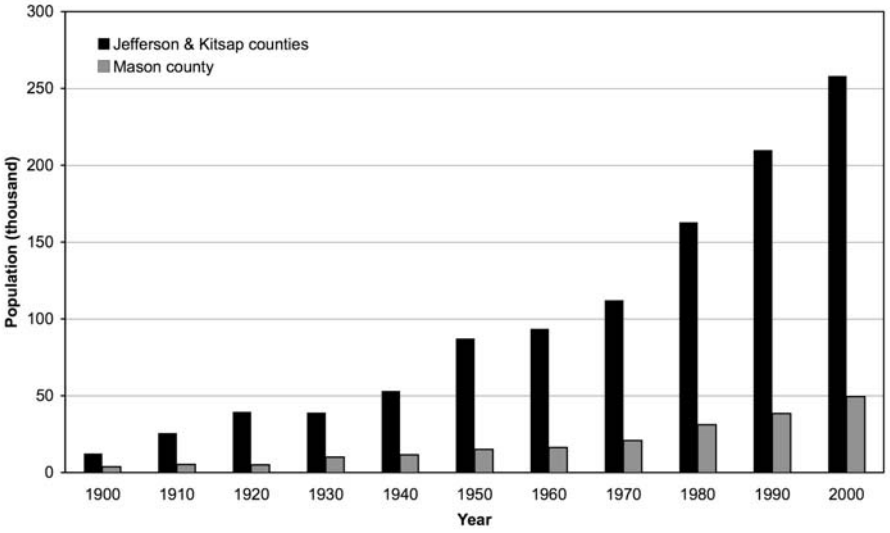

Figure 19. 20th century population growth in (a) basins of central Puget Sound *vs*. Hood Canal, and (b) Jefferson & Kitsap counties *vs*. Mason county. Note that data for central Puget Sound basin is from the populations of King, Kitsap, and Pierce counties, while data of Hood Canal basin is from populations of Jefferson, Kitsap, and Mason counties. HC-5 core is surrounded by Jefferson and Kitsap counties; HC-3 core is within the Mason county (*http://www.ofm.wa.gov/forecasting/key2pop.asp*).

4.3.1.2. Hood Canal cores

As shown in Table 8 and Figures 17c, d, the down-core GBC fluxes of two Hood Canal cores were significantly lower than those from the Puget Sound cores. HC-5 has similar GBC content (0.025-0.041%) as those of Puget Sound cores but with lower sedimentation rate (0.73 cm yr^{-1}). The GBC fluxes in HC-3 were extremely low (0.0048-0.0074 mg cm^{-2} yr^{-1}) due to both the lowest GBC level (0.014-0.024%) and sedimentation rate (0.49 cm yr^{-1}) among the four cores in this study. Such low BC fluxes are comparable to those observed in the deep sediments (deposited during the 11th century) of Stora Frillingen Lake (0.0071 mg cm^{-2} yr^{-1}, Elmquist et al., 2007), and indicate that HC-3 is less impacted by the inputs of combustion products than the urban/suburban environments of the Sound.

The pre-industrial PyPAH fluxes in the two Hood Canal cores (2-4 ng cm^{-2} yr^{-1}) are 4-7 times lower than that of PS-1 (14 ng cm^{-2} yr^{-1}). Throughout the entire cores, the PyPAH fluxes of HC-3 and HC-5 are only a fraction of those observed in Puget Sound cores, which is in line with the observations for GBC fluxes. This again shows that Hood Canal environment receives lower combustion inputs compared to the densely populated central Puget Sound basin (Figure 19a). Similar to their GBC fluxes, the PyPAH fluxes of HC-3 (2-17 ng cm^{-2} yr^{-1}) are lower than those of HC-5 (4-80 ng cm^{-2} yr^{-1}). Distinct vertical distribution patterns were also found in the two Hood Canal cores. In HC-3, the increase of PyPAHs fluxes started around 1930s and reached the down-core maximum in 1970 followed by a rapid decline to recent sediments. In HC-5, PyPAHs fluxes increased slightly in the second half of the 19th century and then showed an abrupt increase from 1900 (10 ng cm^{-2} yr^{-1}) to 1920 (43 ng cm^{-2} yr^{-1}). After being constant for 20 years, the PyPAHs fluxes experienced another steep two-fold increase to reach a maximum during the 1940s-1950s

(from 42 to 80 ng cm^{-2} yr^{-1}). Similar timing of PAH maximum was also reported in a sediment core from Dabob Bay near the HC-5 site (Prahl and Carpenter, 1979). Thereafter, PyPAHs fluxes decreased rapidly from 1955-1980 followed by a small increase in 1990s and decrease again in the last decade returning to the level of the early 20th century. It is noteworthy that the temporal patterns of PyPAHs fluxes in these two cores seem to follow the population growth trends of their surrounding areas during the first half of the 20th century (Figure 19b). The population increase in the area around HC-5 (Jefferson and Kitsap counties) increased from 1900s and had the first large increase (over 60%) during 1940s-1950s, while HC-3 area (Mason county) showed the first significant population increase (over 50%) in 1920s-1930s and later in 1970s-1980s. This suggests that the combustion-derived material inputs in these two rural sites may be directly linked to the urbanization. Furthermore, the timing of PyPAH flux maximum in HC-3 (1970s) is synchronous with the GBC flux maximum. In contrast, the timing of PyPAHs flux maximum in HC-5 (1950s) is different from its GBC flux maximum (1970s). The decoupling between GBC and PyPAH profiles in HC-5 implies that this site might have received PAH and BC inputs from different sources. A nearby Naval munitions depot located in north Hood Canal might be a potential PAHs sources (e.g. oil spill, ship emissions, etc.) for HC-5 during that period.

The apparent difference in pre-1900 GBC fluxes among the four Puget Sound/Hood Canal cores, and in particular the GBC fluxes in presettelement era (pre-1850) in PS-1, HC-5, and HC-3 are noteworthy. The consistently different GBC fluxes in these cores imply that each region of the Sound has its own stable level of GBC sources, which is unlikely just from wildfires. A pioneering study by Dickens and co-workers (2004) indicated that another potential GBC source is petrogenic graphite from erosion of rocks. Graphite can survive in

the harsh thermo-chemical treatments of soot-BC methods and be counted as part of GBC. The discrepancy among the background fluxes in Puget Sound/Canal cores thus can be reasonably explained by different degrees of petrogenic graphite inputs from erosion of bedrock in the nearby watersheds. The inputs of petrogenic graphite was also considered as the major source of GBC in the sediments from Lake Washington during presettlement era (Wakeham et al., 2004). Furthermore, the surficial GBC fluxes of these four cores are all lower than the pre-industrial values (Figure 17). Surficial sediments should receive more combustion-derived materials than the pre-industrial counterparts since the corresponding PyPAH flux profiles all show elevated PyPAH fluxes in the surface sediments compared to the deep sections (Figure 17). This might be the result of the shift of petrogenic graphite inputs due to the human-induced alteration of watershed characteristics during the 20th century, particularly the decreased sediment inputs due to sediment retention behind hydroelectric dams (Wakeham et al., 2004).

4.3.2. Combustion sources identification by molecular markers

4.3.2.1. PAH diagnostic ratios

PAH diagnostic ratios have often been used in source apportionment studies because PAH composition pattern is both source and process specific (Youngblood and Blumer, 1979; Yunker et al., 2002). For example, combustion processes often generate PAHs with less methyl-substituted homologues compared to petrogenic processes. Yunker et al. (2002) suggested that the ratio of the sum of fluoranthene and pyrene to their monomethyl-substituted homologues ($C_0/(C_0+C_1)_{Fl/Py}$) is a good indicator for pyrogenic/petrogenic source identification since there is a clear $C_0/(C_0+C_1)_{Fl/Py}$ transition value (0.5) between these two sources (> 0.5 points to pyrogenic origins; < 0.5 indicates petrogenic origins). As shown in

Figure 20, the $C_0/(C_0+C_1)_{Fl/Py}$ values suggest that the PAHs in the four Puget Sound/Hood Canal cores were predominantly derived from combustion. Our observations are in line with the statement by Lima and co-workers (2005) that the most prominent and ubiquitous source of PAHs in the environment is the incomplete combustion of biomass and/or fossil fuels.

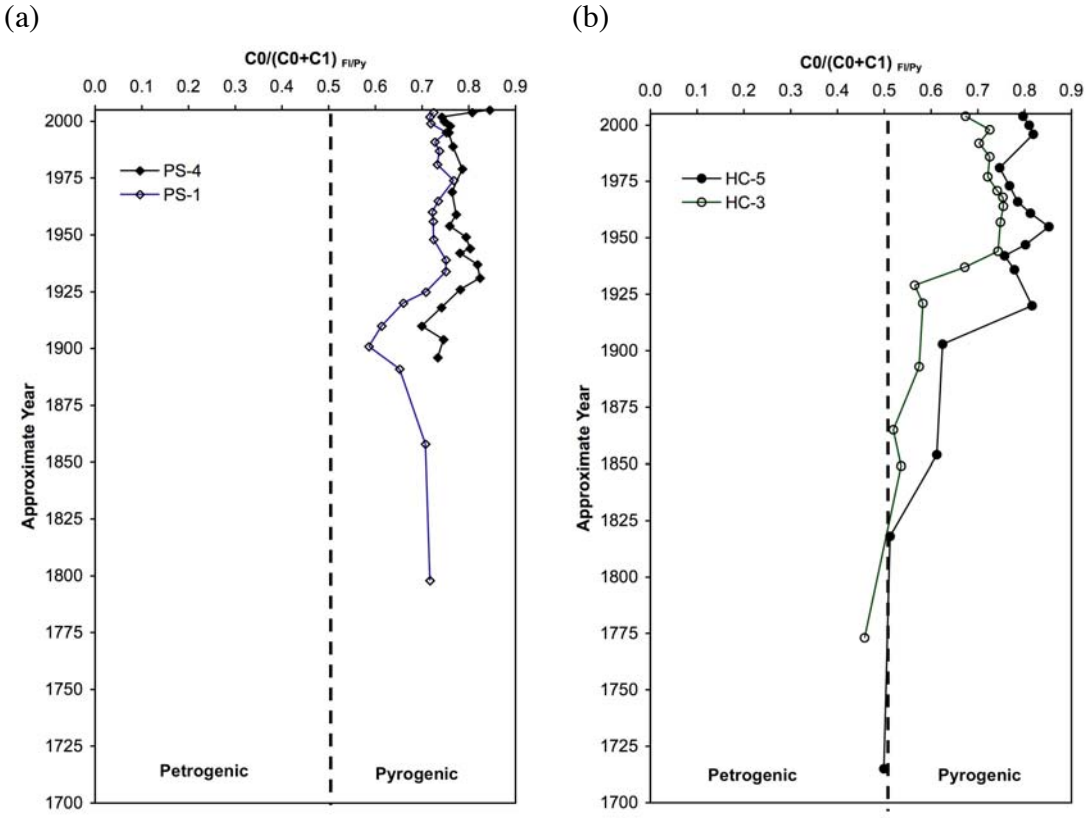

Figure 20. Temporal profiles for source diagnostic ratio of parent (C_0) versus monomethyl (C_1) fluoranthene and pyrene ($C_0/(C_0+C_1)_{Fl/Py}$) in (a) Puget Sound cores, and (b) Hood Canal cores.

1,7-dimethylphenanthrene (1,7-DMP) and retene (7-isopropyl-1-methylphenanthrene) are recognized as specific markers for biomass burning because they have been found in high concentrations in the smoke from softwood combustion (Ramdahl, 1983; Benner et al., 1995). PAH diagnostic ratios based on these two markers include 1,7-DMP to the sum of

1,7- and 2,6-dimethylphenanthrenes (1,7-DMP/1,7-+2,6-DMP) and retene to retene+chrysene (Ret/(Ret+Chy)). These two ratios are used specifically for distinguishing the combustion sources of PAHs (Benner et al., 1995; Yunker et al., 2002; Yan et al., 2005; Elmquist et al., 2007). For 1,7-DMP/(1,7-+2,6-DMP) ratio, vehicle emissions are generally characterized by values < 0.45, whereas values between 0.7-0.9 point to wood combustion (particularly softwood). The values between 0.45 and 0.7 may be generated by a mixture of the above two sources, coal combustion, or the presence of oil and shales (Yunker et al., 2002). The ratio of Ret/(Ret+Chy) can also be used to distinguish between petroleum combustion (0.15-0.5), coal combustion (0.3-0.45), and softwood combustion (0.83-0.9) (Yan et al., 2005). These two diagnostic ratios were plotted for the four Puget Sound/Hood Canal cores to characterize potential combustion fuel sources since softwood combustion is dominant in the study region (Fahnestock and Agee, 1983; Yunker et al., 2002). Both Puget Sound cores show high Ret/(Ret+Chy) ratios (0.9-1.0) in the beginning of the 20th century, suggesting a strong influence from softwood combustion inputs prior to major development of the drainage basin (Figure 21). In the early part of the 20th century, a steep shift occurred in PS-4 toward sources dominated by fossil fuel combustion in ~1940s followed by a mixture of sources in the mid-to late 20th century. The recent dramatic shift towards fossil fuel combustion signatures in this core confirms that the large increases in PyPAHs fluxes in recent years were driven by fossil fuel combustion. In contrast to PS-4, the Ret/(Ret+Chy) ratios in PS-1 core remain in the softwood combustion zone throughout the entire core. Similar information is obtained from the 1,7-DMP/(1,7-+2,6-DMP) ratio with less pronounced changes, however, for core PS-4 (Figure 22). The Ret/(Ret+Chy) ratios in the Hood Canal cores suggest that this system was dominated by softwood combustion inputs

from pre-1900s to the early 20th century, followed by mixed combustion inputs during the 1950s-1970s, and later return to a predominance of softwood combustion inputs in the recent years (Figure 21).

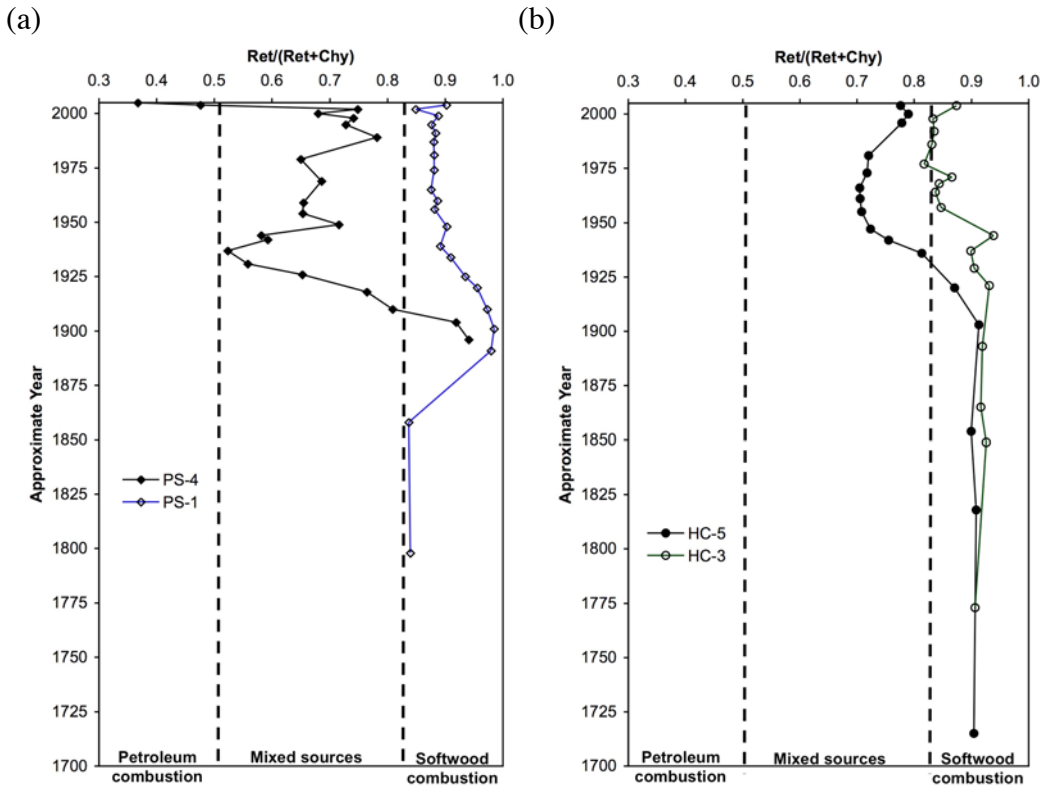

Figure 21. Temporal profiles for source diagnostic ratio of retene to summation of retene and chrysene (Ret/(Ret+Chy)) in (a) Puget Sound cores, and (b) Hood Canal cores.

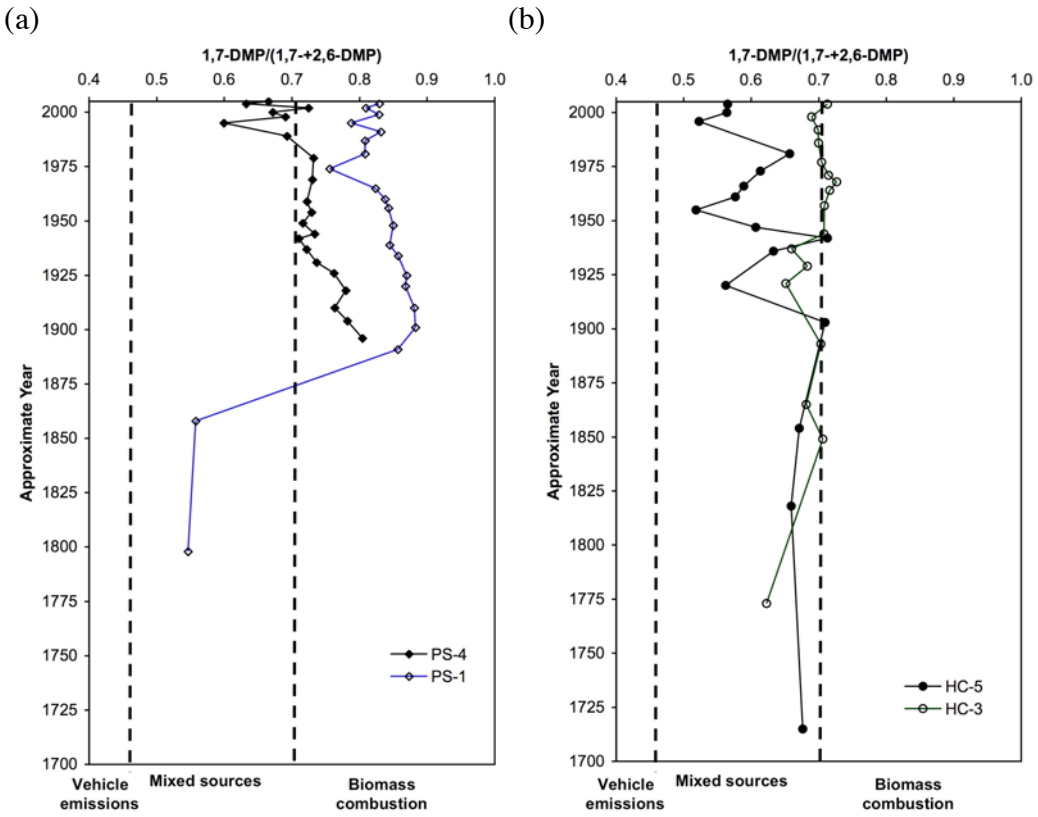

Figure 22. Temporal profiles for source diagnostic ratio of 1,7-DMP to summation of 1,7-DMP and 2,6-DMP (1,7-DMP/1,7-+2,6-DMP) in (a) Puget Sound cores, and (b) Hood Canal cores.

The PAH source diagnostic results for PS-1 are surprising since they fail to show significant fossil fuel combustion inputs in this core. PS-1 has relatively high GBC and PyPAH fluxes with respect to the other cores and it is located near the populated Tacoma area. Therefore, PS-1 is expected to receive large inputs from fossil fuel combustion, as observed in PS-4 and Lake Washington cores (Wakeham et al., 2004). However, retene and DMP may also come from other sources than combustion, such as pulp/paper mill effluents, anaerobic transformation of dehydroabietic acid, and tire debris (Wakeham et al., 1980b;

Rogge et al., 1993; Tavendale et al., 1997; Leppanen et al., 2000). But the effects from inputs of those alternative sources should also be seen in PS-4. Moreover, the peak of terrestrial organic matter inputs in both PS-1 and PS-4 due to the activities of logging and pulp/paper mills were recorded in the sediment sections from the 1940s-1960s (Brandenberger et al., 2008a; Louchouarn et al., 2009). If the deposited terrestrial OM, mostly from softwood, were precursors of retene and dimethylphenanthrenes in the sediments, then both Ret/(Ret+Chy) and 1,7-DMP/(1,7-+2,6-DMP) ratios would peak during 1940s-1960s, rather than the observed 1900s-1930s in PS-1. Some earlier Puget Sound studies have indicated the presence of coal fragments in a core located near PS-1 site (Furlong and Carpenter, 1982; Barrick et al., 1984; Barick and Prahl, 1987). During our core sampling, some coal-like particles were also visually recognized in intervals of this core. Barrick et al. (1984) analyzed the hydrocarbon compositions in 16 western Washington coal samples as well as coal particles from a sediment core near Tacoma, and found several dominant components including retene, methylphenanthrenes, and dimethylchrysenes. To examine the potential coal inputs, we plotted the down-core trend of retene, DMP, and dimethylchrysene of our four cores. Interestingly, compared to the other three cores, PS-1 is unique, showing very high concentrations of these three compounds from late 19th century to 1930s, when the highest Ret/(Ret+Chy) and 1,7-DMP/(1,7-+2,6-DMP) ratios are observed (Figure 23). PS-4 also shows a smaller peak at the same time. Since 1-methylphenanthrene (1-MP) was reported to be a dominant component in the coal particles collected from Puyallup and Nisqually River deltas in south Sound (Barrick et al., 1984), we further compared the trends of ratio of 1-MP to MP for the four cores (Figure 23d). The results indicate that core PS-1 is the only one showing elevated 1-MP level. Its 1-MP/MP ratios

peaked during the early 20th century and increased again from 1970s. All of these molecular marker signatures suggest that the presence of coal particles may be responsible for the abnormal PAH diagnostic ratio patterns in PS-1 as well as part of PS-4.

To collect more information about the potential interferences that unburned coal particles may generate on PAH diagnostic ratios, we conducted PAH analysis on several coal standards as well as three char-BC standards from our previous study (Table 2). Large PAH signature variations in coals were observed in this test (Table 10). The variations are highly dependent on the coal rank, in agreement with earlier findings (Radke et al., 1982; Barrick et al., 1984; Stout and Emsbo-Mattingly, 2008). Notably, both retene and DMP ratios decrease with increasing coal maturity. The low-rank coals (lignite, high-volatile bituminous) have Ret/(Ret+Chy) > 0.83 and 1,7-DMP/(1,7-+2,6-DMP) > 0.8, which are comparable to those of char-BC and within the biomass combustion zone of these two diagnostic ratios. Since Barrick et al. (1984) indicated that the coal fragments sieved from a Puget Sound core probably are sub-bituminous and bituminous coals, the observed high Ret/(Ret+Chy) and 1,7-DMP/(1,7-+2,6-DMP) ratios in PS-1 are presumably caused by the inputs of unburned coal fragments. This is also in line with the Washington coal production history, which started in 1853, peaked in 1918 followed by a sharp decrease until the 1970s (State coal profile, Energy Information Administration, 1994). Tacoma was the major coal trans-shipment center until 1920 (Barrick and Prahl, 1987). As such, the contributions of biomass combustion in Puget Sound cores from PAH signatures, especially in PS-1, may be overestimated. The case of Puget Sound cores demonstrates the potential uncertainties in source identification from the use of PAH source diagnostic ratios.

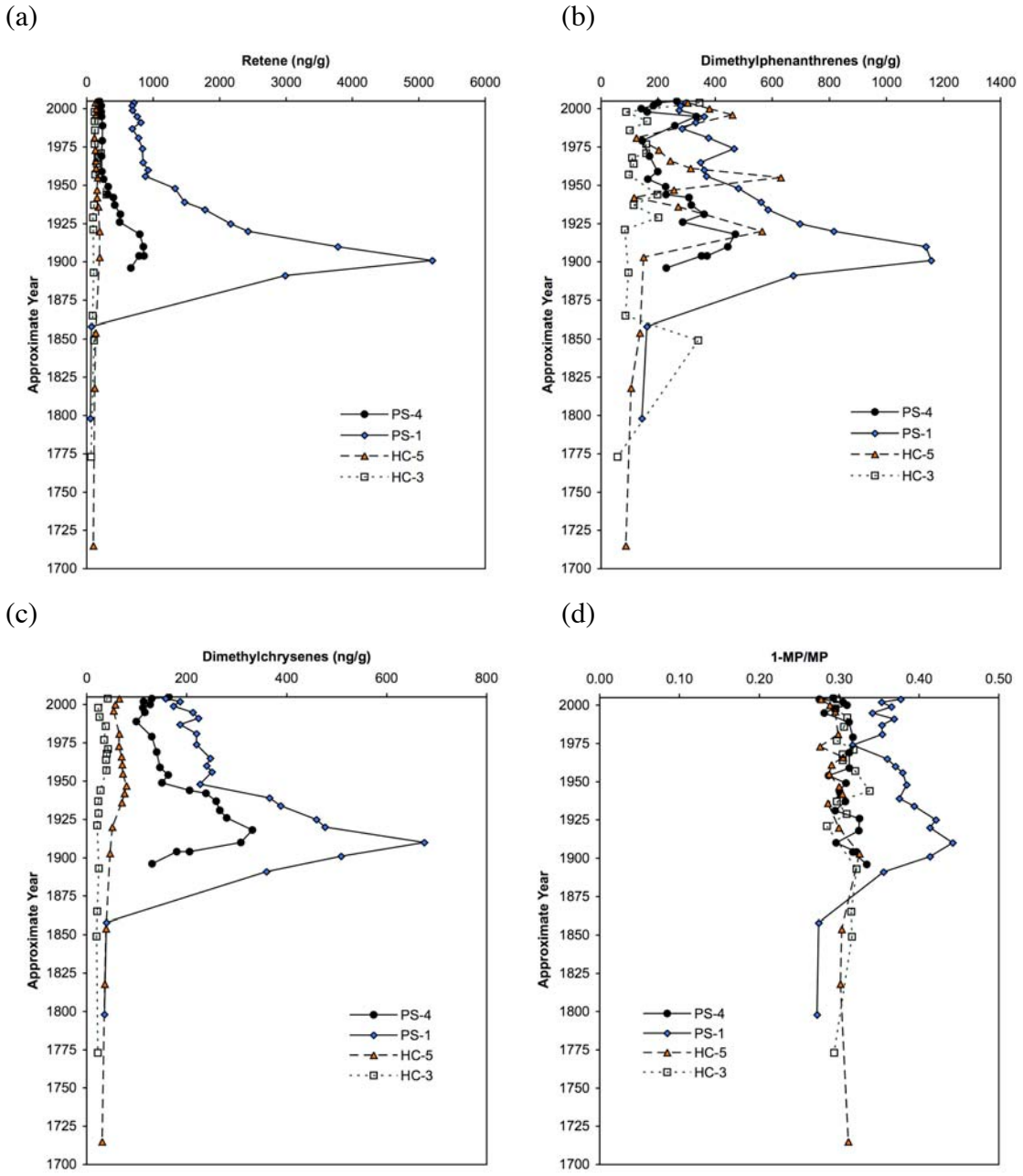

Figure 23. Comparisons of temporal profiles of (a) retene concentrations, (b) dimethylphenanthrenes concentrations, (c) dimethylchrysenes concentrations, and (d) ratios of 1-methylphenanthrene to mono-methylphenanthrene/anthracene (1-MP/MP) of Puget Sound/Hood Canal cores.

Table 10. Selected PAH source diagnostic ratios of synthetic chars and coal standards

Materials	1,7-DMP/(1,7-+2,6-DMP)[a]	Ret/(Ret+Chy)[a]	MP/P[a]
PI 300 char[b]	1.00	1.00	7.92
HM 300 char[b]	0.94	0.71	1.92
CG 300 char[b]	0.84	0.00	0.95
ANL lignite[c]	0.84	0.92	3.05
ANL bituminous 1[c]	0.83	0.85	4.20
ANL bituminous 2[c]	0.75	0.40	2.45
ANL bituminous 3[c]	0.34	0.06	2.03
SRM 1632c (bituminous)[d]	0.74	0.46	2.48
SRM 2689 (coal fly ash)[d]	-	0.00	0.72

a. PAH source diagnostic ratios: 1,7-DMP/(1,7-+2,6-DMP): 1,7-dimethylphenanthrene/(1,7-+2,6-dimethylphenanthrene); Ret/(Ret+Chy): retene/(retene+chrysene); MP/P: monomethylphenanthrene & anthracene/ phenanthrene.

b. 300°C combusted synthetic chars from loblolly pine (PI), honey mesquite (HM), and cordgrass (CG).

c. Argonne National Laboratory (ANL) coal standards: lignite: lignite from the Beulah-Zap seam in North Dakota; bituminous 1: high-volatile bituminous from the Blind Canyon seam in Utah; bituminous 2: high-volatile bituminous from the Pittsburgh seam in Pennsylvania; bituminous 3: low-volatile bituminous from the Pocahontas #3 seam in Virginia.

d. Standard reference materials (SRM) from National Institute of Standards and Technology (NIST): SRM 1632c is a bituminous coal from the Pittsburgh seam in Pennsylvania; SRM 2689 is coal fly ash collected from coal-fired power plant.

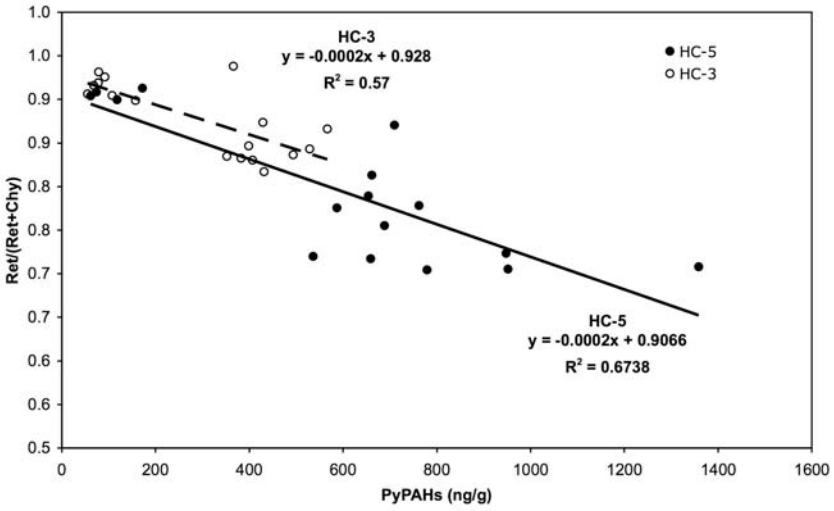

Figure 24. Ret/(Ret+Chy) ratio *vs*. total combustion PAHs (PyPAHs) (ng g^{-1}) for HC-3 and HC-5 cores.

Nevertheless, the dramatic shifts of PAH signatures in PS-4 between biomass burning and fossil fuel combustion during the 20th century (Figure 21) is noteworthy. The strong signal of fossil fuel combustion in1940s fits well with the GBC profile and the historical energy consumption trend (Figure 17, 18). Additionally, the significant increase in fossil fuel combustion signature in the surficial sediments resembles the features observed in major urban area in the US. Because PS-1 and PS-4 have synchronous PAH flux maxima and both are located near the highly urbanized/industrialized area of Seattle/Tacoma, the changing pattern of combustion sources in PS-1 is presumably similar to that of PS-4, except for the surfical sediments. This later difference suggests sub-basin variations in watershed development and eventually differences in the transfer of contaminants to different regions of the Sound. In Hood Canal, the lower anthropogenic impacts and lack of coal interference (Figure 23) lead to much simpler profiles of retene ratio compared to the Puget Sound cores. The intrusion of fossil fuel combustion in these two cores is evident in the shift of PAH signatures. Notably, the timings of such change (1970s and 1950s for HC-3 and HC-5, respectively) are in agreement with the significant urbanization of the surrounding areas (Figure 19). Moreover, the Ret/(Ret+Chy) ratios of both Hood Canal cores are inversely correlated with PyPAHs concentrations (r^2 = 0.57 and 0.67 for HC-3 and HC-5, respectively, $p < 0.01$) (Figure 24). The identical slopes of these two regression lines suggest a binary mixture in the Hood Canal system with biomass combustion as one end-member and a common fossil fuel combustion source as the other.

4.3.2.2. Levoglucosan

Levoglucosan, a specific biomarker for low temperature char-BC, can provide direct information of BC inputs from biomass combustion. Levoglucosan is the product of

cellulose combustion and can be generated from a broad suite of plant tissues (softwood, hardwood, grasses) (Kuo et al., 2008). Our previous work showed that coals don't contain levoglucosan, hence the interferences from unburned coals is not an issue. There is also no detectable levoglucosan in smokes from coal combustion except for some specific brown coals, which are limited in use (Santos et al., 2004; Fabbri et al., 2008; Fabbri et al., 2009). Since wildfires and open biomass burning may generate both char-BC and GBC under their highly variable combustion conditions, the down-core levoglucosan profile may be linked to the temporal variations of both char-BC and GBC inputs.

Large variations in sedimentary levoglucosan concentrations were found in Puget Sound/Hood Canal cores (Table 8). In contrast to the observations from GBC and PyPAHs profiles, higher concentrations were found in HC-3 (69-782 ng/g), followed by HC-5 (79-323 ng/g) and PS-1 (60-142 ng/g). Levoglucosan was undetectable in sediments from PS-4 so the data of this core is not presented. These results demonstrate that levoglucosan represents different combustion-derived materials from GBC and PAHs in these cores. Very low levoglucosan concentrations in Puget Sound cores may be a result of sediment dilution due to the high sedimentation rate in the main basin of the Sound (Brandenberger et al., 2008a). It also indicates that low temperature char-BC is a minor component in the Puget Sound sediments. Significant differences in temporal trends were also found between levoglucosan fluxes and those of GBC and PyPAHs (Figure 25a). HC-3 shows five significant historical peaks from the early 19th century to the 20th century. The temporal profiles of PS-1 and HC-5 are more variable and not as pronounced as HC-3, probably because they have lower levoglucosan concentrations, and these two sites received more disturbances from water circulation and/or human activities. In contrast, being the most pristine site in this study, the

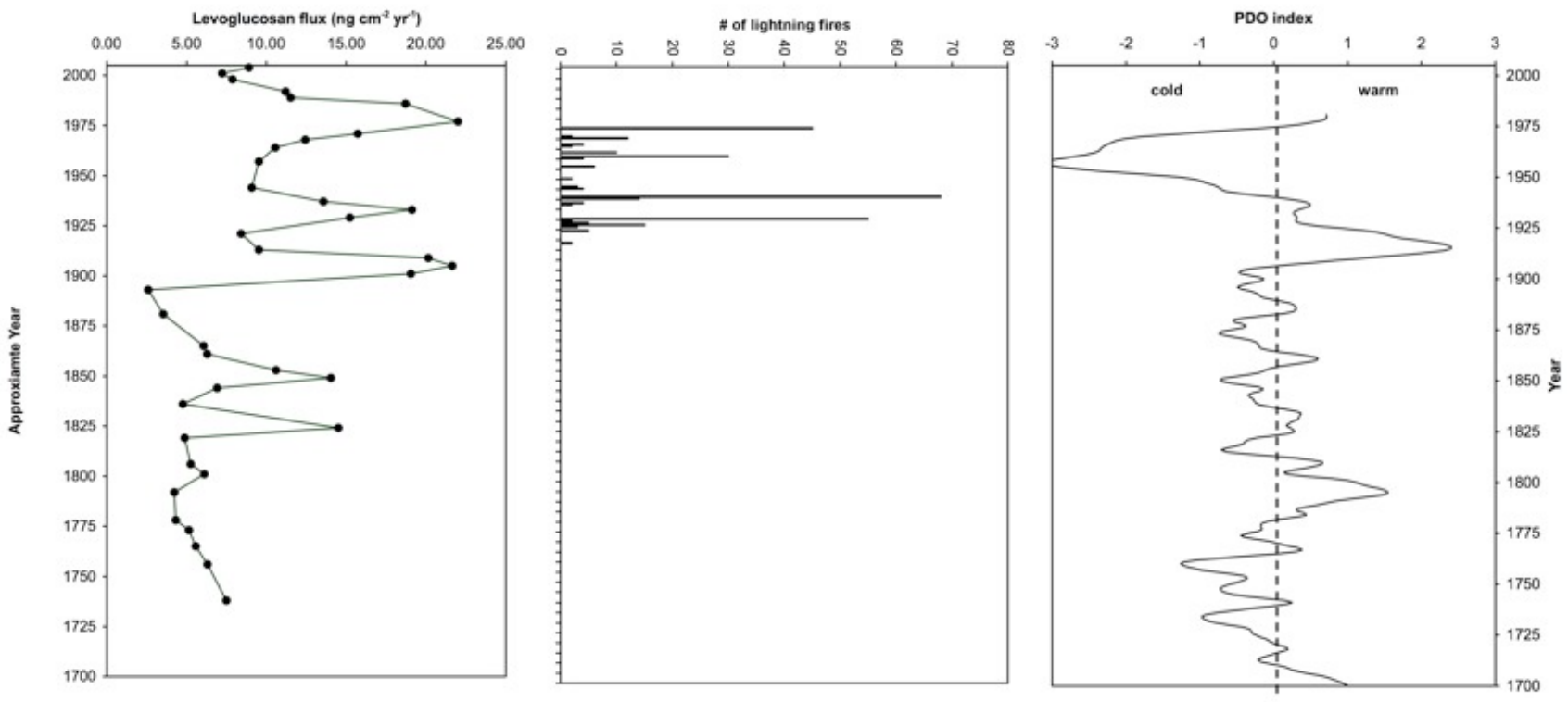

Figure 25. Comparison between the (a) temporal trend of levoglucosan fluxes in HC-3, (b) numbers of lightning fire in Olympic National Park (Pickford et al., 1980), and (c) Pacific Decadal Oscillation (PDO) index (Biondi et al., 2001). Note that PDO is smoothed by 20 yr moving average.

south Hood Canal, where the HC-3 located, is characterized by weak physical circulation of the water (Mackas and Harrison, 1997). These features make HC-3 an ideal deposition environment for recording low-level inputs of low temperature char-BC.

The magnitudes of down-core levoglucosan fluxes of the three cores are similar (6.3-16.6, 2.6-22.0, 4.4-19.1 ng cm^{-2} yr^{-1} for PS-1, HC-3, HC-5, respectively; Table 8). This striking observation indicates that, unlike GBC and combustion PAHs, which might be dominated by localized fossil fuel combustion inputs, levoglucosan in Puget Sound/Hood Canal cores may be derived from regional inputs, presumably transported through atmospheric deposition. This also highlights the presence of micro-size char-BC, which can travel long distances through atmospheric transport (Masiello, 2004; Kuo et al., 2008).

Because of the clearer changes in levoglucosan concentrations and fluxes in HC-3, we focus the rest of the discussion on this core. Major levoglucosan flux peaks in this core were observed in 1820s, 1850s, 1900s-1910s, 1930s-1940s, and 1970s-1980s. During the last few decades, some of these peak coicinde with periods characterized by a higher number of forest fires, mostly from lightning, in the nearby Olympic National Park (Figure 25) (Pickford et al., 1980; Wetzel and Fonda, 2000). Researchers have also explored the linkages between atmospheric and climate variability and the historical fire records in Pacific Northwest and pointed out that wildfire activities might correlate with the Pacific Decadal Oscillation (PDO) (Hessl et al., 2004; Gedalof et al., 2005; Heyerdahl et al., 2008). The positive phase of PDO (PDO index > 0) is associated with warmer, drier winters, whereas the negative phase (PDO index < 0) tends to produce cooler, wetter winters in Pacific Northwest (Mantua et al., 1997). The PDO may affect the snowpack as well as the moisture of fuel (biomass) and thus be linked to the length of fire seasons. As shown in Figure 25, the levoglucosan peaks are

consistent with cool-to-warm transitions of PDO, including the most significant PDO episodes of the last 200 years (1905 and 1977). The similiarlity between the trend of levoglucosan fluxes and PDO suggests that climate oscillations may play a role in the historical wildfire activities (Hessl et al., 2004; Gedalof et al., 2005; Heyerdahl et al., 2008; Marlon et al., 2008) and thus influence the char-BC inputs to the environment. Furthermore, the elevated background levoglucosan flux in 20th century, compared to 19th century, points to the generally increased char-BC inputs in this region over the last century. This is in line with the increases in wildfires activity, a possible consequence of climate oscillation and human-induced climate change, in the western US and Canada during past decades (Gillett et al., 2004; Gedalof et al., 2005; Westerling et al., 2006).

4.3.3. Implications from Puget Sound/Hood Canal cores

The distinct temporal distribution pattern of GBC and PyPAHs fluxes between central Puget Sound basin and Hood Canal basin observed in the present study demonstrate that environmental soot-BC deposition may not reflect a nation- or region-wide phenomenon but is rather highly controlled by local inputs. This is also supported by the large differences in magnitudes of fluxes among cores, especially between PS-4 and HC-3. In a study of soot-BC deposition in the Great Lakes by Buckley and co-workers (2004), distinct BC temporal profiles were found in cores from the same lake. The cores near the metropolitan areas (Chicago, Detroit) always possessed significantly higher BC concentrations than distant cores. Large differences in soot-BC flux profiles were also found between an urban lake in Stockholm, Sweden, and a rural lake outside of the Stockholm metropolitan area (Routh et al., 2004; Elmquist et al., 2007). In the present study, two Puget Sound cores presumably received high inputs of combustion-derived products from the nearby Seattle/Tacoma

metropolitan area. The Hood Canal cores, however, are located in a rural area that might receive much less anthropogenic combustion products inputs from domestic heating, vehicular combustion as well as industrial activities. The significant role of local point sources is especially highlighted in the Puget Sound cores. In contrast to the observations from GBC and PAHs, PS-1 historically received higher inputs of anthropogenically-derived metals (natural background subtracted Pb, Cu, As) than PS-4 (Brandenberger et al., 2008a). PS-1 is near Tacoma which is a more industrialized area housing a major metal smelter from the late 19th century to late 20th century. PS-4 is located near the predominantly urban Seattle area which is the most populated region of the Puget Sound. The very different distribution pattern between heavy metals and combustion-derived materials in PS-1 and PS-4 demonstrate the distinct point sources of these two contaminant classes. Urban environments are hot spots of energy consumption due to the high population density and human activities (Grimm et al., 2008). Significant GBC and PAHs sources such as vehicular emissions, domestic heating, road dust, tire wear, and incineration of municipal solid wastes, are highly concentrated in these urban areas (Wakeham et al., 1980a; Barrick, 1982; Van Metre et al., 2000; Yunker et al., 2002; Wakeham et al., 2004; Lima et al., 2005; Mahler et al., 2005; Van Metre and Mahler, 2005; Yan et al., 2005; Louchouarn et al., 2007). Throughout the 20th century, the population in Seattle was always 2-3 times greater than that of Tacoma (Office of Financial Management, WA, 2007). Thus it is not surprising that PS-4 possessed the highest GBC and PAHs fluxes in this study.

The data of Puget Sound/Hood Canal cores in the present study also demonstrate regional-specific features. The historical GBC concentrations and fluxes of Puget Sound cores (0.02-0.04% and 0.02-0.08 mg cm^{-2} yr^{-1}), except for the PS-4 maxima, were all about

one order of magnitude lower than the observed values in other urban lakes in eastern US and northern Europe (Gustafsson et al., 1997; Gustafsson and Gschwend, 1998; Routh et al., 2004; Louchouarn et al., 2007). Because similar GBC concentrations and fluxes were also found in the sediment cores from Lake Washington and the Washington coast (Dickens et al., 2004; Wakeham et al., 2004), the additional information from our study further demonstrates the lower GBC inputs in the Pacific Northwest region. This may result in part from the high usage of hydroelectric power in Washington State. Hydroelectric power accounts for nearly three-fourths of the State's electricity generation (EIA, 2009). As shown in Figure 18b, hydroelectric power is historically comparable to petroleum consumption in Washington State. Furthermore, distinct combustion sources between northeastern and northwestern US could be seen from PAH signatures of sediment cores from these two regions. The cross plot of Ret/(Ret+Chy) *vs*. 1,7-DMP/(1,7-+2,6-DMP) ratios (Figure 26) shows that the cluster of data from the Puget Sound/Hood Canal cores is distinct from that of a sediment core from Central Park Lake (CPL) in New York City (Yan et al., 2005). Excluding the questionable PS-1 data, stronger biomass combustion signatures are still predominant in the Puget Sound/Hood Canal sediments, whereas CPL sediments obviously received more inputs from fossil fuel combustion except for the late 19th century intervals which also suggest large inputs from biomass combustion (Yan et al., 2005). As an early-settled and densely populated city, NYC shows a different energy consumption pattern from that of the Pacific Northwest region. However, the distribution of data from the urban site PS-4 seems to plot in the general fossil fuel direction as for CPL, again showing the impacts of urbanization on the environmental inputs of combustion-derived materials to this site.

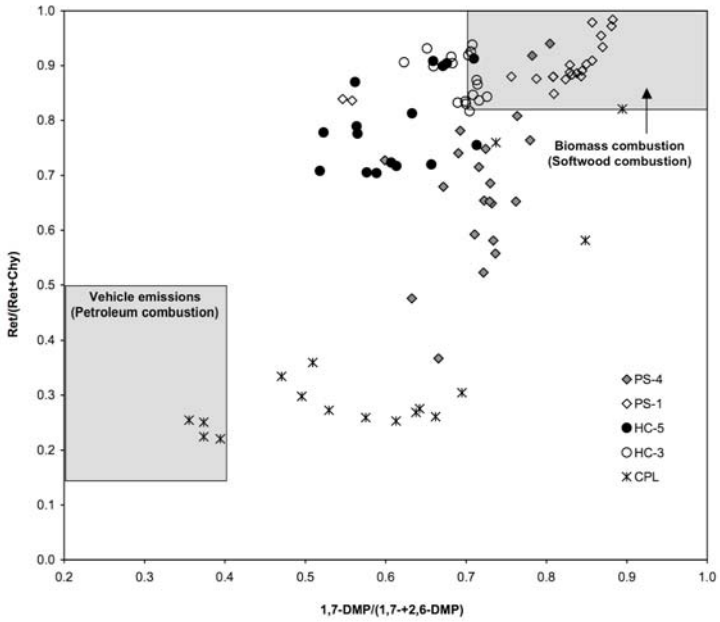

Figure 26. Comparison of combustion sources between Puget Sound/Hood Canal cores to a sediment core from Central Park Lake (CPL) in New York City (Yan et al., 2005) via cross plot of Ret/(Ret+Chy) vs. 1,7-DMP/(1,7-+2,6-DMP) ratios.

4.4. Conclusions

The recalcitrant nature of BC and PAHs make them ideal indicators for researchers to reconstruct the past contamination loadings to the environment and their relationship with many factors of human society development. Most importantly, the reconstructed history of contamination can also help us constrain the potential sources, evaluate the effectiveness of enacted environmental regulations, as well as develop more effective mitigation strategies. In the present study, GBC and combustion PAHs profiles of four cores from central Puget Sound and Hood Canal basins illustrate the evolution of energy consumption in the region and the positive effects of environmental regulations enacted in mid-to-late 20th century. However, the distinct temporal patterns and the differences in flux magnitude among these cores indicate that urbanization is a crucial factor controlling the inputs of combustion byproducts to the environment. The lack of 1940s-1950s GBC peak in pristine deposition

environments, like Hood Canal, further shows that temporal GBC profile tend to be very localized. Another example of local pattern is the recent combustion PAH increases in PS-4, which is not seen in the other three cores of this study, but is in line with other highly urbanized area around the US. On the other hand, our results also show that specific regional energy consumption can affect the GBC inputs to aquatic systems. Compared to other urban lakes in the eastern US and northern Europe, the Puget Sound cores have relatively low GBC fluxes, probably due to the high hydroelectric power usage in the Pacific Northwest. Different from high temperature-derived GBC, the inputs of low temperature char-BC may be more relevant to the climate oscillations and thus also showed a more regional pattern. As such, the observed historical and geographical heterogeneities in the BC and PAH temporal profiles from four cores in this study demonstrate that the environmental loading of these combustion byproducts is a complex function of urbanization and land use, fuel usage, combustion technology, environmental policies, and climate changes. Better assessment of the impacts of combustion-derived products on the human ecosystem thus should be based on their regional or local scale distribution, rather than on national level inventory estimations.

5. GENERAL CONCLUSIONS AND IMPLICATIONS

This research includes three individual studies related to BC. The topics span from method development, molecular signature characterization, to environmental applications. The observations enhance our understanding of how to measure diverse fraction of complex BC continuum, which improve our ability to do better environmental interpretation of BC distribution. The important observations and implications of the present research are listed below.

To our knowledge, the levoglucosan study is the first study that evaluates the role of the molecular marker levoglucosan in the BC method continuum. The findings indicate that a) levoglucosan only exists in BC originating from biomass combustion, b) levoglucosan is a specific molecular marker of low temperature (≤ 350°C) char/charcoal BC, c) it is not a quantitative tool for determining BC in environmental samples since levoglucosan yield is strongly affected by combustion conditions and biomass sources, and d) it can be extracted reproducibly from standard reference materials that are relevant to researches in both aquatic and atmospheric sciences. In particular, we suggest that the NIST urban dust standard reference material (SRM 1649a) can be used as a working standard for levoglucosan analysis. Finally, the comparisons between the analytical window of levoglucosan and those from other BC methods demonstrate that this molecular marker is unique in the current BC method continuum due to its specificity to low temperature char/charcoal BC. The present study shows the weaknesses of most BC methods on characterizing low temperature chars, and the potential for the levoglucosan approach to fill in this gap.

The lignin study brings new information of the effects of thermal degradation on lignin and shows the potential impacts of char-BC inputs on the overall lignin signatures of SOM. To our knowledge, this is the first study that systematically investigates the potential influences of char-BC on the signatures of CuO-derived lignin LOP from SOM. The findings indicate that a) thermal degradation can greatly affect the lignin signatures in low temperature chars and totally eliminate the common LOP (syringyl, vanillyl, and cinnamyl phenols) at temperatures ≥ 400°C, b) syringyl/vanillyl phenols ratios of chars from angiosperms and cinnamyl/vanilyl phenols ratios of chars from noon-woody tissues decrease sharply at temperatures known to form chars (150-250°C) reaching negligible values at 400°C, c) the acid/aldehyde ratios of vanillyl and syringyl phenols and the ratio of 3,5-dihydroxybenzoic acid/vanillyl phenols all increase with increasing combustion temperature, reaching maxima at 300-350°C, d) the changes in signatures and ratios of LOP in chars can be used to assess the char-BC forming temperature, and e) the amount of char-BC and the relative difference in lignin signature between char-BC and SOM can help determine the effects of char inputs on the lignin signatures of SOM. The present study demonstrates that, in addition to biological and photochemical degradations, thermal alteration is an important degradation process for lignin in the environment. It may lead to shifts in lignin signatures in environmental samples receiving char-BC inputs.

With multi-proxy approach on four cores from Puget Sound/Hood Canal basins, a comprehensive environmental BC assessment of Pacific Northwest was conducted. This study presents a unique dataset including high temperature soot-BC and low temperature char-BC, as well as PAHs. Our results suggest that historical soot-BC inputs in Pacific Northwest are lower than the reported data in eastern US and Europe. In addition, compared

to New York City, our study area historically received more combustion products from biomass combustion. These observations demonstrate the regional difference in environmental BC inputs. The causes may include differences in human society development (the onset of settlement and urbanization), the energy usage pattern, and the type of energy use. Comparisons among four cores in this study, located from densely populated area to pristine environment, further reveal the localized BC distributions, which are linked to the degree of urbanization of surrounding environments. Historical inputs of low temperature char-BC, based on levoglucosan distribution, show large difference from soot-BC trends and thus point to distinct sources. The temporal distribution of low temperature char-BC, mostly derived from wildfire, is likely related to the regional climate oscillation such as Pacific Decadal Oscillation (PDO). Our results thus illustrate the linkages of combustion products inputs with both human and environmental systems. The local- and regional-specific temporal distributions of combustion byproducts observed in Puget Sound/Hood Canal basins further demonstrate that local records is critical in developing effective environmental policies. Accurate assessment of environmental inputs of diverse combustion byproducts is only possible by applying multi-proxy approach.

REFERENCES

Accardi-Dey, A., 2003. Black carbon in marine sediments: quantification and implications for the sorption of polycyclic aromatic hydrocarbons. Ph.D. dissertation, MIT-WHOI, Woods Hole, MA.

Accardi-Dey, A., Gschwend, P. M., 2003. Reinterpreting literature sorption data considering both absorption into organic carbon and adsorption onto black carbon. Environmental Science & Technology 37, 99-106.

Ackerman, A. S., Toon, O. B., Stevens, D. E., Heymsfield, A. J., Ramanathan, V., Welton, E. J., 2000. Reduction of tropical cloudiness by soot. Science 288, 1042-1047.

Alexis, M. A., Rasse, D. P., Rumpel, C., Bardoux, G., Péchot, N., Schmalzer, P., Drake, B., Mariotti, A., 2007. Fire impact on C and N losses and charcoal production in a scrub oak ecosystem. Biogeochemistry 82, 201-216.

Almendros, G., Knicker, H., Gonzalez-Vila, F. J., 2003. Rearrangement of carbon and nitrogen forms in peat after progressive thermal oxidation as determined by solid-state ^{13}C and ^{15}N NMR spectroscopy. Organic Geochemistry 34, 1559-1568.

Antal, M. J., Varhegyi G., 1995. Cellulose pyrolysis kinetics - the current state of knowledge. Industrial & Engineering Chemistry Research 34, 703-717.

ASTM, 2000. D1102-84 (Reapproved 1995) Standard Test Method for Ash in Wood. American Society for Testing and Materials, West Conshohocken, PA.

Baldock, J. A., Smernik, R. J., 2002. Chemical composition and bioavailability of thermally, altered Pinus resinosa (Red Pine) wood. Organic Geochemistry 33, 1093-1109.

Barrick, R. C., 1982. Flux of aliphatic and polycyclic aromatic hydrocarbons to central Puget Sound from Seattle (Westpoint) primary sewage effluent. Environmental Science & Technology 16, 682-692.

Barrick, R. C., Furlong, E. T., Carpenter, R., 1984. Hydrocarbon and azaarene markers of coal transport to aquatic sediments. Environmental Science & Technology 18, 846-854.

Barrick, R. C., Prahl, F. G., 1987. Hydrocarbon geochemistry of the Puget Sound region-III. Polycyclic aromatic hydrocarbons in sediments. Estuarie, Coastal and Shelf Science 25, 175-191.

Bates, T. S., Hamilton, S. E., Cline, J. D., 1984. Vertical transport and sedimentation of hydrocarbons in the Central Main Basin of Puget-Sound, Washington. Environmental Science & Technology 18, 299-305.

Behar, F., Hatcher, P. G., 1995. Artificial coalification of a fossil wood from brown coal by confined system pyrolysis. Energy & Fuels 9, 984-994.

Benner, J., B. A., Wise, S. A., Currie, L. A., Klouda, G. A., Klinedinst, D. B., Zweidinger, R. B., Stevens, R. K., Lewis, C. W., 1995. Distinguishing the contributions of residential wood combustion and mobile source emissions using relative concentrations of dimethylphenanthrene isomers. Environmental Science & Technology 29, 2382-2389.

Benner, R., Opsahl, S., 2001. Molecular indicators of the sources and transformations of dissolved organic matter in the Mississippi river plume. Organic Geochemistry 32, 597-611.

Benner, R., Louchouarn, P., Amon, R. M. W., 2005. Terrigenous dissolved organic matter in the Arctic Ocean and its transport to surface and deep waters of the North Atlantic. Global Biogeochemical Cycles 19, GB2025, doi:10.1029/2004GB002398.

bin Abas, M. R., Oros, D. R. Simoneit, B. R. T., 2004a. Biomass burning as the main source of organic aerosol particulate matter in Malaysia during haze episodes. Chemosphere 55, 1089-1095.

bin Abas, M. R., Rahman, N. A., Omar, N. Y. M. J., Maah, M. J., Abu Samah, A., Oros, D. R., Otto, A. Simoneit, B. R. T., 2004b. Organic composition of aerosol particulate matter during a haze episode in Kuala Lumpur, Malaysia. Atmospheric Environment 38, 4223-4241.

Biondi, F., Gershunov, A., Cayan, D. R., 2001. North Pacific decadal climate variability since 1661. Journal of Climate 14, 5-10.

Bird, M. I., Gröcke, D. R., 1997. Determination of the abundance and carbon isotope composition of elemental carbon in sediments. Geochimica et Cosmochimica Acta 61, 3413-3423.

Bird, M. I., Cali, J. A., 1998. A million-year record of fire in sub-Saharan Africa. Nature 394, 767-769.

Bond, T. C., Streets, D. G., Yarber, K. F., Nelson, S. M., Woo, J.-H., Klimont, Z., 2004. A technology-based global inventory of black carbon and organic carbon emissions from combustion. Journal of Geophysical Research 109, D14203, doi: 10.1029/2003JD003697.

Bond, T. C., Bhardwaj, E., Dong, R., Jogani, R., Jung, S., Roden, C., Streets, D. G., Trautmann, N. M., 2007. Historical emissions of black and organic carbon aerosol from energy-related combustion, 1850-2000. Global Biogeochemical Cycles 21, GB2018, doi: 10.1029/2006GB002840.

Boon, J. J., Pastorova, I., Botto, R. E., Arisz P. W., 1994. Structural studies on cellulose pyrolysis and cellulose chars by PY-MS, PY-GC-MS, FTIR, NMR and by wet chemical techniques. Biomass & Bioenergy 7, 25-32.

Braadbaart, F., Boon, J. J., van der Horst, J., van Bergen, P. F., 2004. Laboratory simulations of the transformation of peas as a result of heating: the change of the molecular composition by DTMS. Journal of Analytical and Applied Pyrolysis 71, 997-1026.

Brandenberger, J. M., Crecelius, E. A., Louchouarn, P., 2008a. Historical inputs and natural recovery rates for heavy metals and organic biomarkers in Puget Sound during the 20th century. Environmental Science & Technology 42, 6786-6790.

Brandenberger, J. M., Crecelius, E. A., Louchouarn, P., Cooper, S. R., McDougall, K., Leopold, E., and Liu, G., 2008b. Reconstructing trends in hypoxia using multiple paleoecological indicators recorded in sediment cores from Puget Sound, WA. NOAA, Washington DC.

Brodowski, S., Rodionov, A., Haumaier, L., Glaser, B., Amelung, W., 2005. Revised black carbon assessment using benzene polycarboxylic acids. Organic Geochemistry 36, 1299-1310.

Bucheli, T. D., Gustafsson, Ö., 2003. Soot sorption of non-ortho and ortho substituted PCBs. Chemosphere 53, 515-522.

Bucheli, T. D., Blum, F., Desaules, A., Gustafsson, Ö., 2004. Polycyclic aromatic hydrocarbons, black carbon, and molecular markers in soils of Switzerland. Chemosphere 56, 1061-1076.

Buckley, D. R., Rockne, K. J., Li, A., Mills, W. J., 2004. Soot deposition in the Great Lakes: Implications for semi-volatile hydrophobic organic pollutant deposition. Environmental Science & Technology 38, 1732-1739.

Burgess, R. M., Lohmann, R., 2004. Role of black carbon in the partitioning and bioavailability of organic pollutants. Environmental Toxicology and Chemistry 23, 2531-2533.

Burgess, R. M., Ryba, S. A., Perron, M. M., Tien, R., Thibodeau, L. M., Cantwell, M. G., 2004. Sorption of 2,4 '-dichlorobiphenyl and fluoranthene to a marine sediment amended with different types of black carbon. Environmental Toxicology and Chemistry 23, 2534-2544.

Cachier, H., Pertuisot, M. H., 1994. Particulate carbon in Arctic ice. Analusis 22, M34-M37.

Christman, R. F., Oglesby, R. T., 1971. Microbiological degradation and the formation of humus. In: Sarkanen, K.V., Ludwig, C.H. (Eds.), Lignins: Occurence, Formation, Structure, and Reactions. Wiley-Interscience, New York, pp. 769-795.

Chylek, P., Kou, L., Johnson, B., Boudala, F., Lesins, G., 1999. Black carbon concentrations in precipitation and near surface air in and near Halifax, Nova Scotia. Atmospheric Environment 33, 2269-2277.

Clark, J. S., Patterson, W. A. I., 1997. Background and local charcoal in sediments: Scales of fire evidence in the paleorecord. In: Clark, J. S., Cachier, H., Goldammer, J. G., Stocks, B. (Eds.), Sediment Records of Biomass Burning and Global Change. Springer-Verlag, Berlin, pp. 23-48.

Colberg, P. J., 1988. Anaerobic microbial degradation of cellulose, lignin, oligolignols, and monoaromatic lignin derivatives. In: Zehnder, A. J. B. (Ed.), Biology of Anaerobic Microorganisms. John Wiley and Sons, New York, pp. 333-372.

Cope, M. J., Chaloner, W. G., 1980. Fossil charcoal as evidence of past atmospheric composition. Nature 283, 647-649.

Cornelissen, G., Elmquist, M., Groth, I., Gustafsson, Ö., 2004. Effect of sorbate planarity on environmental black carbon sorption. Environmental Science & Technology 38, 3574-3580.

Cornelissen, G., Gustaffson, Ö., 2005. Importance of unburned coal carbon, black carbon, and amorphous organic carbon to phenanthrene sorption in sediments. Environmental Science & Technology 39, 764-769.

Cornelissen, G., Gustafsson, Ö., Bucheli, T. D., Jonker, M. T. O., Koelmans, A. A., Van Noort, P. C. M., 2005. Extensive sorption of organic compounds to black carbon, coal, and kerogen in sediments and soils: Mechanisms and consequences for distribution, bioaccumulation, and biodegradation. Environmental Science & Technology 39, 6881-6895.

Cornelissen, G., Breedveld, G. D., Nas, K., Oen, A. M. P., Ruus, A., 2006. Bioaccumulation of native polycyclic aromatic hydrocarbons from sediment by a polychaete and a gastropod: Freely dissolved concentrations and activated carbon amendment. Environmental Toxicology and Chemistry 25, 2349-2355.

Cornelissen, G., Cousins, I. T., Wiberg, K., Tysklind, M., Holmstrom, H., Broman, D., 2008a. Black carbon-dominated PCDD/Fs sorption to soils at a former wood impregnation site. Chemosphere 72, 1455-1461.

Cornelissen, G., Wiberg, K., Broman, D., Arp, H. P. H., Persson, Y., Sundqvist, K., Jonsson, P., 2008b. Freely dissolved concentrations and sediment-water activity ratios of PCDD/Fs and PCBs in the open Baltic Sea. Environmental Science & Technology 42, 8733-8739.

Crutzen, P. J., Andreae, M. O., 1990. Biomass burning in the tropics: Impact on atmospheric chemistry and biogeochemical cycles. Science 250, 1669-1678.

Currie, L. A., Benner, B. A., Kessler, J. D., Klinedinst, D. B., Klouda, G. A., Marolf, J. V., Slater, J. F., Wise, S. A., Cachier, H., Cary, R., Chow, J. C., Watson, J., Druffel, E. R. M., Masiello, C. A., Eglinton, T. I., Pearson, A., Reddy, C. M., Gustafsson, Ö., Quinn, J. G., Hartmann, P. C., Hedges, J. I., Prentice, K. M., Kirchstetter, T. W., Novakov, T., Puxbaum, H., Schmid, H., 2002. A critical evaluation of interlaboratory data on total, elemental, and isotopic carbon in the carbonaceous particle reference material, NIST SRM 1649a. Journal of Research of the National Institute of Standards and Technology 107, 279-298.

Czimczik, C., Masiello, C. A., 2007. Controls on black carbon storage in soils. Global Biogeochemical Cycles, 21, GB3005, doi: 10.1029/2006GB002798.

Dalzell, B. J., Filley, T. R., Harbor, J. M., 2005. Flood pulse influences on terrestrial organic matter export from an agricultural watershed. Journal of Geophysical Research-Biogeosciences 110, G02011, doi:10.1029/2005JG000043.

de Leeuw, J. W., Largeau, C., 1993. A review of macromolecular organic compounds that comprise living organisms and their role in kerogen, coal, and petroleum formation. In: Engel, M.H., Macko, S.A. (Eds.), Organic Geochemistry: Principles and Applications. Plenum Press, New York, pp. 23-72.

DeLuca, T. H., Applet, G. H., 2008. Charcoal and carbon storage in forest soils of the Rocky Mountain West. Frontiers in Ecology and the Environment 6, 18-24.

Dickens, A. F., Gélinas, Y., Masiello, C. A., Wakeham, S., Hedges, J. I., 2004. Reburial of fossil organic carbon in marine sediments. Nature 427, 336-339.

Dickens, A. F., Gudeman, J. A., Gélinas, Y., Baldock, J. A., Tinner, W., Hu, F. S., Hedges, J. I., 2007. Sources and distribution of CuO-derived benzenecarboxylic acids in soils and sediments. Organic Geochemistry 38, 1256-1276.

Dignac, M. F., Bahri, H., Rumpel, C., Rasse, D. P., Bardoux, G., Balesdent, J., Girardin, C., Chenu, C., Mariotti, A., 2005. Carbon-13 natural abundance as a tool to study the dynamics of lignin monomers in soil: an appraisal at the Closeaux experimental field (France). Geoderma 128, 3-17.

Dittmar, T., 2008. The molecular level determination of black carbon in marine dissolved organic matter. Organic Geochemistry 39, 396-407.

Drage, T. C., Vane, C. H., Abbott, G. D., 2002. The closed system pyrolysis of β-O-4 lignin substructure model compounds. Organic Geochemistry 33, 1523-1531.

Druffel, E. R. M., 2004. Comments on the importance of black carbon in the global carbon cycle. Marine Chemistry 92, 197-200.

EIA Annual Review 2007, Energy Information Administration, Report DOE/EIA-0384(2007), June 2008.

Elias, V. O., Simoneit, B. R. T., Cordeiro, R. C., Turcq, B., 2001. Evaluating levoglucosan as an indicator of biomass burning in Carajas, Amazonia: A comparison to the charcoal record. Geochimica et Cosmochimica Acta 65, 267-272.

Elmquist, M., Cornelissen, G., Kukulska, Z., Gustafsson, Ö., 2006. Distinct oxidative stabilities of char versus soot black carbon: Implications for quantification and environmental recalcitrance. Global Biogeochemical Cycles 20, GB2009, doi:10.1029/2005GB002629.

Elmquist, M., Zencak, Z., Gustafsson, O., 2007. A 700 year sediment record of black carbon and polycyclic aromatic hydrocarbons near the EMEP air monitoring station in Aspvreten, Sweden. Environmental Science & Technology, 41, 6926-6932.

Engling, G., Lee, J. J., Tsai, Y.-W., Lung, S.-C. C., Chou, C. C.-K., Chan, C.-Y., 2009. Size-resolved anhydrosugar composition in smoke aerosol from controlled field burning of rice straw. Aerosol Science and Technology 43, 662-672.

Ertel, J. R., Hedges, J. I., 1984. The lignin component of humic substances; distribution among soil and sedimentary humic, fulvic, and base-insoluble fractions. Geochimica et Cosmochimica Acta 48, 2065-2074.

Ertel, J. R., Hedges, J. I., 1985. Sources of sedimentary humic substances; vascular plant debris. Geochimica et Cosmochimica Acta 49, 2097-2107.

Fabbri, D., Marynowski, L., Fabianska, M. J., Zaton, M. Simoneit, B. R. T., 2008. Levoglucosan and other cellulose markers in pyrolysates of Miocene lignites – geochemical and environmental implications. Environmental Science and Technology 42, 2957–2963.

Fabbri, D., Torri, C., Simoneit, B. R. T., Marynowski, L., Rushdi, A. I., Fabianska, M. J., 2009. Levoglucosan and other cellulose and lignin markers in emissions from burning of Miocene lignites. Atmospheric Environment 43, 2286-2295.

Fahnestock, G. R., Agee, J. K., 1983. Biomass consumption and smoke production by prehistoric and modern forest fires in Western Washington. Journal of Forestry 81, 653-657.

Farella, N., Lucotte, M., Louchouarn, P., Roulet, M., 2001. Deforestation modifying terrestrial organic transport in the Rio Tapajos, Brazilian Amazon. Organic Geochemistry 32, 1443-1458.

Fine, P. M., Chakrabarti, B., Krudysz, M., Schauer, J. J. Sioutas, C., 2004. Diurnal variations of individual organic compound constituents of ultrafine and accumulation mode particulate matter in the Los Angeles basin. Environmental Science & Technology 38, 1296-1304.

Fraser, M. P., Lakshmanan, K., 2000. Using levoglucosan as a molecular marker for the long-range transport of biomass combustion aerosols. Environmental Science & Technology 34, 4560-4564.

Fraser, M. P., Yue, Z. W., Buzcu, B., 2003. Source apportionment of fine particulate matter in Houston, TX, using organic molecular markers. Atmospheric Environment 37, 2117-2123.

Furlong, E. T., Carpenter, R., 1982. Azzaarenes in Puget Sound sediments. Geochimica et Cosmochimica Acta 46, 1385-1396.

Gedalof, Z., Peterson, D. L., Mantua, N. J., 2005. Atmospheric, climatic, and ecological controls on extreme wildfire years in the Northwestern United States. Ecological Applications 15, 154-174.

Gélinas, Y., Prentice, K. M., Baldock, J. A., Hedges, J. I., 2001. An improved thermal oxidation method for the quantification of soot/graphitic black carbon in sediments and soils. Environmental Science & Technology 35, 3519-3525.

Ghosh, U., Zimmerman, J. R., and Luthy, R. G., 2003. PCB and PAH speciation among particle types in contaminated harbor sediments and effects on PAH bioavailability. Environmental Science & Technology 37, 2209-2217.

Gillett, N. P., Weaver, A. J., Zwiers, F. W., Flannigan, M. D., 2004. Detecting the effect of climate change on Canadian forest fires. Geophysical Research Letter 31, L18211, doi: 10.1029/2004GL020876.

Glaser, B., Haumaier, L., Guggenberger, G., Zech, W., 1998. Black carbon in soils: The use of benzenecarboxylic acids as specific markers. Organic Geochemistry 29, 811-819.

Goldberg, E. D., 1985. Black Carbon in the Environment: Properties and Distribution. John Wiley & Sons, New York.

Goñi, M. A., Hedges, J. I., 1992. Lignin dimers; structures, distribution, and potential geochemical applications. Geochimica et Cosmochimica Acta 56, 4025-4043.

Goñi, M. A., Nelson, B., Blanchette, R. A., Hedges, J. I., 1993. Fungal degradation of wood lignins: Geochemical perspectives from CuO-derived phenolic dimers and monomers. Geochimica et Cosmochimica Acta 57, 3985-4002.

Goñi, M. A., Hedges, J. I., 1995. Sources and reactivities of marine-derived organic matter in coastal sediments as determined by alkaline CuO oxidation. Geochimica et Cosmochimica Acta 59, 2965-2981.

Goñi, M. A., Ruttenberg, K. C., Eglinton, T. I., 1997. Source and contribution of terrigenous organic carbon to surface sediments in the Gulf of Mexico. Nature 389, 275-278.

Goñi, M. A., Yunker, M. B., Macdonald, R. W., Eglinton, T. I., 2000. Distribution and sources of organic biomarkers in arctic sediments from the Mackenzie River and Beaufort Shelf. Marine Chemistry 71, 23-51.

Gough, M. A., Fauzi, R., Mantoura, C., Preston, M., 1993. Terrestrial plant biopolymers in marine-sediments. Geochimica et Cosmochimica Acta 57, 945-964.

Griffin, J. J., Goldberg, D. E., 1979. Morphologies and origin elemental carbon in the environment. Science 206, 563-565.

Grimm, N. B., Faeth, S. H., Golubiewski, N. E., Redman, C. L., Wu, J., Bai, X., Briggs, J. M., 2008. Global change and the ecology of cities. Science 319, 756-760.

Gschwend, P. M., Hites, R. A., 1981. Fluxes of polycyclic aromatic hydrocarbons to marine and lacuatrine sediments in the Northestern United States. Geochimica et Cosmochimica Acta 45, 2359-2367.

Gustafsson, Ö., Haghseta, F., Chan, C., Macfarlane, J., Gschwend, P. M., 1997. Quantification of the dilute sedimentary soot phase: Implications for PAH speciation and bioavailability. Environmental Science & Technology 31, 203-209.

Gustafsson, Ö., Gschwend, P. M., 1998. The flux of black carbon to surface sediments on the New England continental shelf. Geochimica et Cosmochimica Acta 62, 465-472.

Gustafsson, Ö., Bucheli, T. D., Kukulska, Z., Andersson, M., Largeau, C., Rouzaud, J. N., Reddy, C. M., Eglinton, T. I., 2001. Evaluation of a protocol for the quantification of black carbon in sediments. Global Biogeochemical Cycles 15, 881-890.

Hadley, O.L., Ramanathan, V., Carmichael, G. R., Tang, Y., Corrigan, C. E., Roberts, G. C., Mauger, G. S., 2007. Trans-Pacific transport of black carbon and fine aerosols (D < 2.5 mm) into North America. Journal of Geophysical Research 112, D05309, doi:10.1029/2006JD007632.

Hammes, K., Smernik, R. J., Skjemstad, J. O., Herzog, A., Vogt, U. F., Schmidt, M. W. I., 2006. Synthesis and characterization of laboratory-charred grass straw (*Oryza sativa*) and chestnut wood (*Castanea sativa*) as reference materials for black carbon quantification. Organic Geochemistry 37, 1629-1633.

Hammes, K., Schmidt, M. W. I., Smernik, R. J., Currie, L. A., Ball, W. P., Nguyen, T. H., Louchouarn, P., Houel, S., Gustafsson, Ö., Elmquist, M., Cornelissen, G., Skjemstad, J. O., Masiello, C. A., Song, J., Peng, P., Mitra, S., Dunn, J. C., Hatcher, P. G., Hockaday, W. C., Smith, D. M., Hartkopf-Froeder, C., Boehmer, A., Luer, B., Huebert, B. J., Amelung, W., Brodowski, S., Huang, L., Zhang, W., Gschwend, P. M., Flores-Cervantes, D. X., Largeau, C., Rouzaud, J. N., Rumpel, C., Guggenberger, G., Kaiser, K., Rodionov, A., Gonzalez-Vila, F. J., Gonzalez-Perez, J. A., de la Rosa, J. M., Manning, D. A. C., Lopez-Capel, E., Ding, L., 2007. Comparison of quantification methods to measure fire-derived (black/elemental) carbon in soils and sediments using reference materials from soil, water, sediment and the atmosphere. Global Biogeochemical Cycles 21, GB3016, doi:10.1029/2006GB002914.

Hansen, J. E., Sato, M., 2001. Trends of measured climate forcing agents. Proceedings of the National Academy of Sciences of the United States of America 98, 14778-14783.

Hansen, J., Nazarenko, L., 2004. Soot climate forcing via snow and ice albedos. Proceedings of the National Academy of Sciences of the United States of America 101, 423-428.

Harris, D., Horwath, W. R., van Kessel, C., 2001. Acid fumigation of soils to remove carbonates prior to total organic carbon or carbon-13 isotopic analysis. Soil Science Society of America Journal 65, 1853-1856.

Hatcher, P. G., 1990. Chemical structural models for coalified wood (vitrinite) in low rank coal. Organic Geochemistry 16, 959-968.

Hatcher, P. G., Wenzel, K. A., Cody, G. D., 1994. Coalification reactions of vitrinite derived from coalified wood. ACS Symposium Series 570, 112-135.

Hedges, J. I., Parker, P. L., 1976. Land-derived organic-matter in surface sediments from Gulf of Mexico. Geochimica et Cosmochimica Acta, 40, 1019-1029.

Hedges, J. I., Mann, D. C., 1979a. The lignin geochemistry of marine sediments from the southern Washington coast. Geochimica et Cosmochimica Acta 43, 1809-1818.

Hedges, J. I., Mann, D. C., 1979b. The characterization of plant tissues of their lignin oxidation products. Geochimica et Cosmochimica Acta 43, 1803-1807.

Hedges, J. I., Ertel, J. R., 1982. Characterization of lignin by gas capillary chromatography of cupric oxide oxidation products. Analytical Chemistry 54, 174-178.

Hedges, J. I., Ertel, J. R., Leopold, E. B., 1982. Lignin geochemistry of a late Quaternary sediment core from Lake Washington. Geochimica et Cosmochimica Acta 46, 1869-1877.

Hedges, J. I. and Stern, J. H., 1984. Carbon and nitrogen determinations of carbonate-containing solids. Limnology and Oceanography 29, 657-663.

Hedges, J. I., Cowie, G. L., Ertel, J. R., Barbour, R. J., Hatcher, P. G., 1985. Degradation of carbohydrates and lignins in buried woods. Geochimica et Cosmochimica Acta 49, 701-711.

Hedges, J. I., Blanchette, R. A., Weliky, K., Devol, A. H., 1988a. Effects of fungal degradation on the CuO oxidation products of lignin; a controlled laboratory study. Geochimica et Cosmochimica Acta 52, 2717-2726.

Hedges, J. I., Clark, W. A., Cowie, G. L., 1988b. Organic matter sources to the water column and surficial sediments of a marine bay. Limnology and Oceanography 33, 1116-1136.

Hedges, J. I., 1991. Lignin, cutin, amino acid and carbohydrate analyses of marine particulate organic matter. In: Hurd, D. C., Spencer, D. W. (Eds.), Marine Particles: Analysis and Characterization, Geophyscial Monograph Series, Vol. 63. American Geophysical Union, Washington DC, pp. 129-137.

Hedges, J. I., Eglinton, G., Hatcher, P. G., Kirchman, D. L., Arnosti, C., Derenne, S., Evershed, R. P., Kögel-Knabner, I., de Leeuw, J. W., Littke, R., Michaelis, W., Rullkotter, J., 2000. The molecularly-uncharacterized component of nonliving organic matter in natural environments. Organic Geochemistry 31, 945-958.

Hernes, P. J., Benner, R., 2003. Photochemical and microbial degradation of dissolved lignin phenols: Implications for the fate of terrigenous dissolved organic matter in marine environments. Journal of Geophysical Research-Oceans 108, doi:10.1029/2002JC001421.

Hernes, P. J., Robinson, A. C., Aufdenkampe, A. K., 2007. Fractionation of lignin during leaching and sorption and implications for organic matter “freshness”. Geophysical Research Letters 34, doi:10.1029/2007GL031017.

Hessl, A. E., McKenzie, D., Schellhaas, R., 2004. Drought and Pacific Decadal Oscillation linked to fire occurrence in the inland Pacific Northwest. Ecological Applications, 14, 425-442.

Heyerdahl, E. K., McKenzie, D., Daniels, L. D., Hessl, A. E., Littell, J. S., Mantua, N. J., 2008. Climate drivers of regionally synchronous fires in the inland Northwest (1651-1900). International Journal of Wildland Fire 17, 40-49.

Hitzenberger, R., Petzold, A., Bauer, H., Ctyroky, P., Pouresmaeil, P., Laskus, L., Puxbaum, H., 2006. Intercomparison of thermal and optical measurement methods for elemental carbon and black carbon at an urban location. Environmental Science & Technology 40, 6377-6383.

Hong, L., Ghosh, U., Mahajan, T., Zare, R. N., Luthy, R. G., 2003. PAH sorption mechanism and partitioning behavior in lampblack-impacted soils from former oil-gas plant sites. Environmental Science & Technology 37, 3625-3634.

Hosoya, T., Kawamoto, H., Saka, S., 2006. Thermal stabilization of levoglucosan in aromatic substances. Carbohydrate Research 341, 2293-2297.

Houel, S., 2003. Dynamics of terrigenous organic matter in boreal reservoirs. Ph.D. dissertation, University of Québec in Montréal (UQAM), Montréal.

Houel, S., Louchouarn, P., Lucotte, M., Canuel, R., Ghaleb, B., 2006. Translocation of soil organic matter following reservoir impoundment in boreal systems: Implications for in situ productivity. Limnology and Oceanography 51, 1497-1513.

Ito, A., Penner, J. E., 2005. Historical emissions of carbonaceous aerosols from biomass and fossil fuel burning for the period 1870 –2000. Global Biogeochemical Cycles 19, GB2028, doi:10.1029/2004GB002374.

Jacobson, M. Z., 2001. Strong radiative heating due to the mixing state of black carbon in atmospheric aerosols. Nature 409, 695-697.

Jones, T. P., Chaloner, W. G., 1991. Fossil charcoal, its recognition and palaeoatmospheric significance. Palaeogeography, Palaeoclimatology, Palaeoecology 97, 39-50.

Jones, T. P., Chaloner, W. G., Kuhlbusch, T. A. J., 1997. Proposed bio-geological and chemical based terminology for fire-altered plant matter. In: Clark, J. S., Cachier, H., Goldammer, J. G., Stocks, B. (Eds.), Sediment Records of Biomass Burning and Global Change. Springer Verlag, Berlin, pp. 9-22.

Jonker, M. T. O., Koelmans, A. A., 2002. Sorption of polycyclic aromatic hydrocarbons and polychlorinated biphenyls to soot and soot-like materials in the aqueous environment mechanistic considerations. Environmental Science & Technology 36, 3725-3734.

Jonker, M. T. O., Hoenderboom, A. M., Koelmans, A. A., 2004. Effects of sedimentary sootlike materials on bioaccumulation and sorption of polychlorinated biphenyls. Environmental Toxicology and Chemistry 23, 2563-2570.

Kaiser, K., Guggenberger, G., 2000. Sorption of dissolved organic nitrogen by acid subsoil horizons and individual mineral phases. European Journal of Soil Science 51, 403-411.

Karls, J. F., Christensen, E. R., 1998. Carbon particles in dated sediments from Lake Michigan, Green Bay, and tributaries. Environmental Science & Technology 32, 225-231.

Kirk, T. K., Farrell, R. L., 1987. Enzymatic combustion - the microbial-Ddegradation of lignin. Annual Review of Microbiology 41, 465-505.

Klap, V.A., Louchouarn, P., Boon, J. J., Hemminga, M. A., van Soelen, J., 1999. Decomposition dynamics of six salt marsh halophytes as determined by cupric oxide oxidation and direct temperature-resolved mass spectrometry. Limnology and Oceanography 44, 1458-1476.

Knicker, H., Gonzalez-Vila, F. J., Polvillo, O., Gonzalez, J. A., Almendros, G., 2005. Fire-induced transformation of C- and N-forms in different organic soil fractions from a Dystric Cambisol under a Mediterranean pine forest (*Pinus pinaster*). Soil Biology & Biochemistry 37, 701-718.

Koelmans, A. A., Jonker, M. T. O., Cornelissen, G., Bucheli, T. D., Van Noort, P. C. M., Gustafsson, Ö., 2006. Black carbon: The reverse of its dark side. Chemosphere 63, 365-377.

Kögel-Knabner, I., Hatcher, P. G., Zech, W., 1991. Chemical structural studies of forest soil humic acids - aromatic carbon fraction. Soil Science Society of America Journal 55, 241-247.

Kralovec, A. C., Christensen, E. R., Van Camp, R. P., 2002. Fossil fuel and wood combustion as recorded by carbon particles in Lake Erie sediments 1850-1998. Environmental Science & Technology 36, 1405-1413.

Krull, E. S., Skjemstad, J. O., Graetz, D., Grice, K., Dunning, W., Cook, G., Parr, J. F., 2003. C-13-depleted charcoal from C_4 grasses and the role of occluded carbon in phytoliths. Organic Geochemistry 34, 1337-1352.

Kuhlbusch, T. A. J., Crutzen, P. J., 1995. Toward a global estimate of black carbon in residues if vegetation fores representing a sink of atmospheric CO_2 and a source of O_2. Global Biogeochemical Cycles 9, 491-501.

Kuhlbusch, T. A. J., 1998. Black carbon and the carbon cycle. Science 280, 1903-1904.

Kukkonen, J. V. K., Landrum, P. F., Mitra, S., Gossiaux, D. C., Gunnarsson, J., Weston, D., 2004. The role of desporption for describing the bioavailability if select polycyclic aromatic hydrocarbon and polychlorinated biphenyl congeners for seven laboratory-spiked sediments. Environmental Toxicology and Chemistry 23, 1842-1851.

Kuo, L.-J., Herbert, B. E., Louchouarn, P., 2008. Can levoglucosan be used to characterize and quantify char/charcoal black carbon in environmental media? Organic Geochemistry 39, 1466-1478.

Larsen, R. K., Schantz, M. M., Wise, S. A., 2006. Determination of levoglucosan in particulate matter reference materials. Aerosol Science and Technology 40, 781-787.

Lefkovitz, L.F., Cullinan, V.I., Crecelius, E.A., 1995. Historical Trends in the Accumulation of Chemicals in Puget Sound. National Oceanic and Atmospheric Administration, Silver Spring, MD.

Lehmann, J., Skjemstad, J. O., Sohi, S., Carter, J., Barson, M., Falloon, P., Coleman, K., Woodbury, P., Krull, E., 2008. Australian climate-carbon cycle feedback reduced by soil black carbon. Nature Geoscience 1, 832-835.

Leppanen, H., Kukkonen, J. V. K., Oikari, A. O. J., 2000. Concentration of retene and resin acids in sedimenting particles collected from a bleached kraft mill effluent receiving lake. Water Research 34, 1604-1610.

Lighty, J. S., Veranth, J. M., Sarofim, A. F., 2000. Combustion aerosols: Factors governing their size and composition and implications to human health. Journal of Air and Waste Management Association 50, 1565-1618.

Lim, B., Cachier, H., 1996. Determination of black carbon by chemical oxidation and thermal treatment in recent marine and lake sediments and Cretaceous-Tertiary clays. Chemical Geology 131, 143-154.

Lima, A. L. C., Eglinton, T. I., Reddy, C. M., 2003. High-resolution record if pyrogenic polycyclic aromatic hydrocarbon deposition during the 20th century. Environmental Science & Technology 37, 53-61.

Lima, A. L. C., Farrington, J. W., Reddy, C. M., 2005. Combustion-derived polycyclic aromatic hydrocarbons in the environment - A review. Environmental Forensics 6, 109-131.

Locke, H. B., 1988. The use of levoglucosan to assess the environmental impact of residential wood-burning on air quality. Ph.D. disseration, Dartmouth College, Hanover, NH.

Lopez-Capel, E., Sohi, S. P., Gaunt, J. L., Manning, D. A. C., 2005. Use of thermogravimetry-differential scanning calorimetry to characterize modelable soil organic matter fractions. Soil Science Society of America Journal 69, 136-140.

Louchouarn, P., Lucotte, M., Farella, N., 1999. Historical and geographical variations of sources and transport of terrigenous organic matter within a large-scale coastal environment. Organic Geochemistry 30, 675-699.

Louchouarn, P., Opsahl, S., Benner, R., 2000. Isolation and quantification of dissolved lignin from natural waters using solid-phase extraction and GC/MS. Analytical Chemistry 72, 2780-2787.

Louchouarn, P., Naehr, T., Silliman, J., Houel, S., 2006. Elemental, stable isotopic ($\delta^{13}C$), and molecular signatures of organic matter in late Pleistocene to Holocene sediments from the Peruvian margin (ODP Site 1229). In: Jørgensen, B.B., D'Hondt, S.L., Miller, D.J. (Eds.), Proceedings of the Ocean Drilling Program, Scientific Results 201 pp. 1-21.

Louchouarn, P., Chillrud, S. N., Houel, S., Yan, B., Chaky, D., Rumpel, C., Largeau, C., Bardoux, G., Walsh, D., Bopp, R. F., 2007. Elemental and molecular evidence of soot- and char-derived black carbon inputs to New York City's atmosphere during the 20th century. Environmental Science & Technology 41, 82-87.

Louchouarn, P., Brandenberger, J. M., Crecelius, E. A., 2009. Natural and post urbanization signatures of hypoxia in two basins of Puget Sound-II: Historical reconstruction of sources and inputs of organic matter. Geochimica et Cosmochimica Acta, in review.

Mackay, D. M., Roberts, P. V., 1982. The dependence of char and carbon yield on lignocellulosic precursor composition. Carbon 20, 87-94.

Mahler, B. J., Van Metre, P. C., Bashara, T. J., Wilson, J. T., Johns, D. A., 2005. Parking lot sealcoat: An unrecognized source of urban polycyclic aromatic hydrocarbons. Environmental Science & Technology 39, 5560-5566.

Mantua, N. J., Hare, S. R., Zhang, Y., Wallace, J. M., Francis, R. C., 1997. A Pacific interdecadal climate oscillation with impacts on salmon production. Bulletin of the American Meteorological Society 78, 1069–1079.

Marlon, J., Bartlein, P. J., Wihitlock, C., 2006. Fire-fuel-climate linkages in the northwestern USA during the Holocene. The Holocene, 16, 1059-1071.

Marris, E., 2006. Putting the carbon back: Black is the new green. Nature 442, 624-626.

Masiello, C. A., Druffel, E. R. M., 1998. Black carbon in deep-sea sediments. Science 280, 1911-1913.

Masiello, C. A., Druffel, E. R. M., Currie, L. A., 2002. Radiocarbon measurements of black carbon in aerosols and ocean sediments. Geochimica et Cosmochimica Acta 66, 1025-1036.

Masiello, C. A., 2004. New directions in black carbon organic geochemistry. Marine Chemistry 92, 201-213.

McGinnes, E. A., Kandeel, S. A., Szopa, P. S., 1971. Some structural changes observed in the structure of wood. Wood Fibre 3, 77-83.

Menon, S., Hansen, J., Nazarenko, L., Luo, Y. F., 2002. Climate effects of black carbon aerosols in China and India. Science 297, 2250-2253.

Middelburg, J. J., Nieuwenhuize, J., van Breugel, P., 1999. Black carbon in marine sediments. Marine Chemistry 65, 245-252.

Müller-Hagedorn, M., Bockhorn, H., Krebs, L., Muller, U., 2003. A comparative kinetic study on the pyrolysis of three different wood species. Journal of Analytical and Applied Pyrolysis 68-69, 231-249.

Muri, G., Cermelj, B., Faganeli, J., Brancelj, A., 2002. Black carbon in Slovenian alpine lacustrine sediments. Chemosphere 46, 1225-1234.

Muri, G., Wakeham, S. G., Rose, N. L., 2006. Records of atmospheric delivery of pyrolysis-derived pollutants in recent mountain lake sediments of the Julian Alps (NW Slovenia). Environmental Pollution 139, 461-468.

Naes, K., Axelman, J., Naf, C., Broman, D., 1998. Role of soot carbon and other carbon matrices in the distribution of PAHs among particles, DOC, and the dissolved phase in the effluent and recipient waters of an aluminum reduction plant. Environmental Science & Technology 32, 1786-1792.

Nelson, B.C., Goñi, M. A., Hedges, J. I., Blanchette, R. A., 1995. Soft-rot fungal degradation of lignin in 2700-year-old archaeological woods. Holzforschung 49, 1-10.

Nguyen, T. H., Brown, R. A., Ball, W. P., 2004. An evaluation of thermal resistance as a measure of black carbon content in diesel soot, wood char, and sediment. Organic Geochemistry 35, 217-234.

Nolte, C. G., Schauer, J. J., Cass, G. R., Simoneit, B. R. T., 2002. Trimethylsilyl derivatives of organic compounds in source samples and in atmospheric fine particulate matter. Environmental Science & Technology 36, 4273-4281.

Novakov, T., 1982. Characterization of aerosol sulfur, carbon, and nitrogen by ESCA and Thermal-Analysis. Transactions of the American Nuclear Society 41, 193-193.

Novakov, T., Ramanathan, V., Hansen, J. E., Kirchstetter, T. W., Sato, M., Sinton, J. E., Sathaye, J. A., 2003. Large historical changes of fossil-fuel black carbon aerosols. Geophysical Research Letters 30, 1324, doi:10.1029/2002GL016345.

Ohta, K., Venkatesan, M. I., 1992. Pyrolysis of wood specimens with and without minerals - Implications for lignin diagenesis. Energy & Fuels 6, 271-277.

Opsahl, S., Benner, R., 1995. Early diagenesis of vascular plant-tissues - Lignin and cutin decomposition and biogeochemical implications. Geochimica et Cosmochimica Acta 59, 4889-4904.

Opsahl, S., Benner, R., 1998. Photochemical reactivity of dissolved lignin in river and ocean waters. Limnology and Oceanography 43, 1297-1304.

Oros, D. R., Mazurek, M. A., Baham, J. E., Simoneit, B. R. T., 2002. Organic tracers from wild fire residues in soils and rain/river wash-out. Water Air and Soil Pollution 137, 203-233.

Otto, A., Shunthirasingham, C., Simpson, M. J., 2005. A comparison of plant and microbial biomarkers in grassland soils from the Prairie Ecozone of Canada. Organic Geochemistry 36, 425–448.

Otto, A., Gondokusumo, R., Simpson, M. J., 2006. Characterization and quantification of biomarkers from biomass burning at a recent wildfire site in Northern Alberta, Canada. Applied Geochemistry 21, 166-183.

Otto, A., Simpson, M. J., 2006. Evaluation of CuO oxidation parameters for determining the source and stage of lignin degradation in soil. Biogeochemistry 80, 121-142.

Park, J. S., Wade, T. L., Sweet, S. T., 2002 Atmospheric deposition of PAHs, PCBs, and organochlorine pesticides to Corpus Christi Bay, Texas. Atmospheric Environment 36, 1707-1720.

Pastorova, I., Arisz, P. W., Boon, J. J., 1993. Preservation of D-glucose-oligosaccharides in cellulose chars. Carbohydrate Research 248, 151-165.

Penner, J. E., Eddleman, H., Novakov, T., 1993. Towards the development of a global inventory for black carbon emissions. Atmospheric Environment Part a-General Topics 27, 1277-1295.

Pessenda, L. C. R., Gouveia, S. E. M., Aravena, R., 2001. Radiocarbon dating of total soil organic matter and humin fraction and its comparison with ^{14}C ages of fossil charcoal. Radiocarbon, 43, 595–601.

Pickford, S. G., Fahnestock, G. R., Ottmar, R., 1980. Weather fuel, and lightning fires in Olympic National Park. Northwest Science 54, 92-105.

Piskorz, J., Radlein, D. S., Scott, D. S., Czernik, S., 1989. Pretreatment of wood and cellulose for production of sugars by fast pyrolysis. Journal of Analytical and Applied Pyrolysis 16, 127-142.

Prahl, F. G., Carpenter, R., 1979. The role of zooplankton fecal pellets in the sedimentation of polycyclic aromatic hydrocarbons in Dabob Bay, Washington. Geochimica et Cosmochimica Acta 43, 1959-1972.

Prahl, F. G., Ertel, J. R., Goñi, M. A., Sparrow, M. A., Eversmeyer, B., 1994. Terrestrial organic carbon contributions to sediments on the Washington margin. Geochimica et Cosmochimica Acta 58, 3035-3048.

Preston, C.M., Schmidt, M. W. I., 2006. Black (pyrogenic) carbon: A synthesis of current knowledge and uncertainties with special consideration of boreal regions. Biogeosciences 3, 397-420.

Quénéa, K., Derenne, S., Rumpel, C., Rouzaud, J. N., Gustafsson, Ö., Carcaillet, C., Mariotti, A., Largeau, C., 2006. Black carbon yields and types in forest and cultivated sandy soils (Landes de Gascogne, France) as determined with different methods: Influence of change in land use. Organic Geochemistry 37, 1185-1189.

Radke, M., Willsch, H., Leythaeuser, D., 1982. Aromatic components of coal: Relation of distribution pattern to rank. Geochimica et Cosmochimica Acta 46, 1831-1848.

Radomski, A., Jurasz, P., Alonoso-Escolano, D., Drews, M., Morandi, M., Malinski, T., Radomski, M. W., 2005. Nanoparticle-induced platelet aggregation and vascular thrombosis. British Journal of Pharmacology 146, 882-893.

Ramanathan, V., Crutzen, P. J., Kiehl, J. T., Rosenfeld, D., 2001. Aerosols, climate, and hydrological cycle. Science 294, 2119-2124.

Ramanathan, V., Carmichael, G. R., 2008. Global and regional climate changes due to black carbon. Nature Geoscience 1, 221-227.

Ramdahl, T., 1983. Retene-a molecular marker of wood combustion in ambient air. Nature 306, 580-582.

Ravi, S., D'Odorico, P., Zobeck, T. M., Over, T. M., Collins, S. L., 2007. Feedbacks between fires and wind erosion in heterogeneous arid lands. Journal of Geophysical Research 112(G04007), doi:10.1029/2007JG000474.

Reddy, C. M., Pearson, A., Xu, L., McNichol, A. P., Benner, B. A., Wise, S. A., Klouda, G. A., Currie, L. A., Eglinton, T. I., 2002. Radiocarbon as a tool to apportion the sources of polycyclic aromatic hydrocarbons and black carbon in environmental samples. Environmental Science & Technology 36, 1774-1782.

Rodionov, A., Amelung, W., Haumaier, L., Urusevskaja, I., Zech, W., 2006. Black carbon in the Zonal steppe soils of Russia. Journal of Plant Nutrition and Soil Science-Zeitschrift Fur Pflanzenernahrung Und Bodenkunde 169, 363-369.

Rose, N. L., Flower, R. J., Appleby, P. G., 2003. Spheroidal carbonaceous particles (SCPs) as indicators of atmospherically deposited pollutants in North African wetlands of conservation importance. Atmospheric Environment 37, 1655-1663.

Routh, J., Meyers, P. A., Gustafsson, O., Baskaran, M., Hallberg, R., Scholdstrom, A., 2004. Sedimentary geochemical record of human-induced environmental changes in the Lake Brunnsviken watershed, Sweden. Limnology and Oceanography 49, 1560-1569.

Ruel, K., Barnoud, B., 1985. Degradation of wood by microorganisms. In: Higuchi, T. (Ed.), Biosynthesis and Biodegradation of Wood Components. Academic Press, Orlando, FL, pp. 441-467.

Rumpel, C., Kogel-Knabner, I., Bruhn, F., 2002. Vertical distribution, age, and chemical composition of organic, carbon in two forest soils of different pedogenesis. Organic Geochemistry 33, 1131-1142.

Rumpel, C., Alexis, M., Chabbi, A., Chaplot, V., Rasse, D. P., Valentin, C., Mariotti, A., 2006. Black carbon contribution to soil organic matter composition in tropical sloping land under slash and bum agriculture. Geoderma 130, 35-46.

Samet, J. M., DeMarini, D. M., Malling, H. V., 2004. Do airborne particles induce heritable mutations? Science 304, 971-972.

Sánchez-García, L., 2007. Geochemical characterization of marine sediments from the Gulf of Cádiz and environmental implications. Distribution and molecular composition of lipids and refractory forms of organic matter. Ph.D. dissertation, Universidad Autónoma de Madrid, Madrid.

Sánchez-García, L., Ramón de-Andrés, J., Martín-Rubí, A., Louchouarn, P., 2009. Diagenetic state and source characterization of marine sediments from the inner continental shelf of the Gulf of Cádiz (SW Spain), constrained by terrigenous biomarkers. Organic Geochemistry 40, 184-194.

Santos, C. Y. M., Azevedo, D. A., Aquino Neto, F. R., 2004 Atmospheric distribution of organic compounds from urban areas near a coal-fired power station. Atmospheric Environment 38, 1247-1257.

Sarkanen, K. V., Ludwig, C. H., 1971. Lignins: Occurence, formation, structure and reactions. Wiley-Interscience, New York, NY.

Schmidl, C., Marr, L. L., Caseiro, A., Kotianova, P., Berner, A., Bauer, H., Kasper-Giebl, A. Puxbaum, H., 2008. Chemical characterisation of fine particle emissions from wood stove combustion of common woods growing in mid-European Alpine regions. Atmospheric Environment 42, 126-141.

Schmidt, M. W. I., Noack, A. G., 2000. Black carbon in soils and sediments: Analysis, distribution, implications, and current challenges. Global Biogeochemical Cycles 14, 777-793.

Schmidt, M. W. I., Skjemstad, J. O., Czimczik, C. I., Glaser, B., Prentice, K. M., Gélinas, Y., Kuhlbusch, T. A. J., 2001. Comparative analysis of black carbon in soils. Global Biogeochemical Cycles 15, 163-167.

Schmidt, M. W. I., 2004. Biogeochemistry - Carbon budget in the black. Nature 427, 305-307.

Schneider, A. R., Stapleton, H. M., Cornwell, J., Baker, J. E., 2001. Recent declines in PAH, PCB, and toxaphene levels in the Northern Great Lakes as determined from high resolution sediment cores. Environmental Science & Technology 35, 3809-3815.

Scott, A. C., 1989. Observations on the nature and origin of fusain. International Journal of Coal Geology 12, 443-475.

Shafizadeh, F., Furneaux, R. H., Cochran, T. G., Scholl, J. P., Sakai, Y., 1979. Production of levoglucosan and glucose from pyrolysis of cellulosic materials. Journal of Applied Polymer Science 23, 3525-3539.

Shindell, D., Faluvegi, G., 2009. Climate response to regional radiative forcing during the twentieth century. Nature Geoscience 2, 294-300.

Simoneit, B. R. T., Schauer, J. J., Nolte, C. G., Oros, D. R., Elias, V. O., Fraser, M. P., Rogge, W. F., Cass, G. R., 1999. Levoglucosan, a tracer for cellulose in biomass burning and atmospheric particles. Atmospheric Environment 33, 173-182.

Simoneit, B. R. T., Elias, V. O., 2000. Organic tracers from biomass burning in atmospheric particulate matter over the ocean. Marine Chemistry 69, 301-312.

Simoneit, B.R.T., 2002. Biomass burning – a review of organic tracers for smoke from incomplete combustion. Applied Geochemistry 17, 129–162.

Simoneit, B. R. T., Elias, V., Kobayashi, M., Kawamura, K., Rushdi, A. I., Medeiros, P. M., Rogge, W. F. Didyk, B. M., 2004. Sugars - Dominant water-soluble organic compounds in soils and characterization as tracers in atmospheric particulate matter. Environmental Science & Technology 38, 5939-5949.

Simpson, C. D., Dills, R. L., Katz, B. S., Kalman, D. A., 2004. Determination of levoglucosan in atmospheric fine particulate matter. Journal of the Air & Waste Management Association 54, 689-694.

Skjemstad, J. O., Taylor, J. A., Smernik, R. J., 1999. Estimation of charcoal (char) in soils. Communications in Soil Science and Plant Analysis 30, 2283-2298.

Skjemstad, J. O., Reicosky, D. C., Wilts, A. R., McGowan, J. A., 2002. Charcoal carbon in U.S. agricultural soils. Soil Science Society of America Journal 66, 1249-1255.

Smith, D. M., Griffin, J. J., Goldberg, D. E., 1973. Elemental carbon in marine sediments: A baseline for burning. Nature 241, 268-270.

State Energy Consumption Estimation, 1960 through 2006, Energy Information Administration, Report DOE/EIA-0214(2006), November 2008.

Stout, S. A., Emsbo-Mattingly, S. D., 2008. Concentration and character of PAHs and other hydrocarbons in coals of varying rank-Implications for environmental studies of soils and sediments containing particulate coal. Organic Geochemistry 39, 801-819.

Tavendale, M. H., McFarlanel, P. N., Mackier, K. L., Wilkins, A. L., Langdon, A. G., 1997. The fate of resin acids-1. The biotransformation and degradation of deuterium labelled dehydroabietic acid in anaerobic sediments. Chemosphere 35, 2137-2151.

Terashima, N., Fukushima, K., 1989. Biogenesis and structure of macromolecular lignin in the cell-wall of tree xylem as studied by microautoradiography. ACS Symposium Series 399, 160-168.

Tollefson, J., 2009. Climate's smoky spectre. Nature 460, 29-32.

Ugolini, F. C., Reanier, R. E., Rau, G. H., Hedges, J. I., 1981. Pedological, isotopic, and geochemical investigations of the soils at the boreal forest and alpine tundra transition in northern Alaska. Soil Science 131, 359-374.

Van Metre, P. C., Mahler, B. J., Furlong, E. T., 2000. Urban sprawl leaves its PAH signature. Environmental Science & Technology 34, 4064-4070.

Van Metre, P. C., Mahler, B. J., 2005. Trends in hydrophobic organic contaminants in urban and reference lake sediments across the United State, 1970-2001. Environmental Science & Technology 39, 5567-5574.

Van Soest, P. J., Robertson, J. B., 1980. Systems of analysis for evaluating fibrous feeds. In: Pigden, W. J., Balch, C. C., Graham, M. (Eds.), Standardization of Analytical Methodology for Feeds. IDRC-134e. International Development Research Centre, Ottawa, Canada, pp. 49-60.

Vane, C. H., Abbott G. D., 1999. Proxies for land plant biomass: Closed system pyrolysis of some methoxyphenols. Organic Geochemistry 30, 1535-1541.

Verardo, D. J., Ruddiman, W. F., 1996. Late Pleistocene charcoal in tropical Atlantic deep-sea sediments: Climatic and geochemical significnace. Geology 24, 855-857.

Wakeham, S. G., Schaffner, C., Giger, W., 1980a. Polycyclic aromatic hydrocarbons in recent lake-sediments .1. compounds having anthropogenic origins. Geochimica et Cosmochimica Acta 44, 403-413.

Wakeham, S. G., Schaffner, C., Giger, W., 1980b. Polycyclic aromatic hydrocarbons in recent lake-sediments .2. compounds derived from biogenic precursors during early diagenesis. Geochimica et Cosmochimica Acta 44, 415-429.

Wakeham, S.G., Forrest, J., Masiello, C.A., Gelinas, Y., Alexander, C.R., Leavitt, P.R., 2004. Hydrocarbons in Lake Washington sediments. A 25-year retrospective in an urban lake. Environmental Science & Technology 38, 431-439.

Ward, T. J., Hamilton, R. F., Dixon, R. W., Paulsen, M. Simpson, C. D., 2006. Characterization and evaluation of smoke tracers in PM: Results from the 2003 Montana wildfire season. Atmospheric Environment 40, 7005-7017.

Westerling, A. L., Hidalgo, H. G., Cayan, D. R., Swetnam, T. W., 2006. Warming and earlier spring increase western U.S. forest wildfire activity. Science 313, 940-943.

Wetzel, S. A., Fonda, R. W., 2000. Fire history of Douglas-fir forests in the Morse Creek drainage of Olympic National Park, Washington. Northwest Science 74, 263-279.

Whitlock, C., Marlon, J., Briles, C., Brunelle, A., Long, C., Bartlein, P. J., 2008. Long-term relations among fire, fuel, and climate in the north-western US based on lake-sediment studies. International Journal of Wildland Fire 17, 72-83.

Wolbach, W. S., Gilmour, I., Anders, E., Orth, C. J., Brooks, R. R., 1988. Global fire at the Cretaceous-Tertiary boundary. Nature 334, 665-669.

Wolbach, W. S., Anders, E., 1989. Elemental carbon in sediments: Determination and isotopic analysis in the presence of kerogen. Geochimica et Cosmochimica Acta 53, 1637-1647.

Yan, B. Z., Abrajano, T. A., Bopp, R. F., Chaky, D. A., Benedict, L. A., Chillrud, S. N., 2005. Molecular tracers of saturated and polycyclic aromatic hydrocarbon inputs into Central Park Lake, New York City. Environmental Science & Technology 39, 7012-7019.

Youngblood, W., Blumer, M., 1975. Polycyclic aromatic hydrocarbons in the environment: Homologous series in soils and recent marine sediments. Geochimica et Cosmochimica Acta 39, 1303-1314.

Yunker, M. B., Macdonald, R. W., Vingarzan, R., Mitchell, R. H., Goyette, D., Sylvestre, S., 2002. PAHs in the Fraser River basin: A critical appraisal of PAH ratios as indicators of PAH source and composition. Organic Geochemistry 33, 489-515.

VITA

Name: Li-Jung Kuo

Address: Department of Geology & Geophysics
Texas A&M University
College Station, TX 77843-3115

Email Address: ljkuo@geo.tamu.edu

Education:

Ph.D. Geology 2009
Texas A&M University, College Station, TX.
M.S. Marine Environment and Engineering 1999
National Sun Yat-sen University, Kaohsiung, Taiwan.
B.S. Marine Environment and Engineering 1996
National Sun Yat-sen University, Taiwan.

Publications:

Kuo, L-J, Louchouarn, P., Herbert, B. E., 2008. Fate of CuO-derived lignin oxidation products during plant combustion: Application to the evaluation of charcoal inputs to soil organic matter. Organic Geochemistry 39, 1522-1536.

Kuo, L-J, Herbert, B. E., Louchouarn, P., 2008. Can levoglucosan be used to characterize and quantify char/charcoal black carbon in environmental media? Organic Geochemistry 39, 1466-1478.

Kuo, L-J, Lee, C-L., 2005. Stage-variation in binding of pyrene to selected humic substances under different ionic strengths. Environmental Toxicology and Chemistry 24, 886-894.

Lee, C-L, Kuo, L-J, Wang, H-L, Hsieh, B-C, 2003. Effects of ionic strength on the binding of phenanthrene and pyrene to the humic substances: three-stage variation model. Water Research 37, 4250-4258.

Lee, C-L, Huang, H-T, Kuo, L-J, 2000. Experimental validation of an OMS model for the sorption behaviors of PAHs onto aluminum oxide coated with humic acids. Journal of Environmental Science and Health A35, 515-536.

Lee, C-L, Kuo, L-J, 1999. Quantification of the dissolved organic matter effect on the sorption of hydrophobic organic pollutant: application of an overall mechanistic sorption model. Chemosphere 38, 807-821.